ESTIMATION OF REQUIRED RESTRAINT FORCES IN Z-PURLIN SUPPORTED, SLOPED ROOFS UNDER GRAVITY LOADS

by

Michael C. Neubert

Thesis submitted to the Faculty of the
Virginia Polytechnic Institute and State University
in partial fulfillment of the requirements for the degree of

MASTER OF SCIENCE

in

Civil and Environmental Engineering

Approved:

_____
T. M. Murray, Chairman

_____ _____
W. S. Easterling T. E. Cousins

August 1999

Blacksburg, VA

Key words: cold-formed steel, metal roof, restraint, Z-purlin

ESTIMATION OF REQUIRED RESTRAINT FORCES IN Z-PURLIN SUPPORTED, SLOPED ROOFS UNDER GRAVITY LOADS

by

Michael C. Neubert

Committee Chairman: Thomas M. Murray

Civil and Environmental Engineering

(ABSTRACT)

The current specification provisions for the prediction of lateral restraint forces in Z-purlin supported roof systems under gravity loads are in Section D3.1 of the 1996 AISI Cold-Formed Specification. The design equations contained in these provisions are empirical and based on statistical analysis. They were developed using elastic stiffness models of flat roofs and were verified by experimental testing. The provisions need refinement, because the treatment of roof slope and system effects is incorrect. Also, the current design provisions are based upon an assumed panel stiffness value, ignoring the significant difference in required restraint force that occurs when panel stiffness is varied.

Therefore, a new restraint force design procedure, having a stronger reliance on engineering principles, is proposed. This new treatment of the static forces in Z-purlin roofs led to a more accurate method of addressing roof slope. Elastic stiffness models, with varying roof slope, panel stiffness, and cross-sectional properties, were used to develop the proposed procedure. The basis of the procedure is to determine the lateral restraint force required for a single purlin system and then extend this result to systems with multiple restrained purlin lines. Roof slope is incorporated into the calculation of the single purlin restraint force, which includes eccentric gravity loads and forces induced by Z-purlin asymmetry. The procedure includes a system effect factor to account for the observed nonlinear increase in restraint force with the number of restrained purlins. An adjustment factor varies the predicted restraint force depending on the shear stiffness of the roof panel. The proposed procedure applies to five bracing configurations: support, third-point, midspan, quarter point, and third-point plus support restraints.

ACKNOWLEDGEMENTS

I first wish to extend my gratitude to Dr. Thomas Murray, principal advisor to this research, for his invaluable direction and assistance. Thank you for urging me to pursue this research and enriching my graduate studies. I also have sincere appreciation for Dr. W. Samuel Easterling and Dr. Thomas Cousins, who aided me greatly as members of the research committee.

I acknowledge the Metal Building Manufacturer's Association and the American Iron and Steel Institute for their financial support of this work. It is truly an honor to have been selected as an MBMA Graduate Fellowship Award Winner. The interest and support of these two organizations made this research possible.

Many friends and family deserve recognition for the support that they have given me in the course of my graduate work. I thank my parents Marilyn and Robert Neubert for their emotional support and their interest in my studies. Many friends assisted me with my research and studies; these friends include Juan Archilla, Mark Boorse, Amy Dalrymple, Anthony Farmer, Rob Krumpen, Rich Meyerson, John Ryan, Rob Schottler, Jolyn Senne, and Anthony Temeles. They made graduate school more enjoyable by providing a supportive environment for me to learn and grow.

TABLE OF CONTENTS

TABLE OF CONTENTS, CONTINUED

TABLE OF CONTENTS, CONTINUED

LIST OF FIGURES

LIST OF FIGURES, CONTINUED

LIST OF TABLES

LIST OF TABLES, CONTINUED

CHAPTER I

INTRODUCTION

1.1 OBJECTIVE

This research is an analytical study to formulate design equations for the estimation of required lateral restraint forces in Z-purlin supported, sloped roofs under gravity loads. The current design equations for these restraints, contained in Section D3.2.1 of the American Iron and Steel Institute's *Specification for the Design of Cold-formed Steel Members* (1996), have several deficiencies. These provisions have an incorrect treatment of roof slope and depend too heavily upon statistical regression. The current specification also does not consider roof panel stiffness, which can have a significant effect on the required restraint force. Furthermore, there is a range of roof slopes for which no lateral restraint is necessary, but Section D3.2.1 does not address this issue.

Thus, the goal of this research is to develop new and more suitable design equations to replace Section D3.2.1 of the Specification. The proposed equations must be less empirical and have a stronger reliance on engineering principles. The other deficiencies must be remedied by using a more accurate treatment of sloped roofs, including an adjustment for roof panel stiffness, and setting a minimum restraint force value for which lateral restraint is necessary.

1.2 BACKGROUND

Metal building systems are commonly used for the construction of low-rise, industrial buildings. The roof system in these buildings is often composed of corrugated metal roof panels connected to cold-formed purlins (either C or Z-sections). Two fastening systems are currently used to attach the roof panels to the purlins. In a through-fastened roof system, the panels are attached directly to the purlins with self-drilling or

self-tapping fasteners, typically spaced every 12 in. along each purlin, that penetrate through the panels. A standing seam roof system has vertical side laps for joining panels, and the panels are attached to the purlins by means of concealed clips, typically spaced every 18-24 in. along each purlin. These clips do not penetrate the panels, making the roof more watertight than a through-fastened system.

Cold-formed Z-purlins come in sizes ranging from 3 to 12 in. in depth, 1.75 to 3.25 in. in flange width, and 0.036 to 0.135 in. in thickness (see Figure 1.1). These purlins are fabricated from steel sheets, which are then subjected to a cold bending process, either press braking or roll-forming, to obtain a Z-shaped cross-section. Cold-forming increases strength due to the strain hardening and strain aging that occurs during the process. The outer edges of the flanges are usually lipped for stiffening, to increase their local buckling strength. The primary advantage of Z-purlins is that the cross-section allows them to be nested for shipping and lapped to provide continuity. Also, Z-purlins are often used in metal roofs because they are lightweight, easily fabricated and erected, and tend to be very economical.

Due to the asymmetric cross-section of a Z-purlin, it will twist and deflect laterally when loaded obliquely to its principal axes, as is the case for gravity loading on a flat roof. The presence of a roof panel usually prevents the purlins from moving relative to each other, but the entire system will tend to move laterally. This lateral movement and twisting is detrimental to flexural strength, and necessitates a restraint system, typically provided by a number of discrete eave braces along each purlin span. The most common bracing schemes are support (or torsional) restraints, third-point restraints, and midpoint restraint, each having braces attached to the purlin web, just below the top flange. The geometry of a Z-purlin, and the composite action between panel and purlin, have made the prediction of the required bracing forces very difficult.

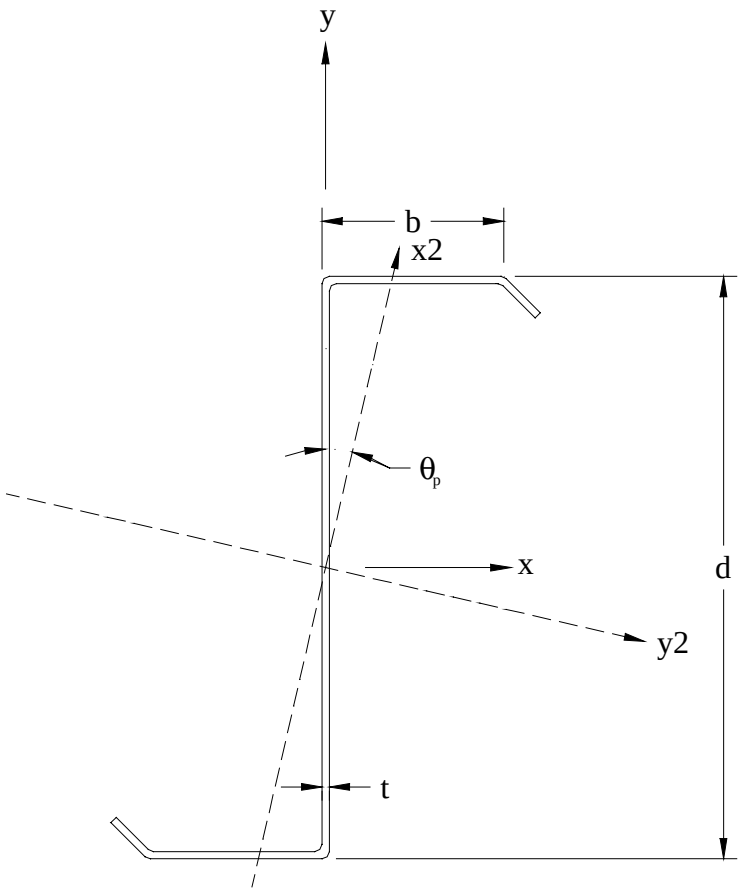

Figure 1.1 Z-purlin Geometry

1.3 LITERATURE REVIEW

Theoretical Studies. Zetlin and Winter (1955) studied single span, simply supported, Z-purlins, with various loadings applied in the plane of the web. They assumed lateral bracing was present at both flanges at all locations of applied loads. Through basic principles of mechanics, the following equation for total restraint force was developed:

$$P_L = \left(I_{xy} / I_x\right) W \tag{1.1}$$

where P_L is the restraint force, I_{xy} is the product moment of inertia, I_x is the moment of inertia with respect to an axis perpendicular to the purlin web, and W is the applied load. This equation shows a linear variation of restraint force with the applied loading, and the ratio of restraint force to applied load depends solely on the cross-sectional properties of

the purlin. Note that torque effects on restraint force, caused by eccentric loading of the top flange, are not accounted for in this expression.

Another limitation of Equation 1.1 is that it considers only a single purlin by itself. In actual roof systems, the shear and torsional stiffness of roof panels gives partial restraint to the purlins. Needham (1981) developed a mathematical model to incorporate these panel forces. Assumptions made in the model were: 1) simply supported purlins, 2) no lateral bracing, 3) the panel acts as an infinitely rigid diaphragm, and 4) the panel cannot move laterally with respect to the purlins. In practice, a gravity loaded purlin has a distributed load acting on its top flange. Needham approximated this loading with a point load acting at $b/6$ away from the web, where b is the flange width (refer to Figure 1.1). The net torque acting on the cross-section was set equal to the sum of torques induced by the applied loading and by panel restraint. The primary force in the panel was taken to be $(I_{xy}/I_x)W$, based on the work of Zetlin and Winter. To satisfy equilibrium, a secondary force in the purlin, W_{ps}, was given to the panel. This force acts at a distance of $d/2$ from the shear center of the purlin, leading to $W_{ps} = T/(d/2)$, where d is the depth of the purlin. Based on these expressions and assumptions, Needham derived an equation for total bracing force, and extended it to account for sloped roofs:

$$P_L = W\left[\left(\frac{I_{xy}}{I_x}\right)(\cos\theta - 1) - \sin\theta + \frac{b}{3d}\right] \tag{1.2}$$

where θ is the roof angle with respect to horizontal. Needham found Equation 1.2 to be in good agreement with laboratory test results, depending on the value of eccentricity ($e = b/6$ was not always accurate).

Ghazanfari and Murray (1983) developed a method to predict restraint forces in simply supported Z-purlins attached to conventional roof panels. Various bracing schemes were examined, all under uniform gravity loading. Assumptions in their model include: 1) no panel rotational restraint, 2) no lateral movement of the purlins relative to the panel, 3) the eccentricity of the vertical load is $b/3$, 4) W_h (lateral panel force) is uniformly distributed and acts at the top flange in a horizontal plane, 5) and all braces are infinitely rigid and connected to immovable supports. In their model, Ghazanfari and

Murray accounted for the effects of panel deformation on restraint forces. Panel deformation cannot be determined unless the lateral force acting on the panel is known. However, this lateral force is depends on the torque loading, which is in turn dependent on the panel deformation. Thus, an iterative computer program was developed to calculate these second order effects. The effect of several parameters on restraint force was studied, and panel stiffness, span, load eccentricity, and principal axes location were found to be the most critical.

The above research had not examined the effects of multiple spans and multiple restrained purlin lines. Elhouar and Murray (1985) remedied this deficiency in developing a design procedure for bracing requirements in through fastened, corrugated steel panel, roof systems. A computer stiffness model (see Figure 1.3) was built and adjusted to match full-scale (Curtis and Murray, 1983) and quarter-scale (Seshappa and Murray, 1985) experimental results. The model was made using STRUDL (Structural Design Language) and represented Z-purlins with space frame line elements and roof panels with plane trusses. Braces were connected to the top line elements of purlins, and the eccentricity of the applied loading was assumed to be *b*/3. Other assumptions were that purlins could not move relative to the roof panel, and that braces and purlins were attached to rigid supports that prevent all translations. Three bracing configurations (see Figure 1.3) were examined: end restraints, third-point restraints, and midpoint restraint.

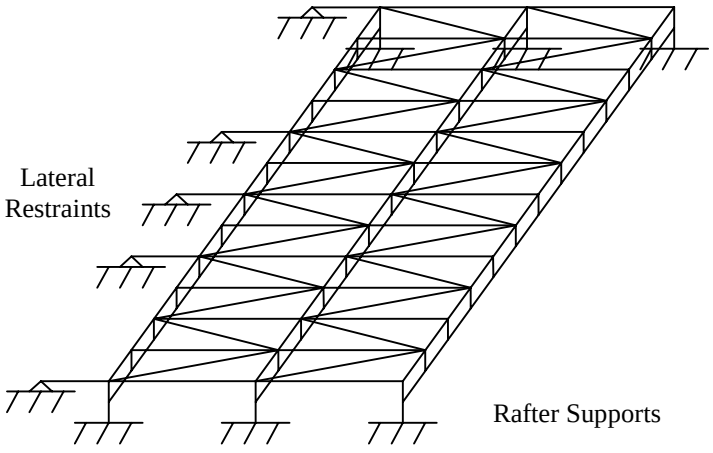

Figure 1.2 Elhouar and Murray's Stiffness Model

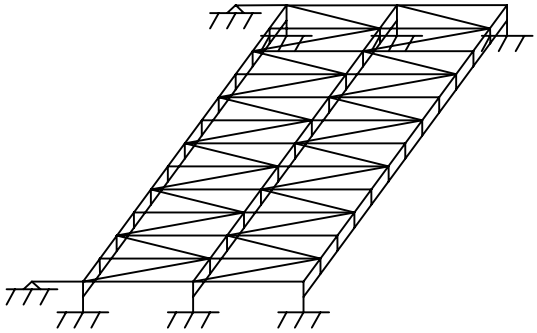

(a) Support Restraints

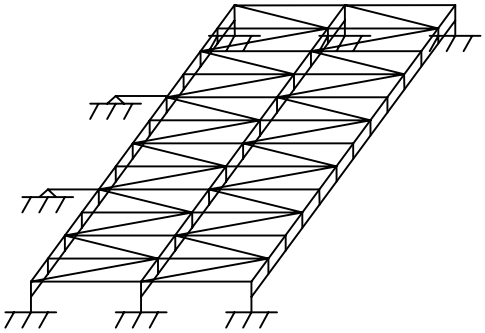

(b) Third-point Restraints

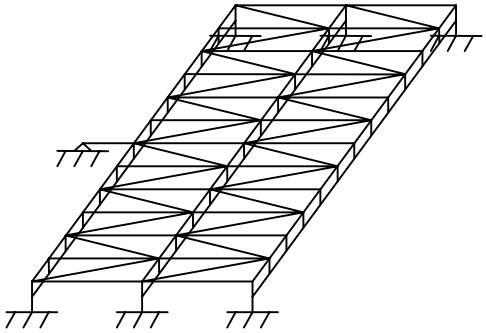

(c) Midpoint Restraint

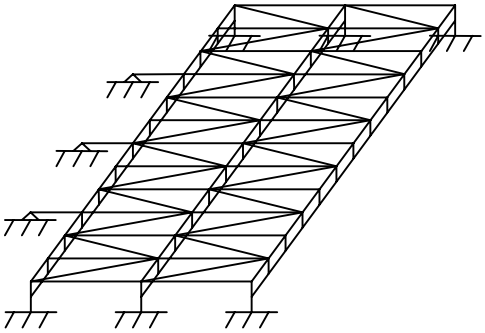

(d) Quarter-point Restraints

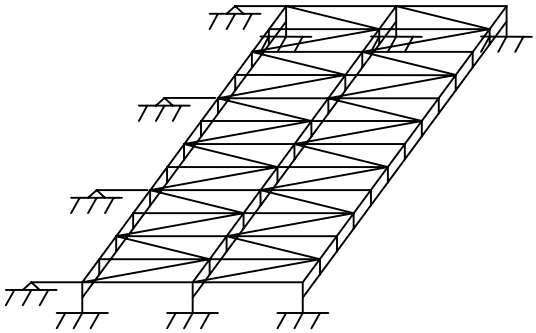

(e) Third-point Plus Support Restraints

Figure 1.3 Bracing Configurations

Based upon data taken from the stiffness model, a parametric study was performed to determine how restraint force is affected by cross-sectional properties, number of restrained purlin lines, span length, number of spans, and the bracing configuration. Roof slope was not included in the parametric study, but based on quarter-scale tests by Seshappa and Murray (1985), Elhouar and Murray (1985) corrected for slope through the following relationship:

$$P_L = P_{L_O} - W \tan\theta \tag{1.3}$$

where P_{L_O} is the restraint force on a flat roof. Roof panel stiffness was also not examined, because a stiffness of 2500 lb/in. was assumed for all cases. It was believed that the increase in required restraint force was negligible for roof panels stiffer than 2500 lb/in, based on experimental results by Ghazanfari and Murray (1983). A regression analysis was then performed on the data to derive prediction equations for the various span and bracing conditions considered. As an example, Elhouar and Murray's equation for the force in each brace of a single span system with end restraints is:

$$P_L = 0.5\left(\frac{0.220 \cdot b^{1.500}}{n_p^{0.716} d^{0.901} t^{0.600}} - \tan\theta\right) W \tag{1.4}$$

where n_p is the number of restrained purlin lines and t is the purlin thickness. Previous experimental results indicated a "system effect" whereby increasing the number of restrained purlin lines in a system decreases the ratio of lateral force to vertical applied force. The primary cause of this system effect is believed to be the torsional resistance of the purlins. Elhouar and Murray's equations take this system effect into account with the regression terms.

Several more recent studies on the modeling of Z-purlin behavior have been conducted. Fenske and Yener (1990) treated Z-purlin roof systems as stiffened plates, with section properties based upon composite action between the roof panel and the purlins. Generalized beam theory was applied to Z-purlin design by Heinz (1994). Lucas et al (1997) developed a non-linear, elasto-plastic finite element model for Z-purlin roof systems.

In 1998, Danza and Murray extended the work done by Elhouar to include two new bracing configurations (refer to Figure 1.3): quarter-point restraints and third-point plus support restraints. A series of computer tests was run using elastic stiffness models, similar to those used by Elhouar, but with minor modifications. The parameters varied included purlin cross-section, number of restrained purlin lines, number of spans, and span length. The study did not include sloped roofs, and assumed a panel stiffness value of 2500 lb/in. A regression analysis was then performed on the stiffness model results, to obtain a set of empirical design equations. The form of the equations was modified slightly from the one used by Elhouar and Murray, and includes span length in the regression. For example, the following is Danza and Murray's design equation for single span systems with quarter-point restraint:

$$P_L = C\left[\left(\frac{t}{L}\right)^{0.16} - \frac{0.407 t^{0.75} d^{0.50} n^{0.39}}{b^{1.25}}\right] W \tag{1.5}$$

where $C = 0.25$ for braces near supports, $C = 0.50$ for brace at midspan, and W is the total applied gravity load (lb).

Experimental Studies. Needham (1981) conducted a small number of full-scale tests on flat roofs to confirm his analysis. The test apparatus had two 9.5 in. deep purlins spaced 5 ft apart, each fastened to roof panels. The bracing configuration was end restraints, and simulated gravity loading was applied. Lateral loads were measured with load cells and found to be between 9.1% and 9.7% of the total applied load.

Ghazanfari and Murray (1982) also did full-scale tests to confirm their analytical results. They performed nine tests on flat, single span, two purlin line systems with four different bracing schemes. Deck stiffness was varied, and results showed a negligible increase in restraint force for two purlin systems, when the deck stiffness was increased above 1500 lb/in. (see Figure 1.4). The predicted restraint forces were in agreement with experimental results, though slightly conservative at loads below the purlin failure load. For systems with intermediate braces, second order effects were negligible. Restraint force was found to vary from 14% to 29% of the total applied load, depending on the span and bracing scheme.

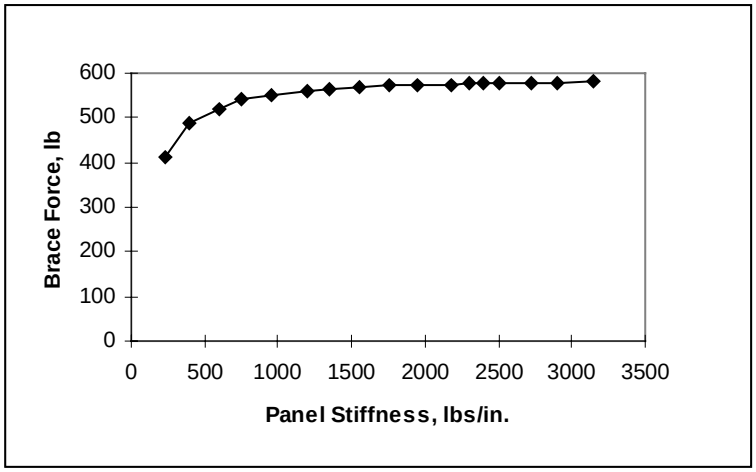

Figure 1.4 Restraint force vs. Panel Stiffness (Ghazanfari and Murray, 1983)

Twenty full-scale tests were conducted by Curtis and Murray (1983) on flat, single-span systems with two, six and seven restrained purlin lines. All tests measured the end restraint restraint forces, which were induced by gravity loading. Their results identified the existence of the system effect in Z-purlin supported roof systems. They determined that increasing the number of restrained purlin lines decreased the lateral restraint force by 5% to 10% of the applied load.

Seshappa and Murray (1985) used quarter-scale model Z-purlins to study through-fastened roof systems under gravity loading. Basic similitude concepts were followed whenever possible, and some identical full-scale tests were done for verification. Roof panels and fasteners did not fully satisfy similitude laws, but it was determined that this difference was negligible. A total of 28 tests were performed to measure lateral restraint forces for multiple span, multiple purlin line systems with end restraints, third point restraints, and midpoint restraint. One series of tests was conducted on systems with roof slopes varying from 0:12 to 1.5:12. The results of this test series are shown in Figure 1.5. It was concluded that the bracing force for sloped roofs could be predicted by subtracting off the lateral component of the applied load from the flat roof prediction (Equation 1.3). The interaction of system effects along with roof slope was not considered.

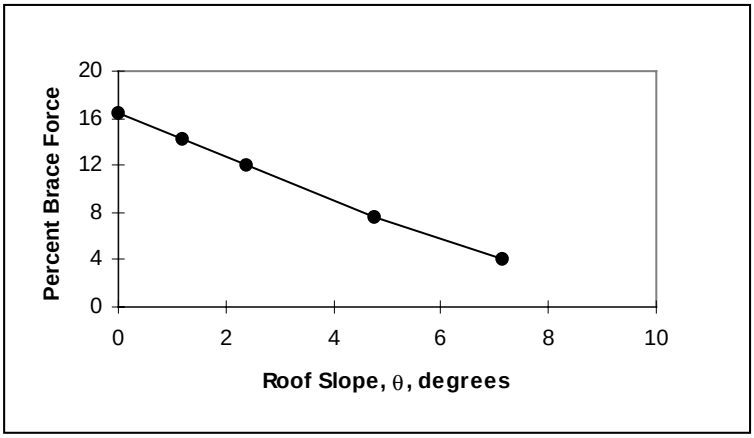

Figure 1.5 Percent Restraint force vs. Roof Slope (Seshappa and Murray, 1985)

Rivard and Murray (1986) performed six single span and six three-span continuous tests for lateral restraint forces in standing seam roof systems with Z-purlins. One single span test was done on a through-fastened system for comparison. The bracing schemes considered were again end restraints, third-point restraints, and midpoint restraint. Two piece clips were used for both pan type and rib type roof panels. The results indicated that the equations developed by Elhouar and Murray (1985) were applicable to standing seam roofs as well as through-fastened roofs.

1.4 CURRENT DESIGN PRACTICE

In the United States, the specification used for the design of lateral bracing for Z-purlin supported roof systems is generally the *Specification for the Design of Cold-Formed Steel Structural Members* (1996). This specification defines the force that lateral restraints must be designed to resist, for single and multiple purlin line systems of any roof slope. Three bracing configurations are addressed: end restraints, third-point restraints, and midpoint restraint. The specification applies to both through-fastened and standing seam roof systems, but only to systems with all purlins facing in the direction of upward roof slope. The design equations are based on the prediction equations developed

by Elhouar and Murray (1985) through regression analysis, with slight modifications. These equations, as they appear in the specification, are as follows:

(1) Single-span System with Restraints at the Supports:

$$P_L = 0.5\left[\frac{0.220b^{1.50}}{n_p^{0.72}d^{0.90}t^{0.60}}\cos\theta - \sin\theta\right]W \qquad (Eq.\ \text{D3.2.1-1})$$

(2) Single-span System with Third-point Restraints:

$$P_L = 0.5\left[\frac{0.474b^{1.22}}{n_p^{0.57}d^{0.89}t^{0.33}}\cos\theta - \sin\theta\right]W \qquad (Eq.\ \text{D3.2.1-2})$$

(3) Single-span System with Midspan Restraint:

$$P_L = 0.5\left[\frac{0.224b^{1.32}}{n_p^{0.65}d^{0.83}t^{0.50}}\cos\theta - \sin\theta\right]W \qquad (Eq.\ \text{D3.2.1-3})$$

(4) Multiple-span System with Restraints at the Supports:

$$P_L = C_{tr}\left[\frac{0.053b^{1.88}L^{0.13}}{n_p^{0.95}d^{1.07}t^{0.94}}\cos\theta - \sin\theta\right]W \qquad (Eq.\ \text{D3.2.1-4})$$

with $C_{tr} = 0.63$ for braces at end supports of multiple-span systems

$C_{tr} = 0.87$ for braces at the first interior supports

$C_{tr} = 0.81$ for all other braces

(5) Multiple-span System with Third-point Restraints:

$$P_L = C_{th}\left[\frac{0.181b^{1.15}L^{0.25}}{n_p^{0.54}d^{1.11}t^{0.29}}\cos\theta - \sin\theta\right]W \qquad (Eq.\ \text{D3.2.1-5})$$

with $C_{th} = 0.57$ for outer braces in exterior spans

$C_{th} = 0.48$ for all other braces

(6) Multiple-span System with Midspan Restraints:

$$P_L = C_{ms}\left[\frac{0.116b^{1.32}L^{0.18}}{n_p^{0.70}dt^{0.50}}\cos\theta - \sin\theta\right]W \qquad (Eq.\ \text{D3.2.1-6})$$

with $C_{ms} = 1.05$ for braces in exterior spans

$C_{ms} = 0.90$ for all other braces

where b = Flange width

d = Depth of section

t = thickness

L = span length

θ = Angle between the vertical and the plane of the web of the Z-section, degrees

n_p = Number of parallel restrained purlin lines

W = Total load supported by the restrained purlin lines between adjacent supports

In these equations, positive restraint force indicates that restraint is needed to keep the purlin flanges from moving in the direction of upward roof slope. Systems having less than four restrained purlin lines have a required bracing force equal to 1.1 times the force given by *Eq*. D3.2.1-1 through *Eq*. D3.2.1-6, calculated using $n_p = 4$. Systems having more than twenty restrained purlin lines have a required bracing force determined by *Eq*. D3.2.1-1 through *Eq*. D3.2.1-6, calculated using $n_p = 20$.

Compared to Elhouar's Equation 1.4, the only significant difference is the addition of a $\cos\theta$ factor to the regression term, and the replacement of the $\tan\theta$ term with a $\sin\theta$ term. Note that for small angles, $\cos\theta \to 1$ and $\sin\theta \to \tan\theta$, which makes the two equations equivalent for this approximation. For examples showing this design procedure, refer to *A Guide for Designing with Standing Seam Roof Panels* (Fisher and LaBoube, 1997).

1.5 SCOPE OF RESEARCH

The intent of this research is to develop restraint force design equations for five lateral bracing configurations for both single and multiple span roof systems, with multiple Z-restrained purlin lines: support restraints, third-point restraints, midspan restraint, quarter-point restraints, and third-point plus support restraints. A space frame stiffness model was developed to test the restraint force behavior of many different roof

system conditions. Parameters varied in the study include: purlin cross-section, span length, roof panel stiffness, roof slope, and number of restrained purlin lines.

Theoretical design equations were developed based on a new treatment of Z-purlin statics, with coefficients varying for each bracing condition. These coefficients were determined by a regression analysis of the stiffness model results. The result of this work is a set of proposed specification provisions, intended to replace the current provisions in Section D3.2.1 of the *Specification for the Design of Cold-Formed Steel Structural Members* (1996).

CHAPTER II

MATHEMATICAL MODELING

2.1 INTRODUCTION TO MODELING

The purpose of this chapter is to develop a mathematical model of a Z-purlin supported roof system, consisting of parallel purlin lines, a roof panel, rafter supports, and lateral braces. Mathematical modeling, by definition, is a means of approximating an actual physical system with a numerical representation. To develop and verify design equations for the estimation of restraint force in Z-purlin roof systems, a large amount of data is necessary. This data must have the required restraint forces for conditions representing the full range of parameters used in Z-purlin supported roofs. A numerical model is necessary for this research, because the number of experimental tests needed to collect this data would be impractical, and the existing data from previous tests is insufficient. Also, experimental research on sloped, full-scale Z-purlin roof systems is difficult due to the possibility of test apparatus collapse.

2.2 SELECTION OF MODEL

After identifying the need for modeling, the next step is to choose the most appropriate model. The model has to be an accurate representation of the physical system, so it should be as detailed and representative as possible. The basic principles of structural modeling must be followed: equilibrium of forces and physical compatibility, along with the use of proper material properties. The most accurate model would be a three-dimensional solid that includes second order effects. However, the model must be analyzed thousands of times to collect the necessary data, so execution time must be minimized. This makes highly sophisticated computer models, where each analysis run takes several hours, impractical for this research. Furthermore, this study is only

concerned with the axial forces in the lateral restraints, and not stresses or deflections throughout the system, so complex modeling would not be advantageous.

In their research, Elhouar and Murray (1985) used a space frame stiffness model to generate restraint force data for their design equations. Their model, hereafter referred to as the Elhouar and Murray model, is appropriate because solid effects and second order effects are negligible on the restraint forces of Z-purlin supported roof systems. The Elhouar and Murray model showed excellent agreement with experimental results, and was later used by Danza and Murray (1998) to develop additional restraint force equations. In both the Elhouar and Murray model and the Danza and Murray model, purlins and the roof panel were represented by space trusses, which were attached to form the main roof system, and then braced laterally by restraint members. Uniform gravity loads were approximated by discretizing the total gravity force into point and line loads. The resulting model retains the key aspects of the physical system and has a manageable execution time. The model also allows for roof parameters to be easily modified, which further reduces the time required for data collection. Therefore, an elastic stiffness model, based on the Elhouar and Murray model, was chosen for this investigation and is hereafter called the current model.

2.3 STIFFNESS MODEL DEVELOPMENT

2.3.1 Global Characteristics

The first step towards creating a stiffness model is to establish the global parameters. All of the models used for this project were created in United States Customary (USD) units (kip, in., ft) as is most commonly used in industry in this country. Analysis specifications were set such that shear deformations, torsional warping effects, and second order effects were neglected. Warping and second order effects were not considered, because this study examines only axial forces. The material used for all elements of the model was linear elastic steel. The fundamental material properties are: E=29,000 ksi, G=11,154 ksi, and ν=0.3; thus defining the Young's modulus, shear

modulus, and Poisson's ratio, respectively. The material was assumed to be below yield stress, and therefore elastic, at all times.

2.3.2 Axes Orientation

To define directions and locations in space, local and global axes must be defined for the model. For the current model, the global Y-axis is established normal to the plane of the roof panel, the global Z-axis points down the length of the parallel purlin lines, and the global X-axis is in line with the lateral restraint members. The local axes for each element in the model are defined so that the local x-axis is oriented down the length of the element, and is normal to the plane containing the local y- and z-axes (see Figure 2.1).

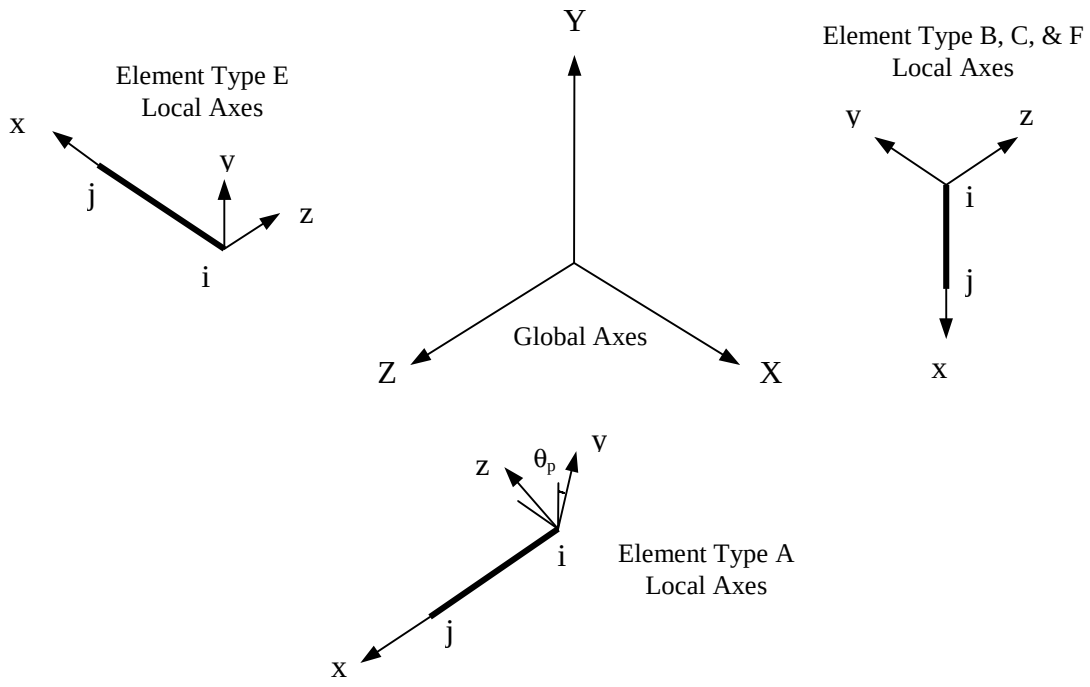

Figure 2.1 Local and Global Axes

2.3.3 Modeling of Purlins

Similar to the Elhouar and Murray model, the current model represents a Z-purlin as a space truss. The truss consists of four different elements, and is divided into twelve sections of equal length (see Figure 2.2). Twelve divisions were chosen so that support, third-point, quarter-point, and midspan lateral restraints could frame into the available joints.

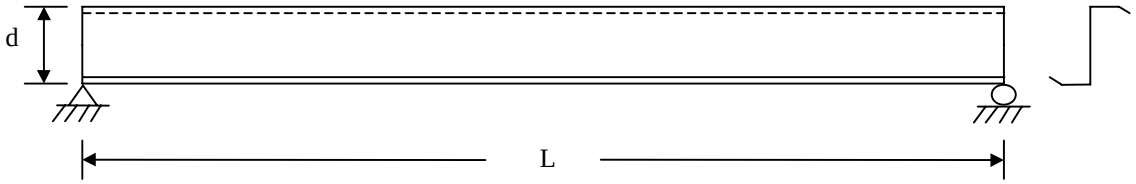

(a) Actual Purlin

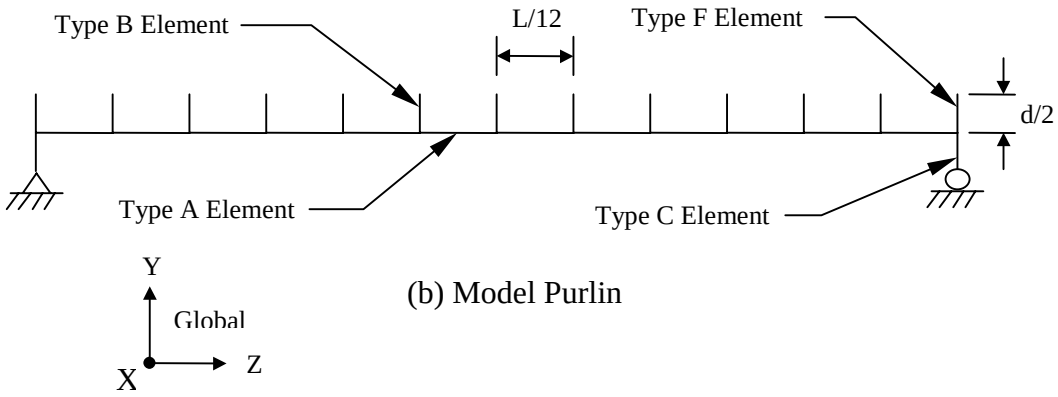

(b) Model Purlin

Figure 2.2 Purlin Modeling

The main purlin elements, oriented along the length of the purlin in the global Z direction, are type A elements. These elements are given different cross-sectional properties depending on the dimensions of the purlin that is being modeled. The section properties given in Table I-3 of the *Cold-Formed Steel Design Manual* (1996), for standard Z-sections with lips were used, with some adjustments. The nomenclature differs between the *Cold-Formed Steel Design Manual* and the current model for some properties (see Table 2.1). Notice that this comparison table pertains only to type A

elements. For this discussion, section properties given in the design manual are referred to as purlin properties, and section properties for the current model are called model properties. Model section properties directly correspond to purlin section properties, except for *J*, the torsion constant. Due to the space truss nature of the purlin model, this model property was set at $J = 10$ in^4 for all cases, to prevent the type A elements from rotating with respect to their adjoining elements. This was done because purlin bending is modeled by the type B and F elements. Had element A been given the *J* values from the *Cold-Formed Steel Design Manual*, which range from $J = 0.000120$ in^4 to $J = 0.0159$ in^4 for standard sections, extreme deformation would occur within the truss. This behavior would not be representative of actual purlins. Finally, to define the orientation of the principal axes of the purlin cross-section in the model, the local x-axis was rotated by the principal angle (refer to Figure 2.1).

Table 2.1 Nomenclature for Section Property Designations (Type A Elements)

Cold-Formed Steel Design Manual	**Current Model**
Area (in^2)	Area (in^2)
I_{x2} (in^4)	I_{yy} (in^4)
I_{y2} (in^4)	I_{zz} (in^4)
J (in^4)	J (in^4)
θ (deg)	x-Axis Rotate (deg)

Perpendicular to the type A elements are the type B and F elements, located at the ends of all twelve sections. The purpose of these elements is to model purlin web bending and connect the main purlin elements (type A) to the roof panel elements (type D). The type B and F elements have a length of half the purlin depth. Type F elements are located on the outside of each purlin line, while type B elements are located on the interior. For type B elements, the model properties are consistent with that of a *L*/12 section of purlin:

$$A = \frac{Lt}{12} \tag{2.1}$$

$$I_{zz} = \frac{Lt^3}{144} \tag{2.2}$$

where $J = I_{x2}$ of the purlin, $I_{yy} = J$ of the purlin, L is the purlin span length (in.), and t is the purlin thickness (in.). Since type F elements are on the outside of each purlin line, they have model section properties corresponding to a $L/24$ length of purlin. These properties are exactly the same as for type B elements, except that:

$$I_{zz} = \frac{Lt^3}{288} \tag{2.3}$$

For these elements, the only difference between the current model and the Elhouar and Murray model is the inclusion of type F elements. Previously, type B elements were used throughout every purlin span. Danza and Murray (1998) introduced the modification of including type F elements.

The last purlin element is type C, which connects the purlin to the rafter supports. The model section properties for this member correspond to a $L/2$ length of purlin:

$$A = \frac{Lt}{2} \tag{2.4}$$

and as before, $J = I_{x2}$ of the purlin and $I_{yy} = J$ of the purlin. However, for the current model, the last model section property is set such that $I_{zz} = 1$ for all cases, instead of the value for a $L/2$ length of purlin:

$$I_{zz} = \frac{Lt^3}{24} \tag{2.5-a}$$

Elhouar and Murray (1985) originally used Equation 2.5-a to define I_{zz} for type C elements. However, they noticed that this method allows type C elements to undergo large amounts of bending, which tended to offset the bending effects of the type B elements. This effect is described in Figure 2.3; note that type C elements are below purlin mid-height while type B elements are above it. If the type C elements are allowed to bend significantly, as in Figure 2.3(b) and Figure 2.3(c), the type A, B, and F elements are allowed to translate laterally to the left with respect to the rafter supports. When this occurs, the net displacement of the roof panel (type D elements) is reduced, because it is attached to the top of the type B and F elements. This reduced roof panel displacement

causes a reduction in the axial force in the restraints and is not representative of Z-purlin supported roof systems. Realizing this, Elhouar and Murray (1985) arbitrarily increased the z-axis moment of inertia as follows:

$$I_{zz} = \frac{Lt^3}{2} \tag{2.5-b}$$

This significantly reduced the amount of bending by type C elements, and was deemed acceptable for their analysis. This modification, though, did not eliminate all bending in type C elements as required. Setting I_{zz} equal to an arbitrarily high value, like I_{zz} = 1 in^4, virtually eliminates all of this bending. This achieves the goal of modeling the purlin such that all bending takes place in the type B elements.

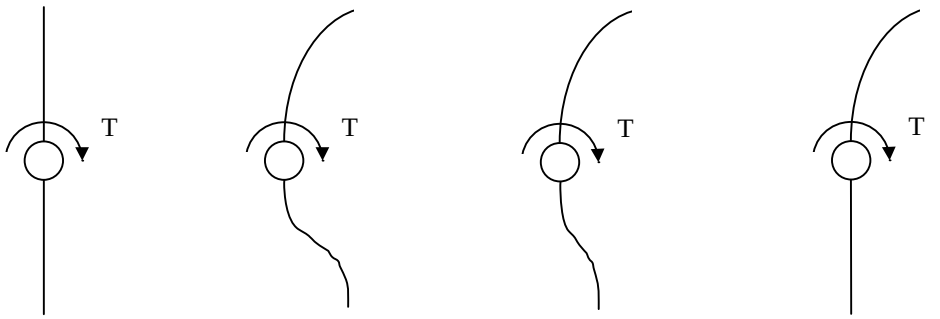

(a) Undeformed Purlin (b) Equation 2.5-a (c) Equation 2.5-b (d) I_{zz} = 1 in^4

Figure 2.3 Effect of I_{zz} in Type C Elements on Purlin Bending (Danza and Murray, 1998)

2.3.4 Modeling of Roof Panel

The two prominent methods of purlin deck fastening are standing seam and through-fastened connections. In the current model, panel bending stiffness is neglected and only shear stiffness is considered. The roof panel is modeled as a space truss, consisting of 5 ft wide sections between each purlin line, each with a series of diagonal members (see Figure 2.4). All of the elements in the roof panel have the same model section properties and are denoted as type D elements. To simulate the lack of bending

stiffness, all moments of inertia for type D elements are made as close to zero as possible: $I_{yy} = I_{zz} = J = 0.001$ in^4.

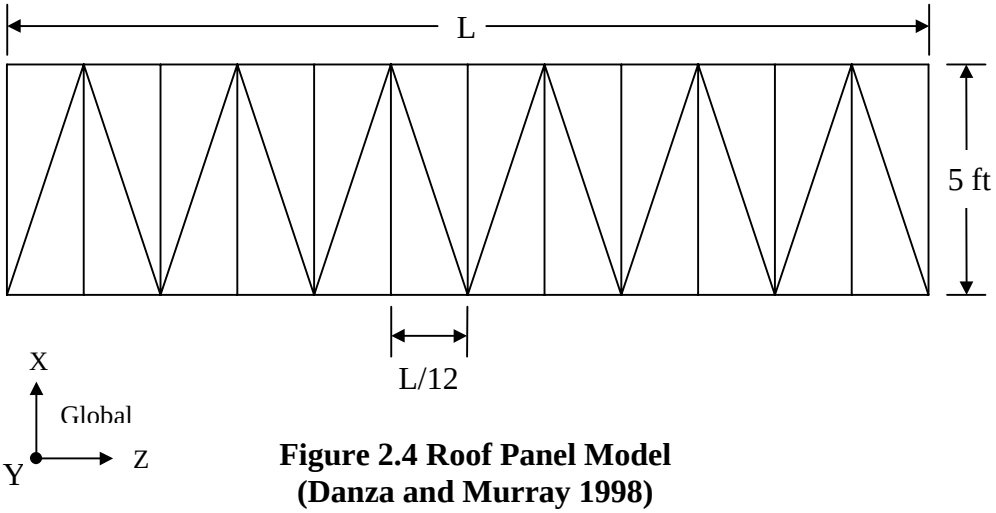

Figure 2.4 Roof Panel Model (Danza and Murray 1998)

The Elhouar and Murray model, used to develop the AISI Provisions in Section D3.2.1, had an assumed roof panel shear stiffness of 2500 lb/in. For this discussion, roof panel stiffness is defined as:

$$G' = \frac{PL}{4a\Delta} \tag{2.6}$$

where P is a point load (lb) applied at midspan of a rectangular roof panel, L is the panel's span length (ft), a is the width of the panel (5 ft for all cases), and Δ is the deflection of the panel (in.) at the location of the point load. Figure 2.5 shows the test setup to calculate panel stiffness; note that the panel has two fully pinned supports and no rollers. Experimental tests done by Ghazanfari and Murray (1983) indicated that the increase in required restraint force for systems with roof panels stiffer than 1500 lb/in. was negligible. An experimental study by Curtis and Murray (1983) determined that a panel stiffness of 2500 lb/in. should be used for all mathematical models. However, these tests only considered systems with three or fewer restrained purlin lines. This research examines how restraint force is affected by roof panel shear stiffness, considering a wide range of parameters.

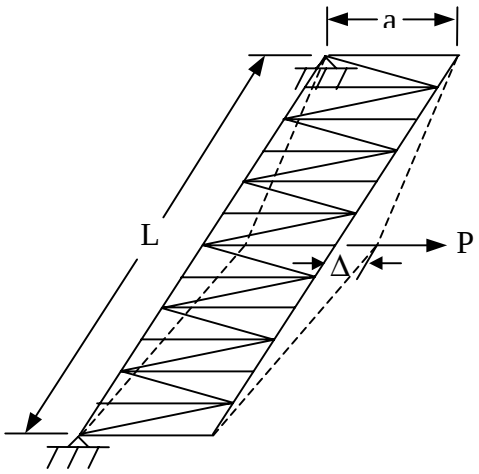

Figure 2.5 Panel Stiffness Test Setup

Despite the fact that shear stiffness is varied in this study, the value of *G'*=2500 lb/in. provides an important base point for the design equations that are formulated in Chapter III. The model section property that defines the shear stiffness of the roof panel is the area of the type D elements. Using Equation 2.6 and the test setup of Figure 2.5, the area of the type D elements corresponding to a shear stiffness of 2500 lb/in. can be obtained for any desired span length. The area values for the span lengths used in this research are presented in Table 2.2 below. Increasing the area of type D elements above the values given in Table 2.2 for each span length increases the panel shear stiffness above 2500 lb/in. Similarly, decreasing the area of these elements decreases the panel stiffness below 2500 lb/in.

Table 2.2 Area of Type D Elements for *G'* = 2500 lb/in.

Area (in^2)	Span length (ft)
0.0321	20
0.0336	25
0.0377	30
0.0437	35
0.0451	36

2.3.5 Modeling of Braces

In the current model, lateral braces for the roof system are axial load only members, and are represented by line elements. To eliminate any bending in these members, referred to as type E elements, the eave connections are given fully pinned boundary conditions, and the restraint to purlin joints are given bending pin releases. Thus, type E elements cannot support any bending moment forces. For all cases, the area of these elements was arbitrarily set at 0.333 in^2, and the element length was set at 8 in. These values are intended to represent the typical lateral restraint used in practice and to match the values used in previous studies. Since no bending resistance is required, all moments of inertia for type D elements are made as small as possible: $I_{yy} = I_{zz} = J = 0.001$ in^4.

2.3.6 Joints and Boundary Conditions

All element connections are modeled as rigid joints, except for the connection of lateral restraints to purlins, where bending pin releases were added, as previously described. This is of particular importance for the purlin to roof panel connection, where rigid joints are representing the deck fastening system. Based on the experimental findings by Rivard and Murray (1986), the restraint force equations formulated by Elhouar and Murray (1985) are applicable to both standing seam and through-fastened roof systems. Since these equations are based on a stiffness model with rigid joints, the current model developed here is appropriate for both standing seam and through-fastened roof systems.

The boundary conditions in the stiffness model are rafter supports and lateral restraint eave connections. The rafter supports (see Figure 2.6) are located at either end of every purlin span, at the base of all type C elements. As in the physical system, all translations are restrained at these boundaries. In the model, these supports are free to rotate about the global X- and Y-axes, but rotation is fixed about the global Z-axis. The Z-axis rotation is fixed because the rafter support is assumed to prevent purlin web bending about this axis. In reality, this boundary is a rotational spring, offering significant resistance to purlin web bending, but allowing for some rotation. The spring

constants needed to model the connection as a rotational spring are dependent on the type of purlins and rafters used, and are beyond the scope of this project. The effect of using fixed rotation restraint versus rotational springs is believed to be negligible.

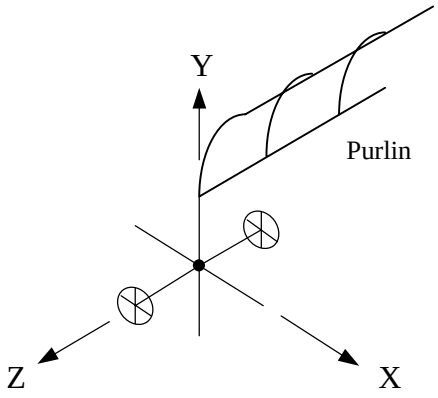

Figure 2.6 Rafter Support

The eave attachments (see Figure 2.7) for all of the lateral restraints are modeled as fully pinned connections, with all translations fixed and all rotations free. These boundaries are pinned connections so that all force in the restraint is taken up by axial load. Thus, it is conservative to ignore the bending resistance of these braces.

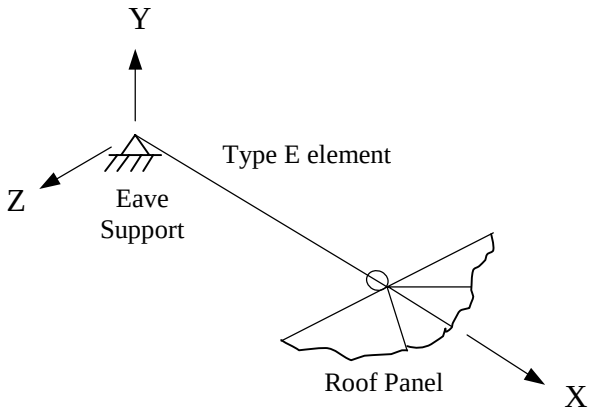

Figure 2.7 Lateral Brace Boundary Conditions

2.3.7 Model Loading

This research deals exclusively with gravity loads and does not address uplift forces. Because load modeling has a critical effect on restraint force, the loading must resemble the physical system as closely as possible. Gravity loads are represented in the current model by sets of distributed line loads and point moments acting along each purlin line. Each purlin has two distributed line loads acting on the principle axes of every type A element. The total gravity load acting on the roof system, W (lb), is distributed equally to all restrained purlin lines (including spandrels) such that the load carried by each is w = 100 plf, for all cases. The distributed load is first split into components parallel and perpendicular to the purlin web, which change depending on the slope angle of the roof:

$$w_{web} = w\cos\theta \tag{2.7}$$

$$w_{ds} = w\sin\theta \tag{2.8}$$

The distributed load acting parallel to the web, w_{web}, was then split into components along each of the principle axes of the type A elements, where the load is applied (see Figure 2.8):

$$w_y = w_{web}\cos\theta_p \tag{2.9}$$

$$w_z = w_{web}\sin\theta_p \tag{2.10}$$

The principle angle, θ_p, is defined as the angle between the purlin web and the major principle axis (refer to Figure 1.1). The distributed load acting perpendicular to the web, also known as the downslope component, w_{ds}, is applied to the type D panel elements on top of each purlin line. The load was applied there to simulate the true point of application of the downslope load to the roof system; the purlin top flange.

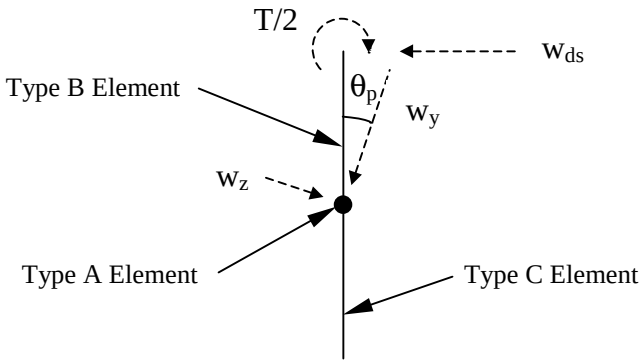

Figure 2.8 Purlin Loads

Due to roof slope and the asymmetry of the Z-purlin cross-section, purlins connected to sheathing receive an eccentric loading. The magnitude of this eccentricity, measured along the purlin top flange, determines the torque loading on each purlin line. In the physical system, the true load distribution on the purlin top flange is unknown, but for this model, a triangular load distribution was assumed (see Figure 2.9). This leads to an eccentricity of one third of the purlin flange width, as used in the studies by Elhouar and Murray (1985) and Danza and Murray (1998). A comparison of theoretical and experimental results by Ghazanfari and Murray (1983) confirmed the validity of this assumption.

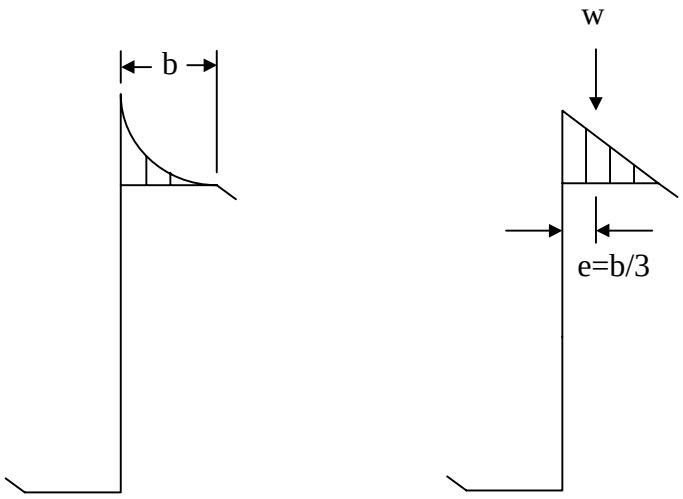

(a) True Load Distribution (b) Model Load Distribution

Figure 2.9 Flange Load Distribution

From statics, the total torque acting on each purlin span is:

$$T = \frac{b w_{web} L}{3} \tag{2.11}$$

where T is the total torque (ft-lb), b is the flange width (ft), w_{web} is given by Equation 2.7 (plf), and L is the span length (ft). A series of point moments is applied to the joints connecting the type B and F elements to the type D elements, along every purlin line. In both the Elhouar and Murray model and the Danza and Murray model, these moments were applied to the joints at both ends of the type A elements, corresponding to the purlin centroid. However, applying moments at those locations causes most of the moment to be balanced by the rafter supports, due to the high stiffness of the type C elements. This is incorrect, because the lateral braces balance much of this moment in an actual roof system. Applying moments at the purlin to roof panel connection allows these moments to be properly transferred to the restraints. Since only half of the purlin depth is flexible in the current model, the point torque must be divided in half to obtain the correct effect on lateral restraint forces. Then, the total torque is distributed equally to every joint along each purlin span (T/24), except for the outside of each purlin line, where T/48 is applied, due to a reduced tributary length.

2.3.8 Summary of Model

The current stiffness model consists of six different elements. Purlins are modeled as a space truss with type A, B, C, and F elements. A space truss of type D elements represents the roof panels, with strength in shear but not in bending. Lateral restraints are modeled with type E elements that are axial force only members. The combined system (see Figure 2.10) is a space frame, with pinned eave connections and rafter supports restricting Z-axis rotation. Model section properties for each element are given in Table 2.3. Gravity loads are approximated by a set of line loads and point moments along every purlin line.

Table 2.3: Element Section Properties

Member Type	Area (in^2)	I_{yy} (in^4)	I_{zz} (in^4)	J (in^4)
A	*A* of purlin	I_{x2} of purlin	I_{y2} of purlin	10
B	(*Lt*)/12	*J* of purlin	(Lt^3)/144	I_{x2} of purlin
C	(*Lt*)/2	*J* of purlin	1	I_{x2} of purlin
D	*f*(*G'*, *L*)	0.001	0.001	0.001
E	0.333	0.001	0.001	0.001
F	(*Lt*)/12	J of purlin	(Lt^3)/288	I_{x2} of purlin

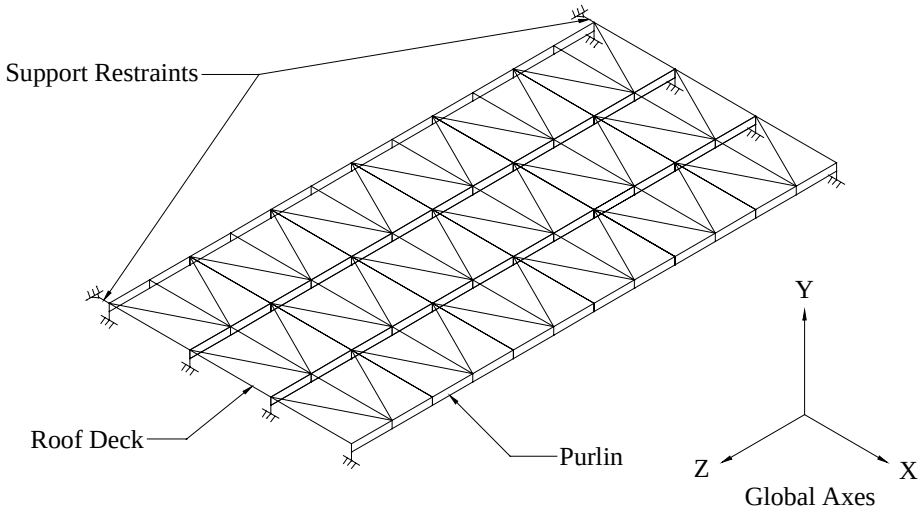

Figure 2.10 Stiffness Model
(Danza and Murray 1998)

2.4 METHOD OF SOLUTION

The stiffness models were assembled and analyzed using a commercial software program on a personal computer. The matrix method of stiffness analysis was used to solve each model case. Computational time for the models, using a 333 MHz computer, was typically two seconds for single span models and four minutes for three span models. An examples showing model input parameters and results is found in Appendix A.

2.5 VALIDATION OF MODEL TO EXPERIMENTAL RESULTS

To ensure the validity of the current modeling technique, results must be compared to those of laboratory tests. Comparison to real Z-purlin supported roof systems is essential to ensuring that the model is appropriate to predict lateral restraint forces. The stiffness models used by Elhouar and Murray (1985) and Danza and Murray (1998) were compared to full-scale tests by Curtis and Murray (1983) and quarter-scale tests by Seshappa and Murray (1985). For uniformity of comparison, the same set of tests used for comparison by Danza and Murray is presented here, with one additional test (3C/2-1). Table 2.4 gives the designations of the six tests used for comparison, along with a description of the parameters for each test.

Table 2.4 Experimental Test Parameters

Test Name	Bracing Scheme	Number of Spans	d (in.)	t (in.)	b (in.)	Purlin Lines	L (ft)
B/2-1-A	Support	1	8	0.088	2.40	2	22.25
C/2-1	Support	1	2	0.025	0.625	2	5
C/6-1	Support	1	2	0.025	0.625	6	5
3C/2-1	Support	3	2	0.025	0.625	2	5
C/2-15	Third-pt.	1	2	0.025	0.625	2	5
C/6-2	Third-pt.	1	2	0.025	0.625	6	5

All of the comparison tests are for zero slope (horizontal) roofs. The first test listed, B/2-1-A, is a full-scale test by Curtis and Murray (1983), while the remaining five tests are quarter-scale tests by Seshappa and Murray (1985). The panel shear stiffness was taken as 2500 lb/in. for all of these tests, which were then modeled accordingly. The tests in Table 2.4 provide a good means of checking model behavior with respect to number of restrained purlin lines, number of spans, purlin cross-section, and span length.

To compare laboratory test and model results, the term brace force ratio, β, is introduced. Brace force ratio represents the percentage of the total applied gravity load, W, that is transferred to the lateral restraints:

$$\beta = \frac{\sum P_L}{W} \tag{2.12}$$

where ΣP_L is the summation of the restraint forces in every brace in the system. All of the tests in Table 2.4, except for test 3C/2-1, are single span support restraints or third-point restraints, so there are only two braces per span. For these tests, the summation of brace forces is thus twice the brace force of each restraint; each restraint has an equal brace force due to symmetry. For comparison, the brace force ratio of the three span test 3C/2-1 is divided into 3C/2-1(E) (where ΣP_L is the sum of the restraint forces in the two symmetric exterior braces), and 3C/2-1(I) (where ΣP_L is the sum of the restraint forces in the two symmetric interior braces). Note this nomenclature in Table 2.5, which compares the brace force ratio results. Comparison of current model results to experimental results is very good (less than 10% difference) for the single span, support restraint tests (B/2-1-A, C/2-1, C/6-1). Correlation was not as good for the third-point restraint tests (C/2-15, C/6-2) or the three span, support restraint test (3C/2-1), but results using the current model erred on the conservative side. Table 2.5 also shows brace force ratio results for the previous models by Elhouar and Murray (1985) and Danza and Murray (1998). These models have excellent agreement with the current model, as shown by the statistical measures in Table 2.6. The current model predicts restraint forces that differ from the previous models, due to the different modeling of the roof panel (refer to Section 2.3.4) and purlin torque loading (refer to Section 2.3.7).

Table 2.5 Comparison of Brace Force Ratio Results

Test Name	Experimental Test	Elhouar and Murray Model (1985)	Danza and Murray Model (1998)	Current Model
B/2-1-A	0.22	0.21	0.21	0.23
C/2-1	0.26	0.23	0.29	0.24
C/6-1	0.19	0.17	0.18	0.20
3C/2-1(E)	0.04	0.05	-	0.07
3C/2-1(I)	0.11	0.10	-	0.15
C/2-15	0.14	0.22	0.27	0.21
C/6-2	0.13	0.17	0.22	0.20

Table 2.6 Statistics for Model Evaluation

Test Name	Ratio of Exper. Test to Current Model	Mean of All Brace Force Ratio Results	Standard Deviation	Standard Error
B/2-1-A	0.96	0.218	0.010	0.005
C/2-1	1.08	0.255	0.027	0.013
C/6-1	0.95	0.185	0.013	0.007
3C/2-1(E)	0.57	0.053	0.015	0.009
3C/2-1(I)	0.73	0.120	0.027	0.015
C/2-15	0.67	0.210	0.054	0.027
C/6-2	0.65	0.180	0.039	0.020

CHAPTER III

THEORETICAL FORMULATION OF DESIGN EQUATION

3.1 INTRODUCTION

The stiffness model presented in Chapter II is now utilized to develop design equations for the prediction of lateral restraint forces in Z-purlin supported roofs under gravity loads. The objective is to form a completely new set of equations to predict these restraint forces, intended as an alternative to the current design equations in Section D3.2.1 of the 1996 *AISI Cold-Formed Specification.* These current specification provisions have some deficiencies, including a flawed treatment of roof slope and the system effect, which will be described later. For every Z-purlin supported roof system, there is a finite range of roof slopes for which no lateral restraint is required, but the specification does not address this aspect. The provisions have a strong reliance upon statistical regression, distancing them from engineering principles. Also, the provisions are based upon an assumed roof panel shear stiffness of 2500 lb/in., ignoring the change in restraint force that occurs when panel stiffness is changed from this assumed value.

New design equations are proposed to address these deficiencies. The proposed equations accurately predict restraint forces for all the bracing configurations addressed in the research by Elhouar and Murray (1985) and Danza and Murray (1998): support, third-point, midpoint, quarter-point, and third-point plus support restraints. Figure 1.3 shows each of these bracing configurations for single span systems. The new equations also account for all of the major parameters observed in Z-purlin supported roofs, including purlin cross-section, number of purlins, number of spans, roof slope, and panel shear stiffness.

3.2 BACKGROUND

The AISI specification provisions of Section D3.2.1 are revisited here. The provisions were developed using elastic stiffness models of horizontal (flat) roofs (Elhouar and Murray, 1985) and verified by full-scale and model testing (Seshappa and Murray, 1985). For example, the predicted force in each brace for single span systems with anti-roll restraints only at the supports is:

$$P_L = 0.5(\beta W) \tag{3.1}$$

where W = the total applied vertical load (parallel to the web), and $\beta = \dfrac{0.220 b^{1.5}}{n_p{}^{0.72} d^{0.90} t^{0.60}}$.

As before, b is the flange width (in.), n_p is the number of restrained purlin lines, d is the section depth (in.), and t is thickness (in.). The restraint force ratio, β, was developed from a regression analysis of stiffness model results. To account for roof slope, the latest balloted AISI provisions for single span systems with anti-roll restraints only at the supports is:

$$P_L = 0.5(\beta \cos\theta - \sin\theta)W \tag{3.2}$$

where θ is roof slope measured from the horizontal. The terms $W\cos\theta$ and $W\sin\theta$ represent the gravity load components parallel and perpendicular to the purlin web as shown in Figure 3.1, respectively. The latter component is also referred to as the downslope component.

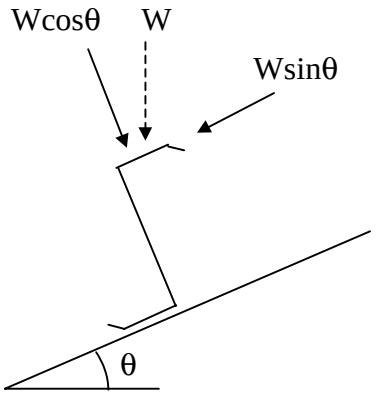

Figure 3.1 Gravity Load Components

From basic principles (Zetlin and Winter, 1955), the required restraint force is:

$$P_L = 0.5\left(\frac{I_{xy}}{I_x}\right)W \tag{3.3}$$

where I_{xy} is the product moment of inertia (in^4) and I_x is the moment of inertia with respect to the centroidal axis perpendicular to the web of the z-section (in^4). The Elhouar and Murray (1985) study showed that the restraint force given by Equation 3.3 is conservative, that is $I_{xy}/I_x > \beta$, because of system effects. Equation 3.1 can be rewritten as:

$$P_L = 0.5\alpha\left(\frac{I_{xy}}{I_x}\right)W \tag{3.4}$$

where $\alpha = \frac{I_x}{I_{xy}}\beta$ = system effect factor. Thus, the system effect is identified as a function of the AISI Specification parameter β.

The system effect is the inherent restraint in the system because of purlin web flexural stiffness and a Vierendeel truss effect caused by interaction of the purlin web with the roof panel and the rafter flange (see Figure 3.2). This Vierendeel truss action explains the relative decrease in restraint force as the number of restrained purlin lines, n_p, increases as shown in Figure 3.3. Figure 3.4 is a plot of restraint force from Equation 3.2 versus the slope angle θ. The value θ_0 is the intercept where the restraint force is equal to zero. For roof slopes less than θ_0, the AISI Specification provision, Equation 3.2, predicts a restraint force in tension. For slopes greater than θ_0, Equation 3.2 predicts the restraint force to be in compression.

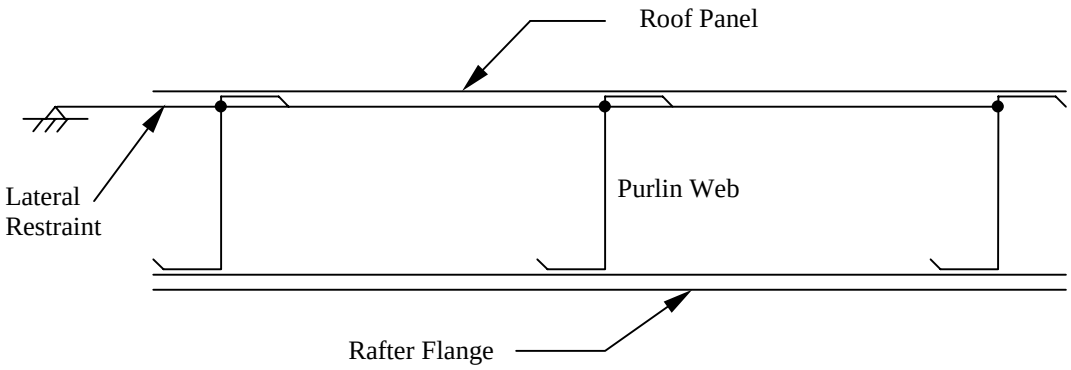

Figure 3.2 Vierendeel Truss Action

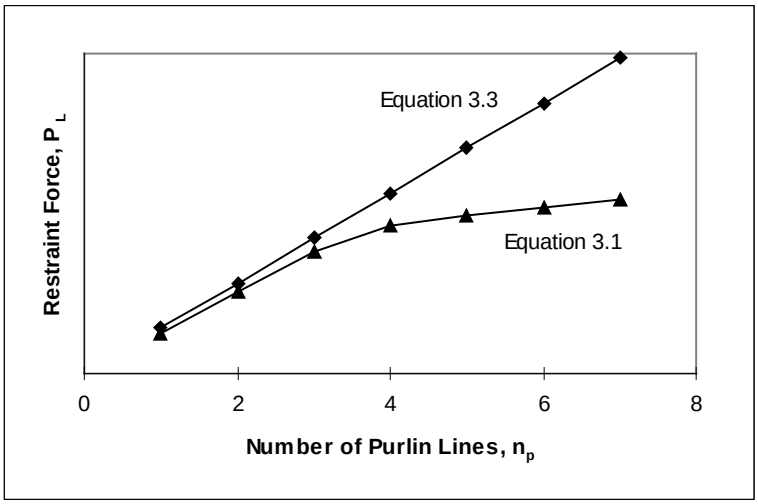

Figure 3.3 Restraint Force vs. Number of Purlins

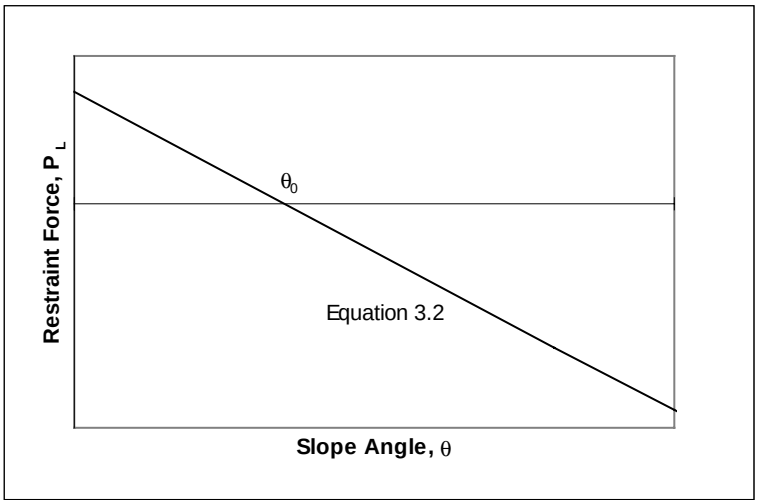

Figure 3.4 Restraint Force vs. Roof Slope (Typical)

Equation 3.2 has a flawed treatment of both the system effect and roof slope, because two important effects are not taken into account. First, the internal system effect applies to both the fictitious force $W\cos\theta(I_{xy}/I_x)$ and the real force $W\sin\theta$. Second, the system effect reverses when the net restraint force, as shown in Figure 3.5, changes from tension to compression with increasing slope angle. As a result of these effects, the intercept value θ_0 is in actuality dependent only on purlin cross-sectional properties, not n_p or the bracing configuration. However, Equation 3.2 has θ_0 dependent on β, which is a function of both n_p and the bracing configuration:

$$\theta_0 = \tan^{-1}\beta \tag{3.5}$$

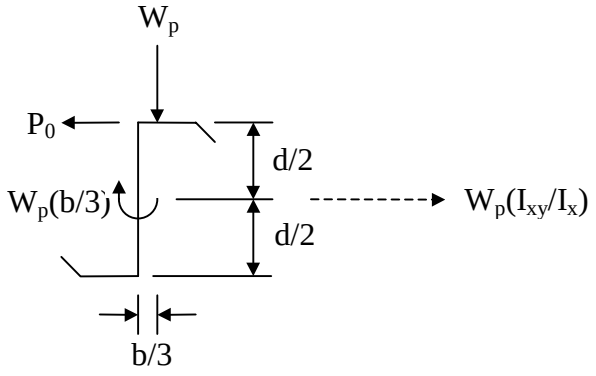

(a) Forces for a Single Purlin on a Flat Roof

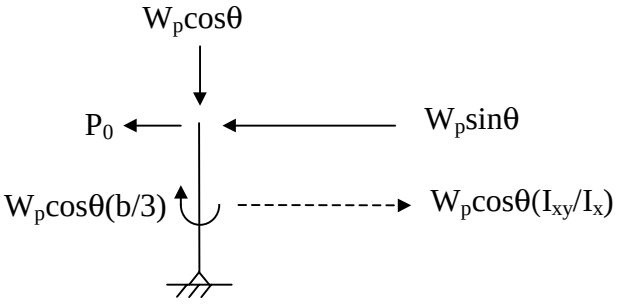

(b) Forces for a Single Purlin on a Sloped Roof

Figure 3.5 Single Purlin Gravity Loads

As mentioned in Section 2.3.4, the Elhouar and Murray stiffness model used to develop the AISI Provisions had an assumed roof panel stiffness of 2500 lb/in. Computer tests run by Elhouar and Murray (1985) indicated that the increase in required restraint force for systems with roof panels stiffer than 2500 lb/in. was negligible. However, these tests only considered systems with three or fewer restrained purlin lines. After examining stiffness models of roof systems with up to eight restrained purlins, results showed that increasing panel stiffness above 2500 lb/in. caused significant increases in the required restraint forces for systems with four or more purlin lines. Thus, the AISI Specification should be modified to address roof panels with varying shear stiffness values.

3.3 EQUATION DEVELOPMENT

3.3.1 Form of Equation

To develop a more accurate set of equations to predict the lateral restraint force in Z-purlin roof systems, the following form was assumed:

$$P_L = P_0 C_1 \left(n_p^* \alpha + n_p \gamma \right) \tag{3.6}$$

where P_0 is the restraint force on a single purlin system, C_1 is the brace location factor, α is the system effect factor, and γ is the panel stiffness factor. The parameter n_p is the number of parallel purlin lines located between restraint anchors. The parameter n_p^* is closely related to n_p as will be described later. Equation 3.6 postulates that the predicted restraint force in any given system is equal to the force on a single purlin multiplied by the total number of purlins, a brace location factor, a reduction factor caused by system effects, and modified by a factor for roof panel stiffness. This equation was formulated by first considering a roof panel stiffness of 2500 lb/in. to obtain a base point along the restraint force versus panel stiffness curve (see Figure 3.6). Notice that Figure 3.6 is shown with panel stiffness in a logarithmic scale. Thus, when G' = 2500 lb/in., $\gamma = 0$ and Equation 3.6 reduces to:

$$P_L = P_0 C_1 n_p^* \alpha \tag{3.7}$$

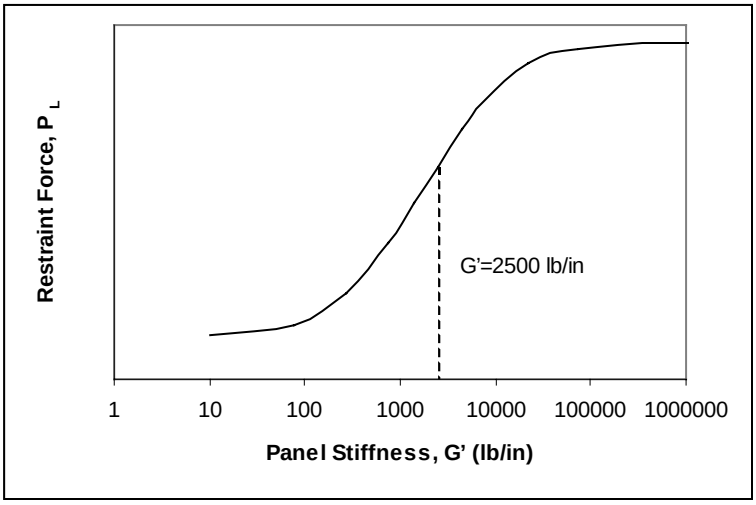

Figure 3.6 Restraint force vs. Panel Stiffness (Model)

3.3.2 Single Purlin Restraint force

To predict the base point restraint force, the diagrams in Figure 3.5 are now used to develop an expression for P_0, which considers the proper application of the system effect and its reversal. The key assumption to this model is that the purlin has a pinned support at the rafter connection. Figure 3.5(a) shows the Z-purlin with a gravity load W_p and zero slope. W_p is the total gravity load (force units) acting on each purlin span:

$$W_p = wL \tag{3.8}$$

where w is the distributed gravity load on each purlin (force/length units) and L is the span length (length units). The fictitious force $W_p(I_{xy}/I_x)$ is the overturning force from basic principles (Zetlin and Winter, 1955).

Figure 3.5(b) shows the set of real and fictitious forces associated with a single purlin on a roof with slope θ. The set of forces account for the following effects: $W_p \sin\theta$ is the downslope component of the gravity loading, $W_p \cos\theta\,(I_{xy}/I_x)$ is the fictitious force as previously discussed, and $W_p \cos\theta (b/3)$ is the torque induced by eccentric loading of the top flange. As with the stiffness model, this static analysis assumes the eccentricity of loading to be one third of the flange width. Here, however, the torque

loading is applied at the centroid of the cross-section as per basic mechanics. Summation of moments about the pinned support results in:

$$P_0 = \left[\left(\frac{I_{xy}}{2I_x} + \frac{b}{3d}\right)\cos\theta - \sin\theta\right]W_p \tag{3.9}$$

which is valid if P_0 is positive (tension) or negative (compression). Equation 3.9 can be solved for the intercept slope angle, where restraint force is zero:

$$\theta_0 = \tan^{-1}\left(\frac{I_{xy}}{2I_x} + \frac{b}{3d}\right) \tag{3.10}$$

Thus, the intercept is dependent only on purlin cross-sectional properties as required. For roof slopes less than θ_0, P_0 is in tension, and for roof slopes greater than θ_0, P_0 is in compression.

3.3.3 System Effect Factor, α

When Elhouar and Murray (1985) used regression analysis to derive Equation 3.4, they assumed that the system effect factor, α, was dependent on the following parameters: I_{xy}, I_x, b, n_p, d, and t. However, if the system effect is taken to be caused purely by purlin bending resistance, then only the parameters n_p, d, and t should affect α. Statistical analysis, based on stiffness model results, was used to develop a new equation for α:

$$\alpha = 1 - C_2\left(\frac{t}{d}\right)\left(n_p^* - 1\right) \tag{3.11}$$

where C_2 is a constant factor that depends on the bracing configuration. Note that α is a dimensionless factor and α=1 when n_p^* =1, as needed for consistency. Since α is a multiplicative factor in Equation 3.6, it accurately models the reversal of the system effect when P_0 changes from tension to compression.

For a rational basis to Equation 3.11, consider a purlin to be a cantilevered, rectangular beam with a point load acting at the free end (see Figure 3.7). The deflection of such a beam is proportional to the ratio $(d/t)^3$. Since α is a measure of bending resistance, it would naturally be assumed to vary with $(t/d)^3$. This does not consider the

effects of panel restraint, though. Elastic stiffness model results indicate a complex relationship between α and n_p, which can be reasonably approximated by giving the slope of α a linear variation with (t/d).

$$\Delta = \frac{Pd^3}{3EI} \propto \frac{d^3}{t^3}$$

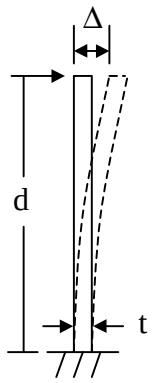

Figure 3.7 Purlin Web Bending

The coefficient C_2 in front of (t/d) in Equation 3.11 was determined from a regression analysis, and is discussed further in Chapter IV. This coefficient differs for each bracing configuration because bending resistance changes depending on a brace's distance from rafter supports and other braces. The values determined for C_2 are presented later in Table 4.10.

3.3.4 Definition of n_p^*

At this point, the variable n_p^* must be explained. Observe that Equation 3.7 is quadratic with respect to n_p, because α is linear in n_p. Thus, for some value of n_p, denoted as $n_{p(max)}$, P_L will reach a maximum point and then decrease as n_p is increased above $n_{p(max)}$. From basic calculus, $n_{p(max)}$ can be determined:

$$n_{p(\max)} = 0.5 + \frac{d}{2C_2 t} \tag{3.12}$$

For very thick purlins, $n_{p(max)}$ can be significantly less than eight, the maximum number of restrained purlin lines for which the proposed equations were initially formulated. Obviously, the required bracing force can never decrease as the number of purlins is

increased. This concern can be eliminated by using n_p^* instead of n_p in Equation 3.7, where n_p^* is defined as the minimum of $n_{p(max)}$ and n_p. This means that adding additional restrained purlin lines above $n_{p(max)}$ will not affect the predicted restraint force; P_L will remain constant (see Figure 3.8).

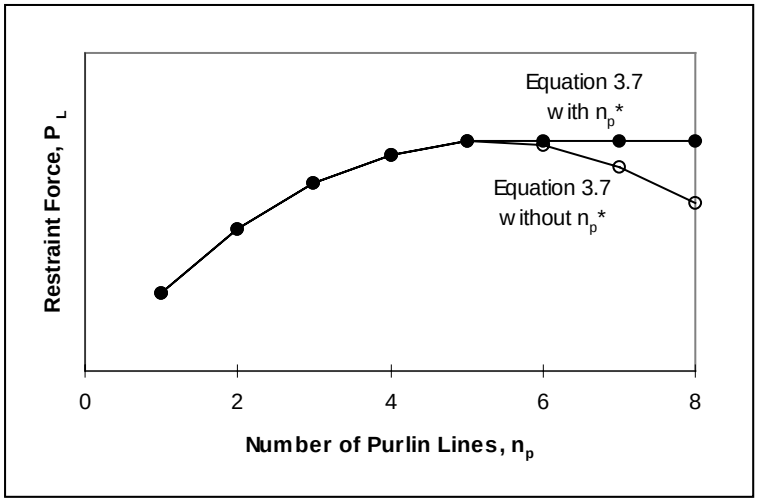

Figure 3.8 Effect of Using n_p^*

3.3.5 Brace Location Factor, C_1

Another key aspect to Equation 3.6 is C_1, the brace location factor. This constant factor represents the percentage of total restraint that is allocated to each brace in the system. By this logic, it is expected that the sum of the C_1 coefficients for each brace in one purlin span length is equal to unity. However, the rafter supports absorb some of the bracing for the gravity load, so this sum is less than unity for some bracing configurations. The sum is also slightly greater than unity for some configurations where a slight factor of safety was required to account for uncertainty in the results. The values for C_1 were determined from a regression analysis and are discussed further in Chapter IV. These values are given for various bracing schemes in Table 4.10. Notice that for multiple span systems, the C_1 values are larger for exterior restraints than the corresponding interior restraints, as expected from elementary mechanics.

3.3.6 Panel Stiffness Modifier, γ

Equation 3.7 establishes the restraint force for the base point of G' = 2500 lb/in. To extend Equation 3.7 to the general form in Equation 3.6, a panel stiffness modifier, γ, is included. After analyzing several different cases, lateral restraint force was shown to vary linearly with the common logarithm of the roof panel stiffness over the range of common panel shear stiffnesses (refer to Figure 3.9). This lead to the following equation for the panel stiffness modifier:

$$\gamma = C_3 \log\left(\frac{G'}{2500}\right) \tag{3.13}$$

where G' is the roof panel shear stiffness (lb/in.), and C_3 is another constant determined by regression analysis of stiffness model results. In Equation 3.13, the denominator constant of 2500 has units of lb/in. to nondimensionalize the term in the log parentheses when G' is in units of lb/in. Equation 3.13 can be used for any units of G', if the denominator constant is first converted from lb/in. to the desired units.

Equation 3.6 is therefore based upon the point-slope method of writing the equation of a line. For roof panels stiffer than the base point value, the required restraint force is increased, and for panels less stiff than the base value, the required restraint force is decreased. Note that $\gamma = 0$ for G' = 2500 lb/in., $\gamma > 0$ for $G' > 2500$ lb/in., and $\gamma < 0$ for $G' < 2500$ lb/in. The values of C_3 are tabulated for various bracing schemes in Chapter IV. The location of a brace with respect to rafter supports and other braces determines how the restraint force varies with roof panel stiffness. The effect of γ is to adjust the system effect factor, α. Notice in Equation 3.6 that γ is multiplied by n_p instead of n_p^*, because as panel stiffness changes, change in restraint force depends on the total number of purlins in the system and $n_{p(max)}$ no longer applies. A roof panel with infinite shear stiffness would transfer all lateral forces to the restraints.

To utilize the panel stiffness modifier, two restrictions are required. First, γ is valid only for 1000 lb/in. $\leq G' \leq$ 100,000 lb/in. This is the range of linear behavior, and most roof panels have a shear stiffness within this limitation. Secondly, a maximum restraint force is set, which can never be exceeded. This maximum force is:

$$\left|P_L\right| \le \left|P_0 C_1 n_p\right| \tag{3.14}$$

and is the expected restraint force if system effects are ignored. Equation 3.14 applies to both tensile and compressive restraint forces. See Figure 3.9 for a typical plot of restraint force versus panel stiffness for Equation 3.6, shown with stiffness model results.

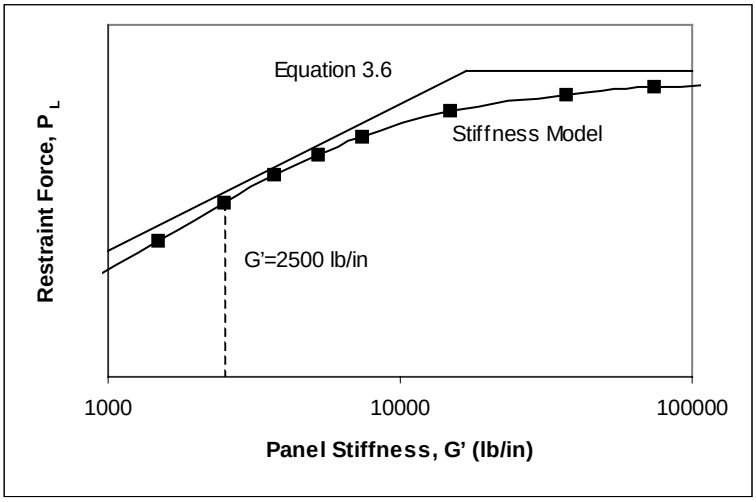

Figure 3.9 Restraint Force vs. Panel Stiffness (Proposed)

3.3.7 Restrictions

Restrictions must be placed on Equation 3.6 to make it applicable for design purposes. Since the stiffness models used to confirm the equation had eight restrained purlin lines or fewer, Equation 3.6 must be used with caution when $n_p > 8$. The proposed equation is believed to apply to the design of lateral restraints in roof systems with $n_p > 8$, but further computer testing is needed for verification. When Equation 3.6 gives a very small predicted magnitude of restraint force, $\left|P_L\right| \le 100$ lb, no lateral bracing is necessary. For every Z-purlin supported roof system, there is a range of roof slopes that corresponds to $\left|P_L\right| \le 100$ lb, and roofs systems having a roof slope within this range require no lateral restraint.

3.3.8 Summary of Design Equation

The proposed design equations accurately predict the lateral bracing forces required for Z-purlin supported roof systems, for five different bracing configurations. The equation is summarized in Figure 3.12 below, where I_{xy} is product moment of inertia, I_x is x-axis moment of inertia, b is purlin flange width, d is purlin depth, t is purlin thickness, w is distributed purlin gravity load, L is purlin span length, θ is roof slope, n_p is number of restrained purlin lines, and G' is roof panel shear stiffness. The required restraint force in any roof system equals the force on a single purlin multiplied by the number of restrained purlin lines, a brace location factor, a system effect factor, and modified by a factor for roof panel shear stiffness. The design equation addresses the deficiencies of the current AISI provisions. The treatment of roof slope and the system effect is more accurate. The proposed equations, while still depending on regression analysis, have a stronger basis in engineering principles. The new design equation accounts for roof panels of different shear stiffness, and identifies the conditions for which no lateral bracing is required. Figure 3.10 shows a typical plot comparing the proposed Equation 3.7 to the AISI Specification, Equation 3.2 with respect to slope angle θ. Figure 3.11 shows a similar plot with respect to the number of restrained purlin lines.

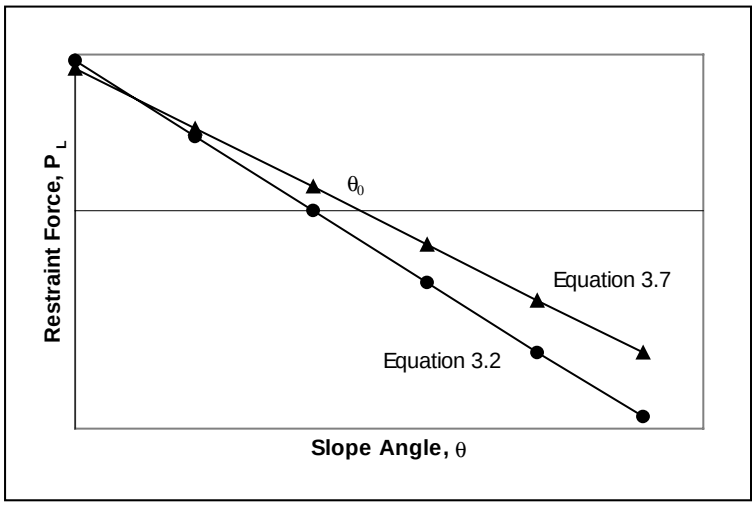

Figure 3.10 Comparison of Restraint Force vs. Roof Slope

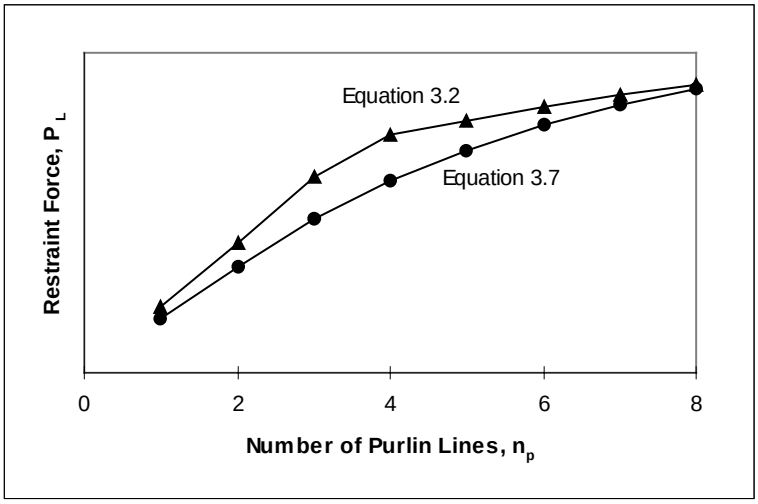

Figure 3.11 Comparison of Restraint Force vs. Number of Restrained

$$P_L = P_0 C_1 \left(n_p^* \alpha + n_p \gamma \right)$$

where:

$$P_0 = \left[\left(\frac{I_{xy}}{2I_x} + \frac{b}{3d} \right) \cos\theta - \sin\theta \right] W_p, \qquad W_p = wL$$

$$n_p^* = \min\left\{ n_p, n_{p(\max)} \right\}, \; n_{p(\max)} = 0.5 + \frac{d}{2C_2 t}$$

$$\alpha = 1 - C_2 \left(\frac{t}{d} \right) \left(n_p^* - 1 \right), \; \gamma = C_3 \log\left(\frac{G'}{2500} \right)$$

Notes:

1) Positive P_L is in tension, negative P_L is in compression.
2) Upper bound: $\left| P_L \right| \le \left| n_p P_0 C_1 \right|$
3) If $\left| P_L \right| \le 100\,\text{lb}$, no lateral bracing is necessary.
4) Applicable range of panel stiffnesses:
   $1000\,\text{lb/in} \le G' \le 100{,}000\,\text{lb/in}$
5) C_1, C_2, and C_3 are regression coefficients.
6) Models used to develop procedure had $n_p \le 8$.

Figure 3.12 Summary of Design Equation

CHAPTER IV

COMPUTER TESTS AND EQUATION DEVELOPMENT

4.1 INTRODUCTION

This chapter discusses the different computer tests performed on the finite element model, and the data analyses used to further develop the design equation. The objective is to fit the theoretical design equation described in Chapter III to the mathematical stiffness model described in Chapter II. An investigation into roof system behavior is made, determining the effect of each parameter upon the required lateral restraint forces. Then, a computer test matrix is developed to define the range of investigation for each parameter. The results of the computer tests are then fit to the proposed design equations using regression analysis. This statistical regression evaluates the coefficients C_1, C_2, and C_3 of the proposed design equations for each bracing configuration. There is also a discussion on the correlation of the resulting final design equation to the stiffness model. Finally, the proposed design equation is verified for the effects of roof slope and roof panel stiffness interaction.

4.2 SYSTEM BEHAVIOR ANALYSIS

Extensive studies on the system behavior of various Z-purlin roof parameters were done by Elhouar and Murray (1985) and Danza and Murray (1998). Each of these analyses investigated the effects of the following parameters on restraint forces: bracing configuration, purlin depth, purlin thickness, purlin flange width, span length, number of restrained purlin lines, and number of spans. Both studies are based upon the lateral restraint forces given by elastic stiffness models. A system behavior analysis is now done using the current model, and the findings are compared to the two previous studies.

4.2.1 Bracing Configuration

Elhouar and Murray (1985) found that "Lateral restraint forces can not be mathematically related to the bracing configuration used and therefore each configuration must be considered separately." Results of the current model, as well as the Danza and Murray model, support this conclusion. The complex system interaction between purlin, roof panel, and restraint makes such a simple mathematical relation impossible. Thus, a separate regression analysis, with different resulting coefficients in the proposed design equation, must be performed for each bracing configuration.

4.2.2 Number of Spans

The cross-sectional shape of Z-purlins allows them to be easily lapped to create continuous spans. The observed restraint forces in a continuous span system can be quite different from those in a single span system under the same loading. Elhouar and Murray (1985) discovered that the brace force ratio, β, decreases significantly (12% to 30%) when the number of spans is increased from one to three, but does not change significantly as the number of spans is increased greater than three. Because of this analysis, two sets of coefficients were developed for the design equations; one for single span systems and one for multiple span systems. A three continuous span model was used to generate the multiple span coefficients in the design equation. The three span model was used because the restraint force results are conservative for systems with more than three continuous spans, and acceptable for two span systems.

Similarly, Danza and Murray (1998) developed design equations for single and multiple span systems, with a three span model representing the multiple span case. The same reasoning is used here to develop the proposed design equations. Regression analysis is used to determine different values of the coefficients C_1, C_2, and C_3 for single and multiple span systems. However, the present system analysis found that restraint forces for braces on the exterior of multiple span systems were almost the same (0% to 10% less) as restraint forces for braces in the same position on single span systems, under the same loading. The primary difference between single and multiple span systems was the restraint force for interior braces on multiple span systems. These braces usually

provide lateral restraint for a different length of purlin than in the single span case, thus causing the difference in restraint force.

4.2.3 Number of Restrained Purlin Lines

Due to the system effect, the required bracing force decreases as the number of restrained purlin lines is increased. As mentioned in Section 3.2, purlin web bending resistance, along with a Vierendeel truss action (between purlin, roof panel, and rafter), causes this effect. The system behavior analyses by Elhouar and Murray (1985) and Danza and Murray (1998) confirmed this finding, and discovered that the reduction in brace force can reach 70% for some cases. Analysis of the current model also agreed with the finding that increasing the number of purlins decreases the restraint force ratio. However, the current model showed that the magnitude of this reduction was a function of other parameters, specifically purlin depth and thickness.

4.2.4 Purlin Span Length

Elhouar and Murray (1985) discovered that varying span length had a negligible effect on the required restraint force for single span systems, and hence span length does not appear in the design equations. They did find that increasing span length increased the required restraint force for multiple span systems, often by 10% or more. Their design equations note a small dependence on span length, with the brace force ratio being proportional to up to $L^{0.25}$ for third-point restraints in multiple span systems. The system behavior analysis by Danza and Murray (1998) found that increasing purlin span length increased the required restraint force for both single and multiple span systems, with greater increases noted in multiple span systems.

Analysis of the current model found a slight increase in restraint force as span length is increased, but the effect is negligible (less than a 10% increase) and does not merit inclusion in the proposed design equations. See Table 4.1 for examples of the variation in brace force ratio with purlin span length, for three span models. In the table, β_1 is the brace force ratio corresponding to L_1, and β_2 is the brace force ratio corresponding to L_2. Note that all of the examples are for models with eight restrained purlin lines, zero roof slope, and the purlin section identifications are those used in the

Cold-Formed Steel Design Manual (1996). The effect of span length is only significant for interior braces in multiple span systems, and is accounted for in the proposed design equation by adjusting the regression coefficients such that a factor of safety is included. The small increase in accuracy that would result from including span length in the design equation is outweighed by the complication to the equation that would result. Thus, the only effect of span length on the proposed equation is to increase the applied gravity load, and there is no contribution to system effects.

Table 4.1 Effect of Span Length on Restraint Force

Purlin Section	Bracing Configuration	L_1 (ft)	β_1	L_2 (ft)	β_2
8ZS2.5x060	Support Restraints	20	0.120	25	0.127
8ZS2.5x090	Support Restraints	20	0.090	25	0.096
10ZS3x075	Support Restraints	30	0.120	35	0.129
10ZS3x135	Support Restraints	30	0.073	35	0.079
8ZS2.5x060	Third-point Restraints	20	0.155	25	0.161
8ZS2.5x090	Third-point Restraints	20	0.134	25	0.140
10ZS3x075	Third-point Restraints	30	0.151	35	0.163
10ZS3x135	Third-point Restraints	30	0.118	35	0.130

4.2.5 Purlin Depth, Thickness, and Flange Width

Elhouar and Murray (1985) investigated several purlin dimensions and section properties, and found purlin depth, thickness, and flange width to have significant effects on the required restraint force. They found that increasing purlin depth and thickness decreases lateral restraint forces, and increasing flange width increases restraint forces. The study by Danza and Murray (1998) found similar results, except that purlin thickness was shown to have a much greater effect on restraint forces. The difference in brace force ratio between relatively thick and relatively thin purlins was found to be up to 20%.

The proposed model also showed these same effects with respect to purlin dimensions. The key parameter in determining the restraint force was found to be the ratio of purlin thickness to depth. As the t/d ratio increases, the lateral restraint force in the system decreases (see Figure 4.1). Figure 4.1 compares the brace force ratio for

single span systems with support restraints, for different values of *t*/*d*. Note that other section properties are varied for each purlin tested, including the moments of inertia. The purlin identifications are given later in Section 4.3. Increasing purlin depth increases the lateral restraint force, because purlin web bending resistance is decreased. Similarly, increasing purlin thickness decreases restraint force because purlin web bending resistance is increased. Increasing flange width increases the restraint force due to the increased torque loading.

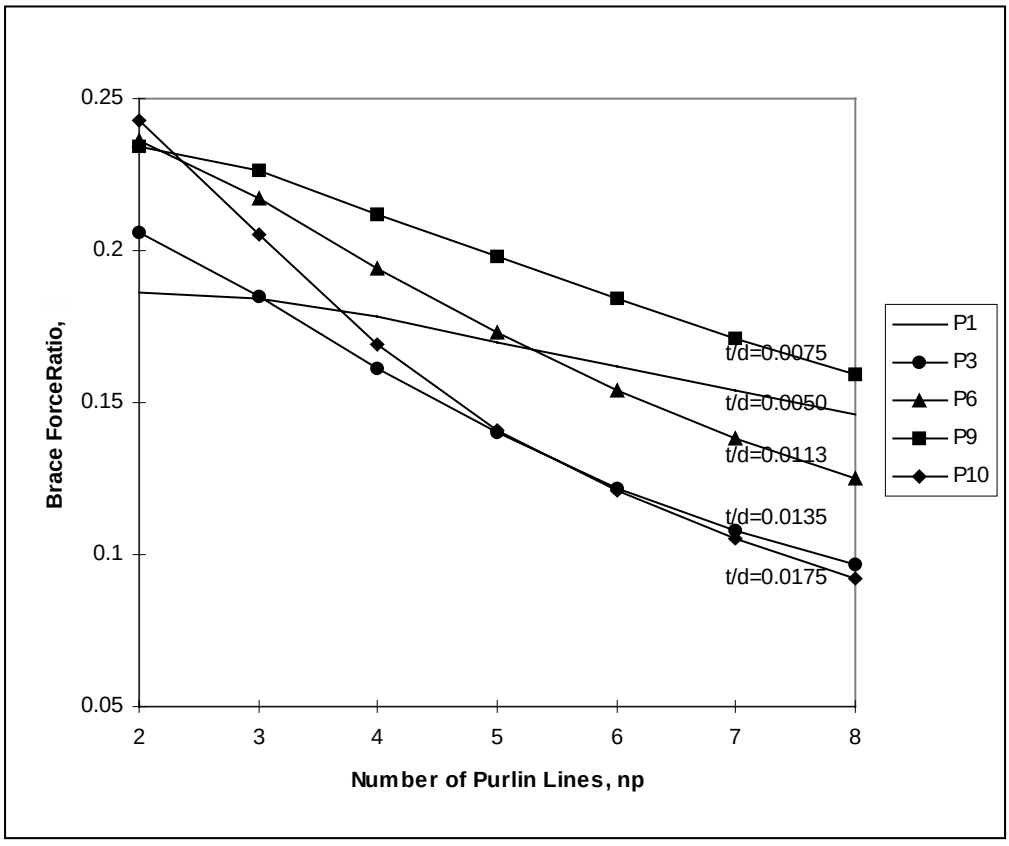

Figure 4.1 Effect of *t*/*d* on Restraint Force

4.2.6 Purlin Moments of Inertia

The previous system behavior analyses did not consider the effects of the moments of inertia I_x and I_{xy} of the purlin cross-section. Analysis of the current model, however, shows that increasing the ratio of I_{xy}/I_x increases the required restraint force. The cause of this effect is the increase in the fictitious force, $W_p \cos\theta (I_{xy}/I_x)$ (see Figure 3.5), resulting from the asymmetry of the cross-section. Figure 4.2 shows an example of this effect, for the case of single span support restraints. The two purlins (see Section 4.3 for purlin identifications) being compared in the figure have the same t/d ratio, to isolate the effect of I_{xy}/I_x on restraint force.

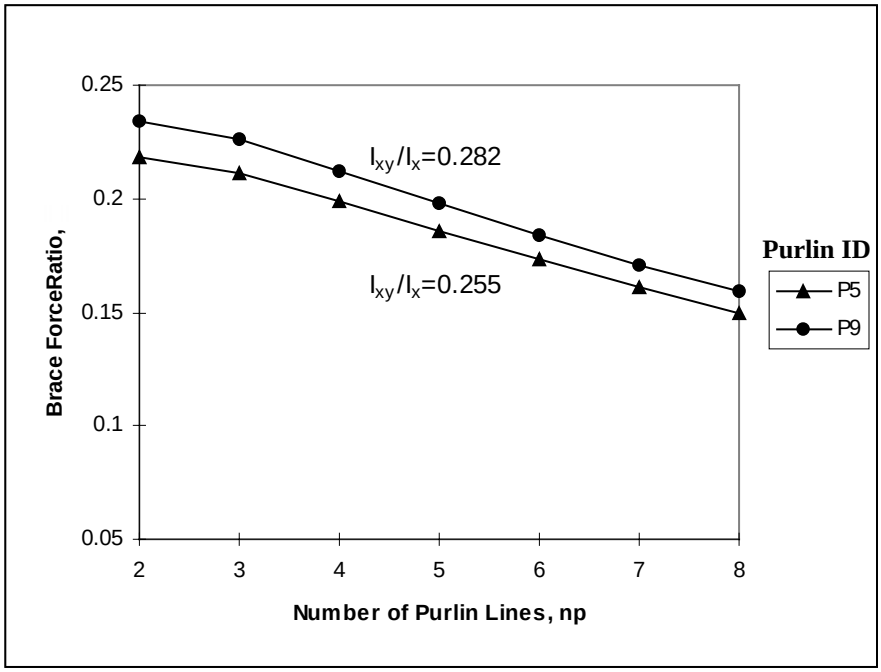

Figure 4.2 Effect of I_{xy}/I_x on Restraint Force

4.2.7 Roof Slope

Elhouar and Murray (1985) did not include roof slope in their parametric study, but instead accounted for roof slope through an adjustment based on a series of five experimental tests on quarter-scale models by Seshappa and Murray (1985). Equation

1.3 was used to correct the design equations for the effect of roof slope. They noted that as roof slope increases, the restraint force changes from tension to compression in a linear fashion with respect to $\tan\theta$. The intercept slope angle, the angle where the restraint force is zero, is given by Equation 3.5, and is a function of the number of restrained purlin lines and the bracing configuration, in addition to purlin cross-sectional properties. Equation 1.3 and Equation 3.5, in that order, are repeated here for convenience:

$$P_L = P_{L_O} - W \tan\theta \tag{4.1}$$

$$\theta_0 = \tan^{-1}\beta \tag{4.2}$$

System behavior analysis of the current model determined that, like the previous study, restraint force changes from tension to compression as roof slope increases. The manner of this variation, however, was not found to agree with Equation 1.3. The theoretical Equation 3.9 was much more accurate in predicting the required restraint force. The intercept slope angle is then given by Equation 3.10, which is dependent only upon purlin cross-sectional properties and remains constant for any number of restrained purlin lines. Equation 3.9 and Equation 3.10, in that order, are repeated here for convenience:

$$P_0 = \left[\left(\frac{I_{xy}}{2I_x} + \frac{b}{3d}\right)\cos\theta - \sin\theta\right]W_p \tag{4.3}$$

$$\theta_0 = \tan^{-1}\left(\frac{I_{xy}}{2I_x} + \frac{b}{3d}\right) \tag{4.4}$$

Table 4.2 compares the current stiffness model results to the values of the slope intercept angle predicted by Equations 3.5 and 3.10. The table compares results from single span, support restraint systems with four or eight restrained purlin lines. Linear interpolation was used to determine the intercept slope angles for the current stiffness model. Notice that the current model results show no significant change in the intercept slope angle for n_p=4 versus n_p=8. The intercept slope angles given by Equation 3.10, for all values of n_p, are very close to the stiffness model results; the maximum difference is 1.13 degrees for purlin P10 (purlin identifications are given in Section 4.3) with eight

restrained purlin lines. The intercept slopes given by Equation 3.5 tend to be lower than the model results by several degrees when n_p=8. However, the intercept slopes given by Equation 3.5 are often higher than the model values when n_p=4. Thus, the dependence of Equation 3.5 upon the number of restrained purlin lines is not representative of the current model behavior.

Table 4.2 Slope Intercept Comparison

Purlin ID	Slope Intercept (degrees)				
	Stiffness Model		Equation 3.5		Equation 3.10
	n_p=4	n_p=8	n_p=4	n_p=8	
P1	11.02	11.19	15.35	9.46	11.29
P3	11.99	11.96	10.00	6.11	12.73
P5	12.63	12.61	14.09	8.67	12.80
P7	13.69	13.63	11.81	7.24	13.74
P9	13.50	13.45	14.94	9.20	13.77
P10	14.31	14.16	10.02	6.12	15.29

4.2.8 Roof Panel Stiffness

As noted previously, the models used by Elhouar and Murray (1985) and Danza and Murray (1998) assumed a value of 2500 lb/in. for roof panel shear stiffness. Thus, panel stiffness was not included in their system behavior analyses. Analysis of the current model showed that restraint force increases significantly as roof panel shear stiffness increases. The increase in restraint force is approximately linear with respect to the common logarithm of panel stiffness, over the range of typical roof panel stiffnesses. Section 3.3.6 has a full discussion of the effect of roof panel shear stiffness upon lateral restraint forces.

4.3 DEVELOPMENT OF COMPUTER TEST MATRIX

Taking note of the parameters affecting required restraint forces in Z-purlin supported roof systems, a computer test matrix was developed. All of the tests in the matrix were then analyzed using the current elastic stiffness model. Five different lateral bracing configurations were examined (refer to Figure 1.3): support, third-point,

midpoint, quarter-point, and third-point plus support restraints. Separate equations are necessary for single and multiple span conditions, so a one span and a three span model were created for each bracing configuration.

A total of ten different purlins were selected for the computer test matrix. The dimensions of these purlins are given in Table 4.3 and the corresponding section properties are shown in Table 4.4. The test purlins have six different cross-sections and five different span lengths. Purlin depth ranges from 6 in. to 12 in., flange width ranges from 2 in. to 3.25 in., thickness varies from 0.060 in. to 0.135 in., and span length varies from 20 ft to 36 ft. These purlin dimensions were chosen as being representative of the typical range of purlins used in industry. Span lengths were selected to be appropriate for use with each section depth. Notice that the sections 10ZS3x135, 10ZS3x075, 8ZS2.5x090, and 8ZS2.5x060 each have two different span lengths. Two different purlin thicknesses were chosen for the 8 in. and 10 in. deep purlins, to examine the effects of varying the thickness to depth ratio. Flange width was not varied independently of depth, however, due to the use of standard sections. The purlins P1 and P10 were selected to represent extreme cases; P1 is a very thin and deep purlin (t/d = 0.005) while P10 is a very thick and shallow purlin (t/d = 0.0175). These extreme cases are included to ensure that the design equations accurately predict restraint forces for any typical purlin section and span length. Notice also in Table 4.4 that the I_{xy}/I_x ratio is different for each of the six purlin sections used, to determine the effects of this parameter on restraint forces. Complete section properties for each of the purlin cross-sections are found in the *Cold Formed Steel Design Manual* (1996).

Table 4.3 Purlin Dimensions

ID	Section	d (in.)	b (in.)	t (in.)	L (ft)
P1	12ZS3.25x060	12	3.25	0.060	36
P2	10ZS3x135	10	3.00	0.135	35
P3	10ZS3x135	10	3.00	0.135	30
P4	10ZS3x075	10	3.00	0.075	35
P5	10ZS3x075	10	3.00	0.075	30
P6	8ZS2.5x090	8	2.50	0.090	25
P7	8ZS2.5x090	8	2.50	0.090	20
P8	8ZS2.5x060	8	2.50	0.060	25
P9	8ZS2.5x060	8	2.50	0.060	20
P10	6ZS2x105	6	2.00	0.105	20

Table 4.4 Purlin Section Properties

ID	Area (in.^{2})	I_x (in.^{4})	I_{xy} (in.^{4})	I_{x2} (in.^{4})	I_{y2} (in.^{4})	θ_p (deg)	J (in.^{4})
P1	1.177	24.62	5.381	1.12	25.85	12.90	0.00141
P2, P3	2.275	33.23	8.374	1.83	35.47	14.93	0.01382
P4, P5	1.279	18.99	4.834	1.07	20.29	15.10	0.00240
P6, P7	1.261	12.01	3.370	0.776	13.02	16.69	0.00340
P8, P9	0.847	8.15	2.298	0.532	8.84	16.79	0.00102
P10	1.151	6.17	2.003	0.491	6.88	19.42	0.00423

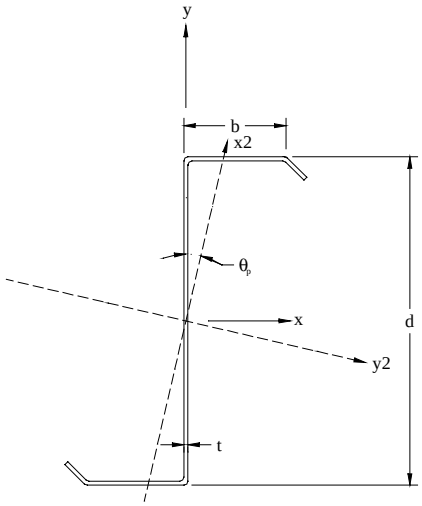

The next parameter in the test matrix is the number of parallel restrained purlin lines. In practice, the number of purlin lines between restraint anchors rarely exceeds eight. Hence, the maximum number of restrained purlin lines considered in the matrix is eight. For flat roofs (zero slope), the number of restrained purlin lines tested was one to eight, inclusive. For models with eight restrained purlin lines, the computer tests varied both the roof slope and the roof panel shear stiffness, independently of each other. Eleven different roof slopes were tested; 0:12, ½:12, 1:12, 2:12, … 9:12. These roof slopes were chosen to be representative of actual Z-purlin supported roofs, and to give enough data points to accurately describe the effect of roof slope on the required restraint forces. Z-purlin supported roof systems can have slopes greater than 9:12, but the general behavior of restraint forces with roof slope can be identified without including tests at these higher roof slopes. For models with n_p=8 and θ=0, six different roof panel shear stiffnesses were tested. The values of roof panel stiffness used for each span length are shown in Table 4.5, along with the corresponding areas of the Type D elements that were used for the roof panel in the current stiffness model. These values of panel shear stiffness represent typical values of actual roof panels and cover the range of log-linear behavior, 1000 lb/in.<*G'*<100,000 lb/in. All span lengths include the shear stiffness of 2500 lb/in., the base point used to formulate the design equations. The set of computer test combinations for roof slope, panel shear stiffness, and number of restrained purlin lines is summarized in Table 4.6 below. The designations G1 through G6 refer to the panel shear stiffness values given in Table 4.5. The models for this set of combinations were analyzed for each bracing configuration, number of spans, and purlin in the test matrix.

Table 4.5 Panel Shear Stiffness Values

ID	L=20 ft		L=25 ft		L=30 ft		L=35 ft		L=36 ft	
	Area (in^2)	G' (lb/in)	Area (in^2)	G' (lb/in)	Area (in^2)	G' (lb/in)	Area (in^2)	G' (lb/in)	Area (in^2)	G' (lb/in)
G1	1.0	76923	1.0	73529	1.0	65217	1.0	56452	1.0	56250
G2	0.3	23256	0.3	22321	0.3	20000	0.3	17157	0.3	16667
G3	0.1	7752	0.1	7440	0.1	6637	0.1	5719	0.1	5538
G4	0.06	4673	0.06	4448	0.07	4644	0.07	4005	0.07	3879
G5	0.0321	2500	0.0336	2495	0.0377	2500	0.0437	2500	0.0451	2500
G6	0.02	1560	0.02	1486	0.02	1326	0.02	1145	0.02	1109

Table 4.6 Combinations of n_p, θ, and G'

Combination	n_p	Roof Slope	G'
1	8	0:12	G5
2	8	½:12	G5
3	8	1:12	G5
4	8	2:12	G5
5	8	3:12	G5
6	8	4:12	G5
7	8	5:12	G5
8	8	6:12	G5
9	8	7:12	G5
10	8	8:12	G5
11	8	9:12	G5
12	1	0:12	G5
13	2	0:12	G5
14	3	0:12	G5
15	4	0:12	G5
16	5	0:12	G5
17	6	0:12	G5
18	7	0:12	G5
19	8	0:12	G1
20	8	0:12	G2
21	8	0:12	G3
22	8	0:12	G4
23	8	0:12	G6

The current stiffness model used to represent Z-purlin supported roof systems is linear and elastic, so the relative magnitude of the applied loading is not important to the model solution. The restraint force is linearly proportional to the applied load. However, a load value must be input to analyze each model for the restraint force. For this reason, a uniform gravity load of w=100 plf was applied to every purlin line for all models in the test matrix.

In summary, the test matrix consists of 2300 computer model tests. This total comes from five bracing configurations (BC), two numbers of continuous spans (S), ten purlins(P), 23 parameter combinations (PC), and one loading (L):

[5BC]x[2S]x[10P]x[23PC]x[1L] = 2300 tests (4.5)

4.4 SOLUTION OF COMPUTER TEST MATRIX

A commercial stiffness analysis program was used to analyze the entire computer test matrix, using the current elastic stiffness model described in Chapter II. A sample model, with input parameters and restraint force results, is presented in Appendix A. The section properties and loads used for all of the models are given in Appendix B.

The restraint force results found by solving the computer test matrix are given in Appendix C, Tables C.1 through C.19. Since the models are symmetric about the midpoint of the system, restraint forces are only given for half of the total restraints in each model. The titles of each result table in Appendix C give the bracing configuration, the number of spans, and the brace location, in that order. Systems with only two symmetric restraints do not have a brace location specified. Exterior denotes the restraints on the outside of each continuous purlin line, while interior refers to braces that are inside of the exterior restraints. Note that the restraint force is not tabulated for every brace location in the system. Some multiple span systems have different interior brace locations with nearly identical restraint forces. For these cases, the results were lumped together, with the largest restraint force (by magnitude) controlling. The parameter combinations listed in the result tables are given in Table 4.6, and the purlin identifications are described in Table 4.3. The restraint forces are given in pounds, and a purlin load of w=100 plf was used for all models.

4.5 STATISTICAL ANALYSES

4.5.1 Regression Characteristics

Engineering principles were used to derive the form of the proposed restraint force design equation, which is summarized in Figure 3.10. The only parts of the equation that remain to be defined are the coefficients C_1, C_2, and C_3. These coefficients are different for each brace location in each lateral restraint configuration. As discussed in Chapter III, C_1 is the brace location factor, C_2 affects the system effect factor, and C_3

influences the panel stiffness modifier. The results of the computer test matrix provide enough data to determine the values of these coefficients for each brace location and configuration, but a means of statistical analysis must be chosen to process the data.

The form of the proposed design equation requires that a multivariable, nonlinear regression analysis be performed. There are ten independent variables in the equation (b, d, t, I_{xy}, I_x, w, L, θ, n_p, and G') and the relationships are nonlinear. For this research, all regression analyses were done using a commercial statistical analysis program, *SigmaPlot 5.0* (1999). Regression analyses were used to determine preliminary values of the three unknown coefficients, which were later adjusted to be more appropriate for design usage.

A weighted, least-squares regression was chosen to analyze the data. Because the computer test matrix includes different roof slopes, some restraint force results are positive (tension) while others are negative (compression). Also, the magnitude of some restraint force results is many times greater than others; for the test matrix, restraint force magnitudes varied from about 10,000 lb to less than 10 lb. When an unweighted regression is performed, residuals are given equal value in the regression, regardless of the magnitude of the corresponding data point. The residual is the difference in restraint force between the stiffness model results and the design equation predictions. However, for the purposes of the restraint force design equation, accuracy is best measured by the percent error between the stiffness model results and the design equation predictions. To create design equations with the smallest percent error, a weighted regression must be used to determine the unknown coefficients. For this analysis, each residual was given a weight of $1/|P_L|$, where P_L is the restraint force given by the stiffness model. Thus, data points having a smaller magnitude of restraint force were given a larger weight in the regression.

Weighted regressions must be handled carefully to ensure that the results are not skewed by overweight on certain data points. For certain roof slopes close to the intercept value, θ_o, the magnitude of the restraint force is close to zero (less than 10 lb in some cases). These data points have very large weights and tend to control the

regression, making the results unrepresentative of all the data points considered. To prevent this distortion from occurring, a select number of data points were eliminated from the regression. All data points where the magnitude of the restraint force given by the stiffness model was less than 100 lb were discarded from the regression. Typically, these discarded data points were those where the roof slope was 3:12 (combination 5 in Table 4.6). Eliminating these points does not damage the validity of the resulting design equations, because the equations are defined such that no lateral restraint is necessary when the magnitude of the predicted restraint force is less than 100 lb.

Another group of data points was discarded from the regression analysis. This group includes all the points for models with only one restrained purlin line (n_p=1, combination 12 in Table 4.6). Since the stiffness models used to generate these data points had only one purlin line, there was no roof panel present to span between purlin lines. The nature of the current model, with very stiff type C elements at the rafter supports, leads to an inordinate amount of restraint force being given to the rafter supports when there is no roof panel diaphragm action. Thus, the force in the lateral restraints is observed to be much smaller than it would be in a real system. This effect is most acute for support restraints (see Table C.1), which are located directly above the rafter supports. The stiffness model results are clearly not accurate for these data points, because the restraint force for two purlin line systems (combination 13 in Table 4.6) is often greater than twice the restraint force for one purlin systems. This would correspond to a system effect that increases restraint force ratio, and is clearly not possible. Thus, all data points with only one purlin line are eliminated.

4.5.2 Determination of Coefficients C_1, C_2, and C_3

All of the data from the computer test matrix, minus the discarded data points mentioned previously, was then statistically analyzed using a weighted, least-squares regression. For ease of data entry, two separate regression analyses were performed; a constant panel stiffness regression and a variable panel stiffness regression. The constant panel stiffness regression included all the data points where G'=2500 lb/in. (combinations 1 through 18 in Table 4.6). The variable panel stiffness regression included all the data

points where *G'* is varied (combinations 1 and 19 through 23 in Table 4.6). The design equation summarized in Figure 3.10 was the regression equation used for both analyses.

As a means of evaluating the effectiveness of the regression model in describing the computer test data, the statistical terms R and R^2 were used. R is the coefficient of correlation and R^2 is the coefficient of determination; each of these measures varies from zero to one. When R=0, no relationship exists between the regression model and the test data, and when R=1, the regression model perfectly predicts the test data. For this research, values of R^2 greater than 0.90 were deemed acceptable for determining the regression coefficients. Appendix D contains a full explanation of the statistical measures calculated in the regression analysis.

To determine final coefficient values for the proposed design equation, three regression trials were performed. For the first trial, only the constant panel stiffness regression was executed, and initial values of C_1 and C_2 were calculated (see Table 4.7). A sample regression analysis for this initial trial is found in Appendix D. Notice that the R^2 values are greater than 0.97 for all restraint configurations, indicating that the regression model is highly accurate at predicting the computer test restraint forces.

Table 4.7 First Regression Trial

Configuration	C_1	C_2	R	R^2
Support Restraints:				
SS	0.4827	5.8234	0.9989	0.9978
MS, exterior	0.4604	5.9264	0.9990	0.9979
MS, interior	0.9373	9.1763	0.9851	0.9704
Third-point Restraints:				
SS	0.4597	3.9651	0.9990	0.9980
MS, exterior	0.4588	4.2003	0.9989	0.9977
MS, interior	0.4321	4.3780	0.9981	0.9961
Midspan Restraints:				
SS	0.8130	5.2671	0.9981	0.9962
MS, exterior	0.7674	5.6286	0.9976	0.9952
MS, interior	0.7435	6.3627	0.9858	0.9719
Quarter-point Restraints:				
SS, exterior	0.2443	4.8359	0.9957	0.9913
SS, interior	0.4255	3.2623	0.9967	0.9934
MS, exterior ¼ span	0.2416	4.9460	0.9953	0.9906
MS, interior ¼ span	0.2175	5.1648	0.9941	0.9883
MS, ½ span	0.4310	3.8545	0.9986	0.9972
Third-point Plus Support Restraints:				
SS, exterior	0.1584	3.4743	0.9890	0.9781
SS, interior	0.3456	2.9515	0.9986	0.9973
MS, exterior support	0.1564	3.4192	0.9919	0.9838
MS, interior support	0.2738	4.9523	0.9851	0.9704
MS, third-point	0.3457	3.1227	0.9978	0.9957

The coefficient values determined by the first trial can be greatly simplified for design purposes. Due to the modeling process, the values are not known to a high degree of accuracy, and only two significant digits are required in the coefficient values. The C_2 values represent Z-purlin bending resistance, and restraints with corresponding locations in single and multiple span systems should have about the same resistance. Thus, these restraints are given the same C_2 value. These adjusted C_2 values were included as known values in the second regression trial, which then calculated revised C_1 values. Again, the constant panel stiffness regression was performed, and the results are shown in Table 4.8. As for the first trial, all R^2 values are greater than 0.97, showing excellent correlation between the regression model and the computer test results.

Table 4.8 Second Regression Trial

Configuration	C_1	C_2	R	R^2
Support Restraints:				
SS	0.4858	5.9	0.9989	0.9978
MS, exterior	0.4594	5.9	0.9990	0.9979
MS, interior	0.9389	9.2	0.9851	0.9704
Third-point Restraints:				
SS	0.4686	4.2	0.9989	0.9978
MS, exterior	0.4588	4.2	0.9989	0.9977
MS, interior	0.4258	4.2	0.9980	0.9961
Midspan Restraints:				
SS	0.8358	5.6	0.9980	0.9961
MS, exterior	0.7656	5.6	0.9976	0.9952
MS, interior	0.6981	5.6	0.9854	0.9710
Quarter-point Restraints:				
SS, exterior	0.2477	5.0	0.9956	0.9913
SS, interior	0.4369	3.6	0.9966	0.9931
MS, exterior ¼ span	0.2427	5.0	0.9953	0.9906
MS, interior ¼ span	0.2145	5.0	0.9941	0.9883
MS, ½ span	0.4222	3.6	0.9985	0.9971
Third-point Plus Support Restraints:				
SS, exterior	0.1587	3.5	0.9890	0.9781
SS, interior	0.3469	3.0	0.9986	0.9973
MS, exterior support	0.1574	3.5	0.9919	0.9838
MS, interior support	0.2749	5.0	0.9851	0.9704
MS, third-point	0.3425	3.0	0.9978	0.9957

Since the regression coefficients are not known to more than two significant digits of accuracy, the resulting C_1 values from the second trial were adjusted to the nearest appropriate value for design purposes. The coefficient C_1 is the brace location factor, which controls the percentage of total restraint force that is allocated to a particular restraint. All C_1 values were increased in the adjustment, because increasing this coefficient always produces a more conservative prediction for restraint forces. For the third trial, the variable panel stiffness regression was performed. The adjusted values for C_1 and C_2 were taken as known quantities, and initial values for the coefficient C_3 were determined (see Table 4.9). The coefficient C_3 controls the panel stiffness modifier (see Equation 3.13). The R^2 values for this trial are greater than 0.90 for all restraint

configurations, with three exceptions. These three exceptions all have R^2 values above 0.89, and are close enough to 0.90 to be acceptable for the final design equation.

Table 4.9 Third Regression Trial

Configuration	C_1	C_2	C_3	R	R^2
Support Restraints:					
SS	0.50	5.9	0.2912	0.9905	0.9812
MS, exterior	0.50	5.9	0.3623	0.9901	0.9803
MS, interior	1.00	9.2	0.4198	0.9915	0.9830
Third-point Restraints:					
SS	0.50	4.2	0.2130	0.9943	0.9886
MS, exterior	0.50	4.2	0.2632	0.9914	0.9830
MS, interior	0.45	4.2	0.3269	0.9850	0.9701
Midspan Restraints:					
SS	0.85	5.6	0.3168	0.9852	0.9706
MS, exterior	0.80	5.6	0.3958	0.9711	0.9430
MS, interior	0.75	5.6	0.4673	0.9479	0.8986
Quarter-point Restraints:					
SS, exterior	0.25	5.0	0.3305	0.9704	0.9416
SS, interior	0.45	3.6	0.1067	0.9458	0.8946
MS, exterior ¼ span	0.25	5.0	0.3585	0.9589	0.9194
MS, interior ¼ span	0.22	5.0	0.4223	0.9448	0.8927
MS, ½ span	0.45	3.6	0.2569	0.9783	0.9571
Third-point Plus Support Restraints:					
SS, exterior	0.17	3.5	0.3566	0.9537	0.9096
SS, interior	0.35	3.0	0.0221	0.9852	0.9706
MS, exterior support	0.17	3.5	0.3553	0.9664	0.9338
MS, interior support	0.30	5.0	0.4564	0.9743	0.9492
MS, third-point	0.35	3.0	0.0718	0.9709	0.9426

After the third regression trial, the final values of the regression coefficients were determined by adjusting the C_3 values. Again, these values need only have two significant digits of accuracy, and are adjusted to values that are appropriate for use in the design equation. The final regression coefficient values are presented in Table 4.10.

Table 4.10 Final Regression Coefficient Values

Configuration	C_1	C_2	C_3
Support Restraints:			
SS	0.50	5.9	0.35
MS, exterior	0.50	5.9	0.35
MS, interior	1.00	9.2	0.45
Third-point Restraints:			
SS	0.50	4.2	0.25
MS, exterior	0.50	4.2	0.25
MS, interior	0.45	4.2	0.35
Midspan Restraints:			
SS	0.85	5.6	0.35
MS, exterior	0.80	5.6	0.35
MS, interior	0.75	5.6	0.45
Quarter-point Restraints:			
SS, exterior	0.25	5.0	0.35
SS, interior	0.45	3.6	0.15
MS, exterior ¼ span	0.25	5.0	0.40
MS, interior ¼ span	0.22	5.0	0.40
MS, ½ span	0.45	3.6	0.25
Third-point Plus Support Restraints:			
SS, exterior	0.17	3.5	0.35
SS, interior	0.35	3.0	0.05
MS, exterior support	0.17	3.5	0.35
MS, interior support	0.30	5.0	0.45
MS, third-point	0.35	3.0	0.10

4.6 VERIFIFICATION OF PANEL STIFFNESS AND ROOF SLOPE INTERACTION

The computer test matrix discussed in Section 4.3 does not include a series of data points where roof slope is varied for values of roof panel shear stiffness other than *G'*=2500 lb/in. The proposed design equation, given in Figure 3.10, must accurately predict the effects on restraint force of the interaction between roof slope and roof panel shear stiffness. To minimize the total data collection time, only four different computer test series were used to verify the proposed design equation for the combined interaction of roof panel stiffness and roof slope. The four test series are described in Table 4.11 and

note that for all tests, n_p=8, the loading is w=100 plf, and the purlin identifications are found in Table 4.4. These four series did not require an extensive number of computer test runs, but the results give a representative description of the interaction behavior. The data points for each test series in this verification, along with restraint force results in lb, are shown in Table 4.12.

Table 4.11 Test Series for Roof Slope and Panel Stiffness Interaction

Test Series	Bracing Configuration	Purlin
1	Single Span, Support Restraints	P6
2	Multiple Span, Third-point Restraints, Interior	P5
3	Single Span, Quarter-point Restraints, Interior	P9
4	Multiple Span, Third-point Plus Support Restraints, Interior Support	P2

Table 4.12 Results of Roof Slope and Panel Stiffness Interaction Tests

Data Point	Roof Slope	Panel Stiffness	Test Series 1	Test Series 2	Test Series 3	Test Series 4
1	0:12	G1	2206	2495	1710	1834
2	0:12	G2	2046	2370	1775	1612
3	0:12	G3	1720	2118	1689	1241
4	0:12	G4	1507	2060	1600	1094
5	0:12	G5	1246	1768	1460	894
6	0:12	G6	1021	1530	1345	591
7	½:12	G1	1806	2011	1401	1471
8	½:12	G2	1678	1913	1456	1292
9	½:12	G3	1417	1714	1390	996
10	½:12	G4	1244	1621	1321	878
11	½:12	G5	1030	1438	1211	717
12	½:12	G6	846	1250	1120	473
13	1:12	G1	1421	1639	1104	1118
14	1:12	G2	1325	1466	1149	981
15	1:12	G3	1125	1319	1103	758
16	1:12	G4	991	1251	1052	668
17	1:12	G5	823	1116	971	546
18	1:12	G6	678	977	903	358
19	2:12	G1	560	596	442	348
20	2:12	G2	535	572	464	305
21	2:12	G3	472	530	461	240
22	2:12	G4	424	510	451	213
23	2:12	G5	359	472	434	174

Table 4.12 Results of Roof Slope and Panel Stiffness Interaction Tests, Continued

24	2:12	G6	300	432	418	109
25	3:12	G1	-181	-401	-130	-331
26	3:12	G2	-146	-373	-126	-293
27	3:12	G3	-91	-305	-92	-219
28	3:12	G4	-65	-274	-65	-192
29	3:12	G5	-40	-212	-27	-157
30	3:12	G6	-24	-150	-	-113
31	4:12	G1	-965	-1255	-734	-1037
32	4:12	G2	-865	-1182	-750	-913
33	4:12	G3	-686	-1019	-677	-694
34	4:12	G4	-581	-943	-613	-609
35	4:12	G5	-463	-794	-517	-498
36	4:12	G6	-368	-643	-441	-341
37	5:12	G1	-1608	-2139	-1230	-1634
38	5:12	G2	-1456	-2019	-1262	-1440
39	5:12	G3	-1174	-1760	-1157	-1138
40	5:12	G4	-1006	-1639	-1062	-966
41	5:12	G5	-810	-1401	-918	-790
42	5:12	G6	-651	-1159	-803	-537
43	6:12	G1	-2283	-2955	-1750	-2241
44	6:12	G2	-2076	-2792	-1800	-1974
45	6:12	G3	-1687	-2444	-1662	-1508
46	6:12	G4	-1451	-2281	-1534	-1326
47	6:12	G5	-1175	-1961	-1340	-1085
48	6:12	G6	-948	-1634	-1185	-734
49	7:12	G1	-2904	-3615	-2229	-2804
50	7:12	G2	-2646	-3418	-2294	-2468
51	7:12	G3	-2159	-2996	-2125	-1887
52	7:12	G4	-1861	-2798	-1968	-1659
53	7:12	G5	-1511	-2411	-1728	-1357
54	7:12	G6	-1221	-2015	-1537	-916
55	8:12	G1	-3461	-4293	-2658	-3309
56	8:12	G2	-3158	-4060	-2739	-2913
57	8:12	G3	-2583	-3564	-2542	-2228
58	8:12	G4	-2229	-3332	-2359	-1959
59	8:12	G5	-1812	-2877	-2078	-1602
60	8:12	G6	-1466	-2411	-1853	-1080
61	9:12	G1	-3973	-4915	-3053	-3710
62	9:12	G2	-3629	-4650	-3146	-3268
63	9:12	G3	-2973	-4086	-2925	-2501
64	9:12	G4	-2568	-3822	-2717	-2200
65	9:12	G5	-2090	-3305	-2399	-1802
66	9:12	G6	-1692	-2775	-2144	-1213

To compare the results of the verification tests to the proposed design equation, a regression analysis was performed. The regression performed on the verification test

results was a weighted, variable panel stiffness regression. The regression equation took the values for C_1 and C_2 given in Table 4.10 as known quantities and then solved for the coefficient C_3 (the panel stiffness modifier coefficient). For each verification test, the statistical measures R and R^2, defined previously, were obtained to evaluate the strength of the correlation between the computer test results and the proposed design equation. Table 4.13 shows the regression results of the verification tests and compares the C_3 values to those of the final coefficient values in the proposed design equation, which are presented in Table 4.10.

Table 4.13 Comparison of Verification Tests to Design Equation

Comparison	C_3	R	R^2
Test Series 1:			
Verification Regression	0.3827	0.9967	0.9934
Design Equation	0.35		
Test Series 2:			
Verification Regression	0.5033	0.9958	0.9916
Design Equation	0.35		
Test Series 3:			
Verification Regression	0.3810	0.9972	0.9944
Design Equation	0.15		
Test Series 4:			
Verification Regression	0.4922	0.9897	0.9795
Design Equation	0.45		

The results of the verification test regression show R^2 values that are all greater than 0.97, indicating a strong correlation between the regression model and the computer test results. The values of the coefficient C_3 determined by the verification test regression are all higher than the values used in the proposed design equation. The reason for this discrepancy is that each of the verification tests considered only one purlin cross-section and span length, whereas the previous regression analyses considered ten different purlins. Thus, the coefficient C_3 shows slight variation with section properties, but this variation does not merit an adjustment to the form of the design equation. The

two sets of coefficient values are similar enough that the validity of the proposed design equation for roof slope and roof panel stiffness interaction is confirmed.

CHAPTER V

APPLICATION OF DESIGN PROCEDURE

5.1 INTRODUCTION

This chapter explains the application of the proposed design procedure to the estimation of lateral restraint forces in Z-purlin supported roof systems. The proposed procedure is summarized in Figure 5.1 and the design equation coefficients are given in Table 5.1. Three design examples, representative of typical Z-purlin roof systems, are presented to illustrate the design procedure.

Table 5.1 Design Equation Coefficient Values

Configuration	C_1	C_2	C_3
Support Restraints:			
SS	0.50	5.9	0.35
MS, exterior	0.50	5.9	0.35
MS, interior	1.00	9.2	0.45
Third-point Restraints:			
SS	0.50	4.2	0.25
MS, exterior	0.50	4.2	0.25
MS, interior	0.45	4.2	0.35
Midspan Restraints:			
SS	0.85	5.6	0.35
MS, exterior	0.80	5.6	0.35
MS, interior	0.75	5.6	0.45
Quarter-point Restraints:			
SS, exterior	0.25	5.0	0.35
SS, interior	0.45	3.6	0.15
MS, exterior ¼ span	0.25	5.0	0.40
MS, interior ¼ span	0.22	5.0	0.40
MS, ½ span	0.45	3.6	0.25
Third-point Plus Support Restraints:			
SS, exterior	0.17	3.5	0.35
SS, interior	0.35	3.0	0.05
MS, exterior support	0.17	3.5	0.35
MS, interior support	0.30	5.0	0.45
MS, third-point	0.35	3.0	0.10

$$P_L = P_0 C_1 \left(n_p^* \alpha + n_p \gamma \right)$$

where:

$$P_0 = \left[\left(\frac{I_{xy}}{2I_x} + \frac{b}{3d} \right) \cos\theta - \sin\theta \right] W_p$$

$$W_p = wL$$

$$\alpha = 1 - C_2 \left(\frac{t}{d} \right) \left(n_p^* - 1 \right)$$

$$n_p^* = \min\left\{ n_p, n_{p(\max)} \right\}$$

$$n_{p(\max)} = 0.5 + \frac{d}{2C_2 t}$$

$$\gamma = C_3 \log\left(\frac{G'}{2500} \right)$$

and

n_p = number of parallel, restrained purlin lines
b = purlin flange width
d = purlin depth
t = purlin thickness
I_{xy} = the product moment of inertia
I_x = the moment of inertia with respect to the centroidal axis perpendicular to the web of the Z-section
θ = roof slope (from horizontal)
w = distributed gravity load along each purlin (force/length)
L = span length
G' = roof panel shear stiffness (lb/in.)

Notes:

1) Positive P_L is in tension, negative P_L is in compression.
2) Upper bound: $\left| P_L \right| \le \left| n_p P_0 C_1 \right|$
3) If $\left| P_L \right| \le 100\,\text{lb}$, no lateral bracing is necessary.
4) Applicable range of panel stiffnesses: $1000\,\text{lb/in} \le G' \le 100{,}000\,\text{lb/in}$
5) C_1, C_2, and C_3 are regression coefficients.
6) Models used to develop procedure had $n_p \le 8$.

Figure 5.1 Summary of Proposed Design Procedure

5.2 Design Examples

Example 1: Determine restraint forces for a three continuous span system having six parallel purlin lines and support restraints. The purlin section is 8ZS2.5x075, the span length is 22.5 ft, and purlin lines are spaced 5ft apart. The roof slope is 1:12 (9.46 degrees) and the roof panel shear stiffness is 2500 lb/in. A uniform gravity load of 20 psf is applied to the system.

Solution: The design equation is given in Figure 5.1:

$$P_L = P_0 C_1 \left(n_p^* \alpha + n_p \gamma \right)$$

From Table 5.1, for multiple span systems with support restraints:

Exterior restraints: C_1=0.50, C_2=5.9, C_3=0.35

Interior restraints: C_1=1.00, C_2=9.2, C_3=0.45

For the purlin section 8ZS2.5x075, Table I-16 of the *Cold-Formed Steel Design Manual*, (1996) gives the following section properties:

d=8 in., b=2.5 in., t=0.075 in., I_{xy}=2.840 in.^{4}, I_x=10.10 in.^{4}

with

$$P_0 = \left[\left(\frac{I_{xy}}{2I_x} + \frac{b}{3d} \right) \cos\theta - \sin\theta \right] W_p \tag{3.9}$$

The $\overline{w} = 20\,\text{psf}$ gravity load is evenly distributed to all purlin lines:

$$w = \frac{\overline{w} a \left(n_p - 1 \right)}{n_p} = \frac{(20\,\text{psf})(5\,\text{ft})(6-1)}{6} = 83.3\,\text{plf}$$

and

$$W_p = wL = (83.3\,\text{plf})(22.5\,\text{ft}) = 1875\,\text{lb} \tag{3.8}$$

thus,

$$P_0 = \left[\left(\frac{2.840\,\text{in.}^4}{2\left(10.10\,\text{in.}^4\right)} + \frac{2.5\,\text{in.}}{3(8\,\text{in.})} \right) \cos 9.46^0 - \sin 9.46^0 \right] (1875\,\text{lb}) = 144.5\,\text{lb}$$

with

$$\alpha = 1 - C_2\left(\frac{t}{d}\right)\left(n_p^* - 1\right) \tag{3.11}$$

and

$$n_p^* = \min\left\{n_p, n_{p(\max)}\right\}, \quad n_{p(\max)} = 0.5 + \frac{d}{2C_2 t} \tag{3.12}$$

For the exterior restraints:

$$n_{p(\max)} = 0.5 + \frac{8\,\text{in.}}{2(5.9)(0.075\,\text{in.})} = 9.54 > 6 \rightarrow n_p^* = 6$$

$$\alpha = 1 - 5.9\left(\frac{0.075\,\text{in.}}{8\,\text{in.}}\right)(6-1) = 0.723$$

For the interior restraints:

$$n_{p(\max)} = 0.5 + \frac{8\,\text{in.}}{2(9.2)(0.075\,\text{in.})} = 5.80 < 6 \rightarrow n_p^* = 5.80$$

$$\alpha = 1 - 9.2\left(\frac{0.075\,\text{in.}}{8\,\text{in.}}\right)(5.80-1) = 0.586$$

The roof panel shear stiffness modifier:

$$\gamma = C_3 \log\left(\frac{G'}{2500\,\text{lb/in.}}\right), \; G' = \; 2500\,\text{lb/in.} \rightarrow \gamma = 0 \tag{3.13}$$

Finally, the design restraint forces are:

Exterior restraints: $P_L = (144.5\,\text{lb})(0.50)\left[(6)(0.723) + (6)(0)\right] = 313\,\text{lb (T)}$

Interior restraints: $P_L = (144.5\,\text{lb})(1.00)\left[(5.80)(0.586) + (6)(0)\right] = 491\,\text{lb (T)}$

Shown graphically, the results are:

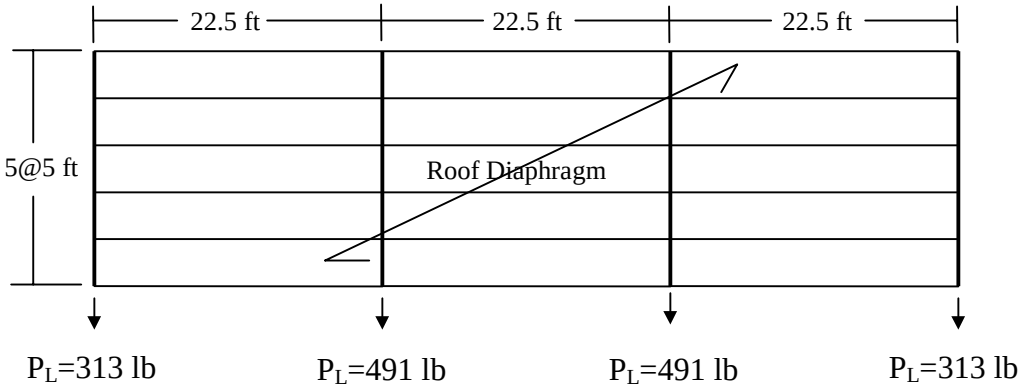

Figure 5.2 Restraint Forces for Example 1

Example 2: Determine restraint forces for a single span system having eight parallel purlin lines and quarter-point restraints. The purlin section is 10ZS3x105, the span length is 30 ft, and purlin lines are spaced 5 ft apart. The system has a roof slope of 5:12 (26.57 degrees) and the panel shear stiffness is 10,000 lb/in. A uniform gravity load of 30 psf is applied to the system.

Solution: The design equation is given in Figure 5.1:

$$P_L = P_0 C_1 \left(n_p^* \alpha + n_p \gamma \right)$$

From Table 5.1, for single span systems with quarter-point restraints:

Exterior restraints: C_1=0.25, C_2=5.0, C_3=0.35

Interior restraints: C_1=0.45, C_2=3.6, C_3=0.15

For the purlin section 10ZS3x105, Table I-16 of the *Cold-Formed Steel Design Manual*, (1996) gives the following section properties:

d=10 in., b=3 in., t=0.105 in., I_{xy}=6.640 in.^{4}, I_x=26.21 in.^{4}

with

$$P_0 = \left[\left(\frac{I_{xy}}{2I_x} + \frac{b}{3d} \right) \cos\theta - \sin\theta \right] W_p \qquad (3.9)$$

The $\overline{w} = 30$ psf gravity load is evenly distributed to all purlin lines:

$$w = \frac{\overline{w}a(n_p - 1)}{n_p} = \frac{(30\text{ psf})(5\text{ ft})(8-1)}{8} = 131.3\text{ plf}$$

and

$$W_p = wL = (131.3\text{ plf})(30\text{ ft}) = 3938\text{ lb} \tag{3.8}$$

thus,

$$P_0 = \left[\left(\frac{6.640\text{ in.}^4}{2(26.21\text{ in.}^4)} + \frac{3\text{ in.}}{3(10\text{ in.})}\right)\cos 26.57^0 - \sin 26.57^0\right](3938\text{ lb}) = -963.1\text{ lb}$$

with

$$\alpha = 1 - C_2\left(\frac{t}{d}\right)(n_p^* - 1) \tag{3.11}$$

and

$$n_p^* = \min\{n_p, n_{p(\max)}\},\quad n_{p(\max)} = 0.5 + \frac{d}{2C_2 t} \tag{3.12}$$

The roof panel shear stiffness modifier:

$$\gamma = C_3 \log\left(\frac{G'}{2500\text{ lb/in.}}\right) \tag{3.13}$$

For the exterior restraints:

$$n_{p(\max)} = 0.5 + \frac{8\text{ in.}}{2(5.9)(0.075\text{ in.})} = 9.54 > 6 \rightarrow n_p^* = 6$$

$$\alpha = 1 - 5.0\left(\frac{0.105\text{ in.}}{10\text{ in.}}\right)(8-1) = 0.633$$

$$\gamma = C_3 \log\left(\frac{G'}{2500\text{ lb/in.}}\right) = (0.35)\log\left(\frac{10{,}000\text{ lb/in.}}{2500\text{ lb/in.}}\right) = 0.211$$

For the interior restraints:

$$n_{p(\max)} = 0.5 + \frac{10\text{ in.}}{2(3.6)(0.105\text{ in.})} = 13.78 > 8 \rightarrow n_p^* = 8$$

$$\alpha = 1 - 3.6\left(\frac{0.105\text{ in.}}{10\text{ in.}}\right)(8-1) = 0.735$$

$$\gamma = C_3 \log\left(\frac{G'}{2500\ \text{lb/in.}}\right) = (0.15)\log\left(\frac{10{,}000\ \text{lb/in.}}{2500\ \text{lb/in.}}\right) = 0.090$$

Finally, the design restraint forces are:

Exterior restraints: $P_L = (-963.1\,\text{lb})(0.25)\left[(8)(0.633)+(8)(0.211)\right] = -1626\,\text{lb (C)}$

Check $\left|P_L\right| \le \left|n_p P_0 C_1\right|$:

$$\left|P_L\right| = 1626\,\text{lb} \le \left|n_p P_0 C_1\right| = (8)(963.1\,\text{lb})(0.25) = 1926\,\text{lb} \rightarrow \text{OK}$$

Interior restraints: $P_L = (-963.1\,\text{lb})(0.45)\left[(8)(0.735)+(8)(0.090)\right] = -2860\,\text{lb (C)}$

Check $\left|P_L\right| \le \left|n_p P_0 C_1\right|$:

$$\left|P_L\right| = 2860\,\text{lb} \le \left|n_p P_0 C_1\right| = (8)(963.1\,\text{lb})(0.45) = 3467\,\text{lb} \rightarrow \text{OK}$$

Shown graphically, the results are:

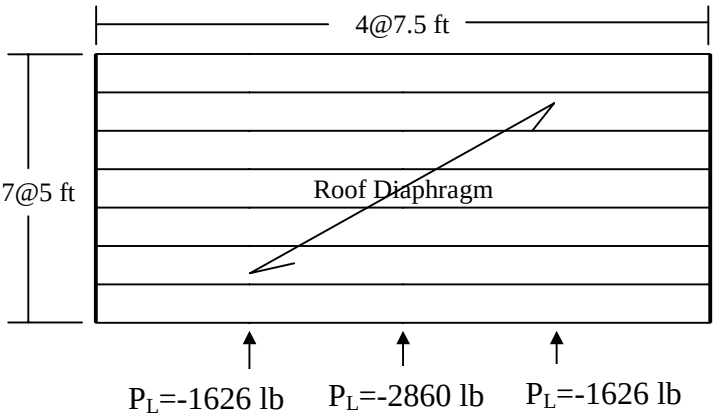

Figure 5.3 Restraint Forces for Example 2

Example 3: Determine restraint forces for a single span system having three parallel purlin lines and third-point plus support restraints. The purlin section is 8ZS2.5x090, the span length is 25 ft, and purlin lines are spaced 5 ft apart. The roof slope is 3:12 and the panel shear stiffness is 2500 lb/in. A uniform gravity load of 20 psf is applied to the system.

Solution: The design equation is given in Figure 5.1:

$$P_L = P_0 C_1 \left(n_p^* \alpha + n_p \gamma \right)$$

From Table 5.1, for multiple span systems with support restraints:

Exterior restraints: C_1=0.17, C_2=3.5, C_3=0.35

Interior restraints: C_1=0.35, C_2=3.0, C_3=0.05

For the purlin section 8ZS2.5x090, Table I-16 of the *Cold-Formed Steel Design Manual*, (1996) gives the following section properties:

d=8 in., b=2.5 in., t=0.090 in., I_{xy}=3.370 in.^{4}, I_x=12.01 in.^{4}

with

$$P_0 = \left[\left(\frac{I_{xy}}{2I_x} + \frac{b}{3d} \right) \cos\theta - \sin\theta \right] W_p \tag{3.9}$$

The $\overline{w} = 20\,\text{psf}$ gravity load is evenly distributed to all purlin lines:

$$w = \frac{\overline{w} a \left(n_p - 1 \right)}{n_p} = \frac{(20\,\text{psf})(5\,\text{ft})(3-1)}{3} = 66.7\,\text{plf}$$

and

$$W_p = wL = (66.7\,\text{plf})(25\,\text{ft}) = 1667\,\text{lb} \tag{3.8}$$

thus,

$$P_0 = \left[\left(\frac{3.370\,\text{in}^4}{2\left(12.01\,\text{in}^4\right)} + \frac{2.5\,\text{in}}{3\left(8\,\text{in}\right)} \right) \cos 14.04^0 - \sin 14.04^0 \right] (1667\,\text{lb}) = -9.2\,\text{lb}$$

with

$$\alpha = 1 - C_2 \left(\frac{t}{d} \right) \left(n_p^* - 1 \right) \tag{3.11}$$

and

$$n_p^* = \min\left\{ n_p, n_{p(\max)} \right\}, \quad n_{p(\max)} = 0.5 + \frac{d}{2C_2 t} \tag{3.12}$$

For the exterior restraints:

$$n_{p(\max)} = 0.5 + \frac{8\,\text{in.}}{2(3.5)(0.090\,\text{in.})} = 13.19 > 3 \rightarrow n_p^* = 3$$

$$\alpha = 1 - 3.5\left(\frac{0.090\,\text{in.}}{8\,\text{in.}}\right)(3-1) = 0.921$$

For the interior restraints:

$$n_{p(\max)} = 0.5 + \frac{8\,\text{in.}}{2(3.0)(0.090\,\text{in.})} = 15.31 < 3 \rightarrow n_p^* = 3$$

$$\alpha = 1 - 3.0\left(\frac{0.090\,\text{in.}}{8\,\text{in.}}\right)(3-1) = 0.933$$

The roof panel shear stiffness modifier:

$$\gamma = C_3 \log\left(\frac{G'}{2500\,\text{lb/in.}}\right) G' = \ 2500\,\text{lb/in.} \rightarrow \gamma = 0 \tag{3.13}$$

Finally, the final design restraint forces are:

Exterior restraints: $P_L = (-9.2\,\text{lb})(0.17)\left[(3)(0.921) + (3)(0)\right] = -4\,\text{lb}$

Interior restraints: $P_L = (-9.2\,\text{lb})(0.35)\left[(3)(0.933) + (3)(0)\right] = -9\,\text{lb}$

Since $\left|P_L\right| \le 100\,\text{lb}$ for all restraints in the system, no lateral restraint is necessary.

CHAPTER VI

SUMMARY, CONCLUSIONS, AND RECOMMENDATIONS

6.1 SUMMARY

A design procedure for the prediction of lateral restraint forces in Z-purlin supported, sloped roofs under gravity loads has been formulated in this research. The procedure applies to both single and multiple span systems for five lateral restraint configurations: support, third-point, midspan, quarter-point, and third-point plus support restraints. To develop the design procedure, a mathematical model was created to collect restraint force data, because experimental research on sloped roofs is both difficult and costly to perform. A first order, linear, elastic stiffness model was used to represent the Z-purlin roof system as a space truss. The model was based on that used by Elhouar and Murray (1985) to develop the current design equations in the American Iron and Steel Institute *Specification for the Design of Cold-Formed Steel Structural Members* (1996).

The data resulting from the stiffness model was used to develop theoretical expressions to predict restraint force. A new treatment of purlin forces and system effects in Z-purlin roof systems led to a new form of restraint force design equation. The proposed equation postulates that the predicted restraint force in any given system is equal to the force on a single purlin multiplied by the total number of purlins, a brace location factor, a reduction factor caused by system effects, and modified by a factor for roof panel stiffness. The equation predicts the restraint force for any value of roof panel shear stiffness between 1000 lb/in. and 100,000 lb/in. The treatment of roof slope in the proposed equation is more accurate than the current specification, and the intercept slope angle (where restraint force is zero) depends only upon purlin cross-sectional properties. The proposed equation also identifies a range of roof slopes for which a given roof system does not require any lateral restraint.

The theoretical equation was developed with three coefficients that are dependent on the bracing configuration. The values of these coefficients were determined by

analyses of the restraint force data collected from the stiffness model. A weighted, least-squares regression was utilized, and the effectiveness of the regression model was measured by R^2, the coefficient of determination.

6.2 CONCLUSIONS

A design procedure has been formulated to predict the required restraint force for Z-purlin supported roof systems under gravity loads. The equation accounts for roof systems of any slope and panel shear stiffness (between 1000 lb/in. and 100,000 lb/in.). The procedure applies to single and multiple span systems with the following bracing configurations: support, third-point, midspan, quarter-point, and third-point plus support restraints. The form of the design equation is based on statics, and was verified by comparison to results of elastic stiffness models. Coefficients, to account for variations in system interactions, were determined by a statistical analysis of the model results and depend on the bracing configuration. The proposed procedure is summarized in Figure 5.1 and the coefficients are given in Table 5.1.

For accuracy, $n_{p(max)}$ should be left in decimal form instead of rounding to whole numbers. This equation applies only to gravity loads, not uplift, and is only valid for systems with all purlin top flanges facing in the same direction (see Figure 3.2). The proposed procedure applies to both standing seam and through-fastened roof systems. Note that all of the relationships in the procedure are dimensionless, except for the roof panel shear stiffness. The panel stiffness modifier, γ, was calibrated such that G' is in lb/in.).

6.3 RECOMMENDATIONS

The American Iron and Steel Institute's *Specification for the Design of Cold-Formed Steel Structural Members* (1996) has provisions for the prediction of restraint forces for Z-purlin supported roofs under gravity loads. This research has developed a design procedure for the prediction of restraint forces for all of the bracing configurations addressed by the AISI Provisions (support, third-point, and midspan restraints) and the

research by Danza and Murray in 1998 (quarter-point and third-point plus support restraints). The empirical equations contained in the AISI Provisions and the Danza and Murray research lack a strong connection to engineering principles, and each work presents different forms for the final solution. The design procedure proposed here is unified for all bracing configurations and is a more accurate representation of Z-purlin roof systems. It is recommended that the current AISI Provisions be revised to include the proposed design equation. Also, the proposed design procedure should be verified for use with roof systems consisting of more than eight purlin lines, by comparison to experimental or model testing.

REFERENCES

Cold-Formed Steel Design Manual, (1996). American Iron and Steel Institute, Washington, D. C.

Curtis, L. E. and Murray, T. M. (1983). "Simple Span Z-purlin Tests to Determine Restraint force Accumulation," Fears Structural Engineering Laboratory Report No. FSEL/MBMA 83-02, University of Oklahoma, Norman, Oklahoma, 197 pages.

Danza, M. A. and Murray, T. M. (1998). "Lateral Restraint Forces in Quarter-point and Third-point Plus Support Braced Z-purlin Supported Roof Systems," Research Report CE/VPI-ST-99/07, Department of Civil and Environmental Engineering, Virginia Polytechnic Institute and State University, Blacksburg, Virginia, 129 pages.

Elhouar, S. and Murray, T. M. (1985). "Prediction of Lateral Restraint Forces for Z-purlin Supported Roof Systems," Fears Structural Engineering Laboratory Report No. FSEL/AISI 85-01, University of Oklahoma, Norman, Oklahoma, 107 pages.

Fenske, T. E. and Yener, M. (1990). "Analysis and Design of Light Gage Steel Roof Systems," *Thin-Walled Structures*, 10(3), 221-234.

Fisher, J. M. and LaBoube R. A. *A Guide for Designing with Standing Seam Roof Panels* (1997). AISI Design Guide CF97-1, American Iron and Steel Institute, Washington, D.C.

Ghazanfari, A. and Murray, T. M. (1982). "Simple Span Z-purlin Tests with Various Restraint Systems," Fears Structural Engineering Laboratory Report No. FSEL/MBMA 82-01A, University of Oklahoma, Norman, Oklahoma, 47 pages.

Ghazanfari, A. and Murray, T. M. (1983). "Prediction of Lateral Restraint Forces of Single Span Z-purlins with Experimental Verification," Fears Structural Engineering Laboratory Report No. FSEL/MBMA 83-04, University of Oklahoma, Norman, Oklahoma, 131 pages.

Heinz, D. A. (1994). "Application of Generalized Beam Theory to the Design of Thin-Walled Purlins," *Thin-Walled Structures*, 19(2-4), 311-335.

Lucas, F. G., Al-Bermani, G. A., and Kitipornchai, S. (1997). "Modelling of Cold-Formed Purlin-Sheeting Systems," *Thin-Walled Structures*, 27(3), 223-243.

Needham, J. R. (1981). "Review of the Bending Mechanics of Cold-Formed Z-purlins," Department of Civil Engineering, University of Kansas.

REFERENCES, CONTINUED

Rivard, P. and Murray, T. M. (1986). "Anchorage Forces in Two Purlin Line Standing Seam Z-purlin Supported Roof Systems," Fears Structural Engineering Laboratory Report No. FSEL/MBMA 86-01, University of Oklahoma, Norman, Oklahoma, 178 pages.

Seshappa, V. and Murray, T. M. (1985). "Experimental Studies of Z-purlin Supported Roof Systems Using Quarter Scale Models," Fears Structural Engineering Laboratory Report No. FSEL/MBMA 85-02, University of Oklahoma, Norman, Oklahoma, 81 pages.

SigmaPlot (1999). Version 5.0, SPSS, Inc., Chicago, Illinois

Specification for the Design of Cold-Formed Steel Structural Members (1996). American Iron and Steel Institute, Washington, D.C.

Zetlin, L. and Winter, G. (1955). "Unsymmetrical Bending of Beams with and without Lateral Bracing," *Proceedings of the American Society of Civil Engineers*, Vol. 81, 774-1 to 774-20.

APPENDIX A: STIFFNESS MODEL EXAMPLE

This appendix describes how to construct a typical stiffness model used in this research. For the example roof system shown in Figure A.1, the section properties for each element in the model are given, along with calculations for determining the applied loads. Then, analysis results given and compared to the restraint forces predicted by the proposed design procedure. Refer to Chapter II for a full discussion of the stiffness model.

Given: A single span system with four purlin lines and third-point restraints. The purlin cross-section is 10ZS3x075, span length is 30 ft, and purlin lines are spaced 5 ft apart. The roof slope is 1:12 and the roof panel shear stiffness is 2500 lb/in. The applied gravity load is w=100 plf along each purlin line.

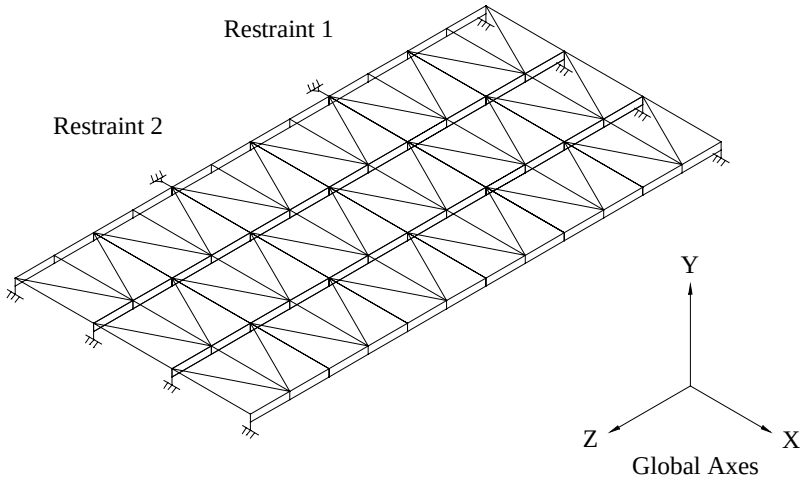

Figure A.1 Example Model

Model Parameters: For the purlin section 10ZS3x075, Table I-16 of the *Cold-Formed Steel Design Manual*, (1996) gives the following section properties:

d=10 in., b=3 in., t=0.075 in., Area=1.279 in.^{2}, I_{x2}=1.07 in.^{4}, I_{y2}=20.29 in.^{4}, θ=74.90 degrees, J=0.00240 in.^{4}

Based on these section properties, the element properties are:

Table A.1 Section Properties for Example Model

Element Type	Area (in.^{2})	I_{yy} (in.^{4})	I_{zz} (in.^{4})	J (in.^{4})
A	1.279	1.07	20.29	10
B	2.25	0.00240	0.001055	1.07
C	13.50	0.00240	1	1.07
D	0.0377	0.001	0.001	0.001
E	0.333	0.001	0.001	0.001
F	2.25	0.00240	0.00527	1.07

The x-axis rotation for type A elements is: $270 + \theta = 270 + 74.90 = 344.9$ degrees

Loading: Distributed load applied to type A elements along the principal axes:

$$w_y = w \cdot \cos\theta \cdot \cos\theta_p = (-100 \text{ plf})\cos(4.76^0)\cos(15.10^0) = -0.0096 \text{ k/ft}$$

$$w_z = w \cdot \cos\theta \cdot \sin\theta_p = (-100 \text{ plf})\cos(4.76^0)\sin(15.10^0) = -0.0026 \text{ k/ft}$$

Distributed downslope load: $w_{ds} = w\sin\theta = (-100 \text{ plf})\sin(4.76^0) = -0.008 \text{ k/ft}$

Total torque acting on each purlin line:

$$T = \frac{bw_{web}L}{3} = \frac{(0.25 \text{ ft})(-0.100 \text{ k/ft})\cos(4.76^0)(30 \text{ ft})}{3} = -0.249 \text{ k} \cdot \text{ft}$$

Point torque on inside joints: $\frac{T}{24} = \frac{-0.249 \text{ k} \cdot \text{ft}}{24} = -0.0104 \text{ k} \cdot \text{ft}$

Point torque on outside joints: $\frac{T}{48} = \frac{-0.249 \text{ k} \cdot \text{ft}}{48} = -0.0052 \text{ k} \cdot \text{ft}$

Analysis Results: Due to symmetry, the two braces have the same restraint force:

Restraints 1 & 2: P_L=734 lb.

Results of Proposed Design Procedure:

Restraints 1 & 2: P_L=780 lb.

APPENDIX B: MODEL LOADS AND SECTION PROPERTIES

Table B.1 Model Loading

Purlin ID	Roof Slope	θ (deg)	w_{ds} (k/ft)	w_y (k/ft)	w_z (k/ft)	Dist. T (k-ft/ft)	Inside Point T (k-ft)	
							L_1	L_2
P1 (L_1=36 ft) x-axis rotate =347.1 deg	0:12	0	0	-0.097	-0.022	-0.00903	-0.014	
	½:12	2.39	-0.004	-0.097	-0.022	-0.00902	-0.014	
	1:12	4.76	-0.008	-0.097	-0.022	-0.00900	-0.013	
	2:12	9.46	-0.016	-0.096	-0.022	-0.00891	-0.013	
	3:12	14.04	-0.024	-0.095	-0.022	-0.00876	-0.013	
	4:12	18.43	-0.032	-0.092	-0.021	-0.00856	-0.013	
	5:12	22.62	-0.039	-0.090	-0.021	-0.00833	-0.012	
	6:12	26.57	-0.045	-0.087	-0.020	-0.00807	-0.012	
	7:12	30.26	-0.050	-0.084	-0.019	-0.00780	-0.012	
	8:12	33.69	-0.056	-0.081	-0.019	-0.00751	-0.011	
	9:12	36.87	-0.060	-0.078	-0.018	-0.00722	-0.011	
P2, P3 (L_1=35 ft) (L_2=30 ft) x-axis rotate =345.1 deg	0:12	0	0	-0.097	-0.026	-0.00833	-0.012	-0.010
	½:12	2.39	-0.004	-0.097	-0.026	-0.00833	-0.012	-0.010
	1:12	4.76	-0.008	-0.096	-0.026	-0.00830	-0.012	-0.010
	2:12	9.46	-0.016	-0.095	-0.025	-0.00822	-0.012	-0.010
	3:12	14.04	-0.024	-0.094	-0.025	-0.00808	-0.012	-0.010
	4:12	18.43	-0.032	-0.092	-0.024	-0.00791	-0.012	-0.010
	5:12	22.62	-0.039	-0.089	-0.024	-0.00769	-0.011	-0.010
	6:12	26.57	-0.045	-0.086	-0.023	-0.00745	-0.011	-0.009
	7:12	30.26	-0.050	-0.083	-0.022	-0.00720	-0.010	-0.009
	8:12	33.69	-0.056	-0.080	-0.021	-0.00693	-0.010	-0.009
	9:12	36.87	-0.060	-0.077	-0.021	-0.00667	-0.010	-0.008
P4, P5 (L_1=35 ft) (L_2=30 ft) x-axis rotate =344.9 deg	0:12	0	0	-0.097	-0.026	-0.00833	-0.012	-0.010
	½:12	2.39	-0.004	-0.096	-0.026	-0.00833	-0.012	-0.010
	1:12	4.76	-0.008	-0.096	-0.026	-0.00830	-0.012	-0.010
	2:12	9.46	-0.016	-0.095	-0.026	-0.00822	-0.012	-0.010
	3:12	14.04	-0.024	-0.094	-0.025	-0.00808	-0.012	-0.010
	4:12	18.43	-0.032	-0.092	-0.025	-0.00791	-0.012	-0.010
	5:12	22.62	-0.039	-0.089	-0.024	-0.00769	-0.011	-0.010
	6:12	26.57	-0.045	-0.086	-0.023	-0.00745	-0.011	-0.009
	7:12	30.26	-0.050	-0.083	-0.023	-0.00720	-0.010	-0.009
	8:12	33.69	-0.056	-0.080	-0.022	-0.00693	-0.010	-0.009
	9:12	36.87	-0.060	-0.077	-0.021	-0.00667	-0.010	-0.008
P6, P7 (L_1=25 ft) (L_2=20 ft) x-axis rotate =343.3 deg	0:12	0	0	-0.096	-0.029	-0.00694	-0.007	-0.006
	½:12	2.39	-0.004	-0.096	-0.029	-0.00694	-0.007	-0.006
	1:12	4.76	-0.008	-0.095	-0.029	-0.00692	-0.007	-0.006
	2:12	9.46	-0.016	-0.094	-0.028	-0.00685	-0.007	-0.006
	3:12	14.04	-0.024	-0.093	-0.028	-0.00674	-0.007	-0.006
	4:12	18.43	-0.032	-0.091	-0.027	-0.00659	-0.007	-0.005
	5:12	22.62	-0.039	-0.088	-0.027	-0.00641	-0.007	-0.005
	6:12	26.57	-0.045	-0.086	-0.026	-0.00621	-0.006	-0.005
	7:12	30.26	-0.050	-0.083	-0.025	-0.00600	-0.006	-0.005
	8:12	33.69	-0.056	-0.080	-0.024	-0.00578	-0.006	-0.005
	9:12	36.87	-0.060	-0.077	-0.023	-0.00556	-0.006	-0.005

Table B.1 Model Loading, Continued

P8, P9 (L_1=25 ft) (L_2=20 ft) x-axis rotate =343.2 deg	0:12	0	0	-0.096	-0.029	-0.00694	-0.007	-0.006
	½:12	2.39	-0.004	-0.096	-0.029	-0.00694	-0.007	-0.006
	1:12	4.76	-0.008	-0.095	-0.029	-0.00692	-0.007	-0.006
	2:12	9.46	-0.016	-0.094	-0.028	-0.00685	-0.007	-0.006
	3:12	14.04	-0.024	-0.093	-0.028	-0.00674	-0.007	-0.006
	4:12	18.43	-0.032	-0.091	-0.027	-0.00659	-0.007	-0.005
	5:12	22.62	-0.039	-0.088	-0.027	-0.00641	-0.007	-0.005
	6:12	26.57	-0.045	-0.086	-0.026	-0.00621	-0.006	-0.005
	7:12	30.26	-0.050	-0.083	-0.025	-0.00600	-0.006	-0.005
	8:12	33.69	-0.056	-0.080	-0.024	-0.00578	-0.006	-0.005
	9:12	36.87	-0.060	-0.077	-0.023	-0.00556	-0.006	-0.005
P10 (L_1=20 ft) x-axis rotate =340.6 deg	0:12	0	0	-0.094	-0.033	-0.00556	-0.005	
	½:12	2.39	-0.004	-0.094	-0.033	-0.00555	-0.005	
	1:12	4.76	-0.008	-0.094	-0.033	-0.00554	-0.005	
	2:12	9.46	-0.016	-0.093	-0.033	-0.00548	-0.005	
	3:12	14.04	-0.024	-0.091	-0.032	-0.00539	-0.004	
	4:12	18.43	-0.032	-0.089	-0.032	-0.00527	-0.004	
	5:12	22.62	-0.039	-0.087	-0.031	-0.00513	-0.004	
	6:12	26.57	-0.045	-0.084	-0.030	-0.00497	-0.004	
	7:12	30.26	-0.050	-0.081	-0.029	-0.00480	-0.004	
	8:12	33.69	-0.056	-0.078	-0.028	-0.00462	-0.004	
	9:12	36.87	-0.060	-0.075	-0.027	-0.00444	-0.004	

Notes:

1) Distributed loads w_y and w_z are applied to type A elements, along the principal axes of the cross-section, which are given by the x-axis rotation.
2) Distributed load w_{ds} is the downslope component of the gravity load.
3) T is the torque loading – the point torque for joints on the outside of each purlin line is half of the tabulated point torque for joints on the inside
4) L_1 and L_2 are the span lengths that were tested for the given purlin cross-section.
5) The gravity load per purlin is w=100 plf.
6) Purlin identifications are given in Table 4.3

Table B.2 Model Section Properties

ID	Elem. Type	Area ($in.^2$)	I_{yy} ($in.^4$)	I_{zz} ($in.^4$)	J ($in.^4$)	ID	Elem. Type	Area ($in.^2$)	I_{yy} ($in.^4$)	I_{zz} ($in.^4$)	J ($in.^4$)
P1	A	1.177	1.12	25.85	10	**P6**	A	1.261	0.776	13.02	10
	B	2.16	0.00141	0.000648	1.12		B	2.25	0.00340	0.001519	0.776
	C	12.96	0.00141	1	1.12		C	13.50	0.00340	1	0.776
	D	0.0451	0.001	0.001	0.001		D	0.0336	0.001	0.001	0.001
	E	0.333	0.001	0.001	0.001		E	0.333	0.001	0.001	0.001
	F	2.16	0.00141	0.000324	1.12		F	2.25	0.00340	0.000759	0.776
P2	A	2.275	1.83	35.47	10	**P7**	A	1.261	0.776	13.02	10
	B	4.73	0.0138	0.007176	1.83		B	1.80	0.00340	0.001215	0.776
	C	28.35	0.0138	1	1.83		C	10.80	0.00340	1	0.776
	D	0.0437	0.001	0.001	0.001		D	0.0321	0.001	0.001	0.001
	E	0.333	0.001	0.001	0.001		E	0.333	0.001	0.001	0.001
	F	4.73	0.0138	0.007176	1.83		F	1.80	0.00340	0.000608	0.776
P3	A	2.275	1.83	35.47	10	**P8**	A	0.847	0.532	8.84	10
	B	4.05	0.0138	0.006151	1.83		B	1.50	0.00102	0.000450	0.532
	C	24.30	0.0138	1	1.83		C	9.00	0.00102	1	0.532
	D	0.0377	0.001	0.001	0.001		D	0.0336	0.001	0.001	0.001
	E	0.333	0.001	0.001	0.001		E	0.333	0.001	0.001	0.001
	F	4.05	0.0138	0.003075	1.83		F	1.50	0.00102	0.000225	0.532
P4	A	1.279	1.07	20.29	10	**P9**	A	0.847	0.532	8.84	10
	B	2.63	0.00240	0.00123	1.07		B	1.20	0.00102	0.000360	0.532
	C	15.75	0.00240	1	1.07		C	7.20	0.00102	1	0.532
	D	0.0437	0.001	0.001	0.001		D	0.0321	0.001	0.001	0.001
	E	0.333	0.001	0.001	0.001		E	0.333	0.001	0.001	0.001
	F	2.63	0.00240	0.000615	1.07		F	1.20	0.00102	0.000180	0.532
P5	A	1.279	1.07	20.29	10	**P10**	A	1.151	0.491	6.88	10
	B	2.25	0.00240	0.001055	1.07		B	2.10	0.00423	0.00193	0.491
	C	13.50	0.00240	1	1.07		C	12.60	0.00423	1	0.491
	D	0.0377	0.001	0.001	0.001		D	0.0321	0.001	0.001	0.001
	E	0.333	0.001	0.001	0.001		E	0.333	0.001	0.001	0.001
	F	2.25	0.00240	0.000527	1.07		F	2.10	0.00423	0.000965	0.491

Note: Purlin identifications are given in Table 4.3

APPENDIX C: RESTRAINT FORCE DATA FROM STIFFNESS MODEL

This appendix contains tables that give the restraint force results from the current stiffness model for every computer test in the test matrix. The stiffness model is described in Chapter II and the computer test matrix is described in Section 4.3. The test combinations are given in Table 4.6. A more extensive explanation of these tables is presented in Section 4.4. Note that all restraint forces are given in pounds.

Table C.1 Support Restraints, Single Span

	Purlin Designation									
Combination	**P1**	**P2**	**P3**	**P4**	**P5**	**P6**	**P7**	**P8**	**P9**	**P10**
1	2108	1370	1160	2169	1802	1246	996	1597	1269	736
2	1753	1095	941	1764	1463	1030	824	1339	1048	611
3	1207	828	716	1370	1135	821	658	1066	834	494
4	320	234	229	583	480	359	292	483	358	258
5	-529	-272	-190	-254	-219	-41	-29	-19	-53	6
6	-1427	-814	-634	-966	-814	-466	-367	-550	-486	-206
7	-2171	-1262	-999	-1712	-1432	-810	-697	-987	-847	-430
8	-2945	-1716	-1381	-2393	-2006	-1177	-934	-1446	-1221	-634
9	-3661	-2148	-1733	-2943	-2461	-1515	-1203	-1868	-1567	-823
10	-4209	-2527	-2050	-3516	-2939	-1812	-1442	-2248	-1879	-992
11	-4801	-2826	-2293	-4035	-3377	-2092	-1665	-2597	-2166	-1147
12	25	25	21	24	21	18	15	21	19	16
13	669	715	617	771	653	589	464	600	468	486
14	993	968	833	1125	951	815	646	865	677	614
15	1280	1130	967	1421	1196	972	772	1080	848	676
16	1532	1232	1050	1666	1397	1079	859	1253	988	707
17	1751	1342	1102	1867	1560	1154	921	1392	1101	723
18	1941	1370	1136	2032	1693	1208	964	1504	1194	732
19	2717	2514	2224	3044	2590	2206	1777	2350	1847	1561
20	2652	2255	2009	2903	2478	2046	1654	2177	1777	1387
21	2488	1793	1612	2582	2217	1720	1398	1939	1609	1086
22	2396	1611	1452	2421	2085	1507	1227	1761	1478	923
23	1876	1018	912	1694	1470	1021	826	1370	1090	613

Table C.2 Support Restraints, Multiple Span, Exterior

	Purlin Designation									
Combination	**P1**	**P2**	**P3**	**P4**	**P5**	**P6**	**P7**	**P8**	**P9**	**P10**
1	2044	1342	1120	2031	1671	1185	922	1490	1166	740
2	1585	1083	906	1652	1356	984	764	1234	960	625
3	1139	831	699	1284	1050	788	610	987	759	512
4	248	273	239	548	438	355	272	437	318	289
5	-605	-206	-159	-234	-212	-17	-22	-39	-64	51
6	-1502	-716	-580	-900	-766	-413	-332	-541	-468	-150
7	-2250	-1138	-929	-1596	-1343	-741	-589	-956	-802	-362
8	-3024	-1571	-1288	-2236	-1876	-1079	-856	-1389	-1149	-555
9	-3739	-1977	-1623	-2829	-2304	-1394	-1103	-1788	-1470	-734
10	-4290	-2338	-1922	-3282	-2746	-1675	-1325	-2147	-1757	-895
11	-4881	-2620	-2155	-3773	-3153	-1936	-1529	-2476	-2022	-1043
12	24	25	21	24	21	18	15	21	18	15
13	557	665	574	665	567	540	427	530	416	479
14	848	930	798	999	854	775	611	793	625	619
15	1131	1102	937	1296	1101	935	734	1012	796	685
16	1398	1208	1019	1544	1301	1039	813	1184	928	716
17	1641	1273	1069	1745	1456	1107	864	1314	1029	730
18	1855	1314	1100	1903	1577	1153	899	1413	1106	738
19	2455	2551	2275	2849	2482	2282	1866	2343	1885	1850
20	2366	2255	1999	2694	2328	2041	1652	2177	1736	1524
21	2245	1772	1570	2417	2079	1675	1344	1939	1532	1132
22	2171	1585	1404	2269	1950	1451	1158	1761	1386	945
23	1702	988	865	1577	1350	963	756	1268	986	612

Table C.3 Support Restraints, Multiple Span, Interior

	Purlin Designation									
Combination	**P1**	**P2**	**P3**	**P4**	**P5**	**P6**	**P7**	**P8**	**P9**	**P10**
1	3656	1981	1525	3383	2634	1707	1235	2307	1712	1035
2	2804	1609	1231	2744	2124	1417	1017	1900	1394	884
3	1975	1247	946	2123	1628	1136	804	1507	1085	737
4	317	453	320	882	635	516	339	640	410	443
5	-1270	-242	-231	-432	-414	-24	-68	-116	-182	131
6	-2926	-968	-802	-1555	-1311	-590	-492	-909	-798	-135
7	-4320	-1574	-1281	-2719	-2245	-1062	-853	-1571	-1318	-413
8	-5749	-2207	-1781	-3803	-3099	-1555	-1219	-2254	-1848	-669
9	-7068	-2784	-2234	-4794	-3793	-2005	1556	-2885	-2336	-906
10	-8098	-3310	-2648	-5570	-4514	-2413	-1866	-3452	-2781	-1118
11	-9180	-3714	-2968	-6388	-5165	-2785	-2143	-3972	-3184	-1314
12	49	53	45	50	44	37	31	42	37	32
13	1287	1222	958	1448	1193	958	711	1072	784	799
14	1885	1605	1255	2061	1650	1315	953	1491	1095	964
15	2372	1785	1388	2493	1980	1485	1077	1770	1303	1015
16	2774	1880	1456	2810	2216	1583	1147	1968	1452	1032
17	3114	1933	1493	3050	2394	1644	1191	2113	1563	1037
18	3401	1959	1510	3232	2527	1680	1216	2220	1645	1035
19	5233	5202	4369	6010	4969	4338	3302	4490	3359	3438
20	5020	4288	3629	5539	4602	3816	2915	4204	3159	2790
21	4419	2963	2506	4504	3751	2835	2154	3476	2610	1867
22	4111	2519	2123	4043	3368	2292	1728	2980	2231	1455
23	2669	1271	1043	2305	1901	1264	922	1811	1329	787

Table C.4 Third-point Restraints, Single Span

	Purlin Designation									
Combination	**P1**	**P2**	**P3**	**P4**	**P5**	**P6**	**P7**	**P8**	**P9**	**P10**
1	2335	1775	1526	2346	1977	1508	1208	1779	1406	1081
2	1825	1431	1238	1910	1611	1254	1006	1478	1166	913
3	1328	1098	958	1487	1255	1007	810	1189	933	748
4	337	352	338	640	543	455	375	540	420	423
5	-612	-278	-197	-261	-214	-13	0	-17	-27	74
6	-1615	-961	-768	-1027	-858	-517	-401	-609	-500	-218
7	-2447	-1506	-1226	-1825	-1539	-932	-722	-1093	-890	-528
8	-3312	-2095	-1719	-2569	-2149	-1355	-1067	-1604	-1291	-811
9	-4112	-2640	-2164	-3161	-2727	-1758	-1386	-2074	-1668	-1073
10	-4727	-3106	-2575	-3765	-3160	-2111	-1665	-2496	-2002	-1308
11	-5385	-3479	-2888	-4335	-3638	-2445	-1929	-2884	-2314	-1524
12	267	304	262	308	263	242	193	242	190	212
13	615	608	530	670	580	507	411	536	430	420
14	945	894	779	1021	878	751	607	806	643	605
15	1258	1141	992	1344	1150	962	776	1050	835	755
16	1554	1349	1170	1638	1396	1140	918	1269	1007	874
17	1832	1522	1316	1902	1614	1289	1035	1462	1159	965
18	2092	1663	1433	2138	1808	1410	1131	1632	1291	1032
19	2720	2518	2236	3047	2596	2215	1786	2355	1852	1576
20	2663	2306	2062	2919	2498	2078	1683	2273	1794	1444
21	2524	2000	1784	2651	2285	1825	1484	2090	1659	1254
22	2450	1897	1684	2527	2183	1676	1361	1957	1558	1166
23	2070	1630	1405	2042	1758	1381	1106	1613	1283	1041

Table C.5 Third-point Restraints, Multiple Span, Exterior

	Purlin Designation									
Combination	**P1**	**P2**	**P3**	**P4**	**P5**	**P6**	**P7**	**P8**	**P9**	**P10**
1	2276	1786	1512	2304	1923	1486	1168	1716	1348	1105
2	1773	1452	1233	1879	1567	1240	975	1428	1117	941
3	1284	1127	963	1465	1222	1002	788	1149	893	782
4	307	402	359	639	530	469	370	528	396	466
5	-628	-214	-155	-241	-205	16	13	-7	-30	128
6	-1614	-877	-707	-989	-830	-471	-369	-575	-484	-156
7	-2434	-1421	-1154	-1775	-1486	-871	-684	-1040	-856	-458
8	-3285	-1978	-1631	-2490	-2085	-1283	-1008	-1530	-1247	-734
9	-4071	-2508	-2071	-3067	-2568	-1672	-1313	-1981	-1609	-989
10	-4674	-2973	-2457	-3664	-3067	-2014	-1584	-2386	-1930	-1218
11	-5324	-3336	-2760	-4219	-3530	-2336	-1836	-2759	-2229	-1429
12	270	317	272	319	270	252	198	249	191	223
13	645	625	544	691	597	520	421	549	442	436
14	983	916	795	1045	896	764	616	818	652	627
15	1286	1164	1006	1361	1160	972	779	1052	836	781
16	1563	1371	1179	1642	1392	1144	912	1257	995	901
17	1820	1539	1317	1891	1594	1284	1019	1435	1133	990
18	2056	1677	1427	2111	1770	1397	1103	1587	1249	1058
19	2723	2664	2329	3090	2611	2290	1815	2372	1839	1798
20	2657	2390	2106	2932	2495	2119	1691	2276	1776	1586
21	2487	2034	1787	2626	2250	1827	1462	2065	1621	1321
22	2402	1920	1679	2494	2139	1663	1329	1920	1509	1209
23	1998	1628	1386	1994	1699	1354	1064	1562	1222	1054

Table C.6 Third-point Restraints, Multiple Span, Interior

	Purlin Designation									
Combination	**P1**	**P2**	**P3**	**P4**	**P5**	**P6**	**P7**	**P8**	**P9**	**P10**
1	2099	1705	1394	2169	1768	1378	1045	1581	1207	1053
2	1621	1395	1140	1768	1437	1153	871	1313	994	903
3	1155	1094	893	1379	1115	934	702	1054	787	758
4	226	434	345	606	471	447	327	478	332	477
5	-664	-150	-126	-226	-212	43	8	-20	-64	177
6	-1597	-763	-628	-930	-794	-415	-339	-547	-478	-104
7	-2378	-1268	-1039	-1666	-1401	-782	-623	-981	-823	-381
8	-3183	-1790	-1472	-2343	-1961	-1163	-917	-1435	-1181	-635
9	-3927	-2279	-1873	-2887	-2411	-1518	-1190	-1854	-1512	-870
10	-4503	-2715	-2229	-3451	-2877	-1834	-1434	-2230	-1809	-1082
11	-5116	-3051	-2505	-3970	-3304	-2128	-1660	-2576	-2082	-1276
12	220	287	242	276	226	221	166	211	154	206
13	584	600	509	652	550	490	384	509	395	429
14	880	884	743	984	823	721	559	757	583	616
15	1153	1121	935	1281	1063	911	702	971	745	762
16	1408	1315	1092	1544	1276	1068	821	1160	891	872
17	1657	1471	1218	1777	1465	1196	915	1324	1015	951
18	1886	1604	1318	1987	1629	1299	989	1464	1120	1011
19	2541	2677	2295	2958	2495	2258	1765	2291	1760	1870
20	2467	2395	2056	2809	2370	2073	1620	2182	1676	1630
21	2310	1992	1700	2509	2118	1752	1363	1957	1503	1314
22	2227	1860	1580	2371	2000	1572	1217	1800	1380	1179
23	1807	1516	1252	1836	1530	1235	935	1417	1074	988

Table C.7 Midpoint Restraint, Single Span

	Purlin Designation									
Combination	**P1**	**P2**	**P3**	**P4**	**P5**	**P6**	**P7**	**P8**	**P9**	**P10**
1	4045	2603	2240	3771	3164	2257	1817	2835	2249	1548
2	3162	2101	1819	3071	2579	1877	1515	2357	1867	1308
3	2303	1618	1414	2395	2014	1512	1223	1896	1498	1075
4	587	532	503	1037	878	690	569	863	671	612
5	-1054	-397	-276	-417	-337	-12	8	-22	-35	117
6	-2790	-1386	-1107	-1641	-1362	-761	-589	-964	-787	-298
7	-4228	-2191	-1783	-2928	-2438	-1370	-1076	-1734	-1404	-739
8	-5725	-3039	-2497	-4115	-3431	-2016	-1590	-2546	-2052	-1152
9	-7110	-3821	-3156	-5212	-4349	-2610	-2064	-3294	-2649	-1534
10	-8167	-4529	-3749	-6049	-5045	-3144	-2491	-3966	-3186	-1848
11	-9312	-5074	-4206	-6965	-5814	-3643	-2887	-4584	-3679	-2165
12	445	516	444	521	441	410	323	407	315	360
13	1090	997	870	1149	997	846	688	924	747	681
14	1708	1452	1266	1766	1521	1244	1008	1397	1120	963
15	2274	1816	1579	2307	1971	1560	1261	1797	1433	1171
16	2786	2099	1818	2769	2351	1807	1459	2132	1696	1320
17	3249	2315	2000	3160	2671	1998	1611	2410	1915	1425
18	3668	2479	2137	3491	2940	2144	1728	2642	2098	1498
19	5367	4653	4163	5927	5060	4220	3412	4598	3621	2864
20	5144	3936	3563	5458	4696	3738	3046	4291	3398	2416
21	4644	3101	2800	4595	3996	2993	2454	3682	2941	1908
22	4398	2863	2568	4243	3700	2622	2148	3295	2642	1715
23	3329	2327	2020	3080	2671	2009	1624	2461	1972	1475

Table C.8 Midpoint Restraints, Multiple Span, Exterior

	Purlin Designation									
Combination	**P1**	**P2**	**P3**	**P4**	**P5**	**P6**	**P7**	**P8**	**P9**	**P10**
1	3679	2502	2081	3489	2857	2085	1614	2533	1969	1512
2	2856	2041	1701	2849	2329	1743	1348	2107	1629	1293
3	2055	1596	1334	2224	1814	1413	1091	1696	1301	1080
4	456	599	512	976	785	674	515	778	571	657
5	-1074	-256	-194	-357	-312	40	20	-13	-60	203
6	-2684	-1166	-944	-1485	-1243	-635	-505	-850	-726	-178
7	-4026	-1909	-1559	-2667	-2215	-1187	-936	-1539	-1276	-582
8	-5415	-2692	-2204	-3757	-3112	-1770	-1389	-2262	-1851	-952
9	-6698	-3415	-2801	-4626	-3830	-2306	-1807	-2927	-2380	-1295
10	-7687	-4066	-3338	-5533	-4576	-2789	-2183	-3526	-2856	-1603
11	-8748	-4560	-3747	-6367	-5262	-3232	-2528	-4077	-3293	-1886
12	383	478	406	468	389	372	285	361	268	338
13	1047	968	833	1107	949	811	647	874	701	676
14	1635	1418	1212	1701	1443	1191	944	1320	1044	958
15	2155	1769	1502	2205	1851	1484	1167	1679	1319	1160
16	2612	2036	1717	2623	2185	1704	1334	1967	1539	1301
17	3014	2235	1876	2967	2456	1868	1456	2197	1715	1397
18	3365	2388	1994	3251	2676	1993	1548	2383	1856	1466
19	5193	4894	4254	5866	4950	4293	4524	4524	3486	3297
20	4919	4004	3514	5306	4509	3697	4150	4150	3213	2630
21	4330	3044	2660	4345	3718	2850	3450	3450	2686	1953
22	4057	2782	2417	3974	3402	2457	3036	3036	2365	1714
23	2955	2201	1855	2808	2378	1839	2203	2203	1704	1419

Table C.9 Midpoint Restraint, Multiple Span, Interior

	Purlin Designation									
Combination	**P1**	**P2**	**P3**	**P4**	**P5**	**P6**	**P7**	**P8**	**P9**	**P10**
1	3400	2366	1911	3274	2620	1924	1438	2330	1761	1435
2	2628	1942	1567	2679	2135	1614	1201	1939	1453	1235
3	1876	1531	1234	2097	1661	1314	972	1561	1155	1042
4	375	614	491	936	715	643	462	720	495	656
5	-1063	-174	-149	-301	-290	67	21	-6	-79	242
6	-2568	-1012	-828	-1352	-1146	-546	-445	-774	-682	-106
7	-3831	-1700	-1386	-2450	-2038	-1049	-830	-1410	-1183	-475
8	-5129	-2422	-1971	-3463	-2861	-1578	-1233	-2072	-1703	-814
9	-6329	-3089	-2512	-4275	-3523	-2066	-1604	-2683	-2182	-1127
10	-7261	-3690	-2999	-5118	-4208	-2505	-1938	-3233	-2613	-1410
11	-8252	-4149	-3371	-5893	-4837	-2909	-2245	-3738	-3008	1669
12	320	436	366	415	335	333	245	313	220	312
13	986	926	784	1053	889	767	600	822	646	656
14	1519	1363	1142	1619	1348	1127	871	1240	957	931
15	1989	1699	1409	2091	1722	1398	1070	1570	1203	1123
16	2409	1950	1603	2481	2025	1598	1213	1832	1397	1254
17	2782	2135	1743	2801	2269	1744	1315	2040	1550	1342
18	3110	2267	1840	3061	2463	1847	1386	2201	1667	1397
19	4863	4992	4246	5673	4773	4280	3320	4421	3381	3447
20	4610	4031	3453	5147	4335	3651	2831	4032	3080	2706
21	4056	2956	2521	4172	3520	2736	2113	3297	2517	1932
22	3784	2669	2262	3782	3189	2315	1777	2857	2176	1661
23	2659	2042	1675	2570	2129	1670	1247	1991	1490	1328

Table C.10 Quarter-point Restraints, Single Span, Exterior

	Purlin Designation									
Combination	**P1**	**P2**	**P3**	**P4**	**P5**	**P6**	**P7**	**P8**	**P9**	**P10**
1	1235	967	774	1268	996	737	549	869	643	521
2	975	795	635	1050	820	618	459	728	534	442
3	723	629	500	838	648	503	371	591	429	364
4	217	256	198	413	304	246	176	286	195	211
5	-267	-64	-61	-41	-63	25	8	24	-7	47
6	-779	-405	-337	-425	-374	-210	-170	-254	-220	-90
7	-1204	-683	-563	-829	-700	-402	-317	-483	-396	-236
8	-1645	-977	-800	-1201	-1001	-605	-470	-723	-580	-370
9	-2053	-1248	-1020	-1498	-1242	-792	-612	-945	-750	-493
10	-2367	-1492	-1217	-1809	-1492	-960	-740	-1144	-902	-604
11	-2705	-1678	-1368	-2094	-1723	-1115	-857	-1328	-1043	-706
12	184	216	185	218	182	171	132	169	130	147
13	450	422	342	493	392	323	241	349	256	252
14	601	560	449	662	518	421	311	456	332	324
15	732	671	538	802	628	504	375	553	405	384
16	862	766	615	933	733	578	431	645	474	433
17	991	847	679	1055	830	642	479	728	538	471
18	1116	913	732	1167	918	694	518	803	594	500
19	1566	1651	1350	1819	1481	1269	974	1319	999	918
20	1475	1446	1178	1684	1359	1126	853	1205	901	785
21	1364	1161	955	1482	1199	941	712	1067	797	634
22	1313	1070	882	1394	1130	872	637	980	733	573
23	1061	860	703	1061	859	663	495	770	574	503

Table C.11 Quarter-point Restraint, Single Span, Interior

	Purlin Designation									
Combination	**P1**	**P2**	**P3**	**P4**	**P5**	**P6**	**P7**	**P8**	**P9**	**P10**
1	2197	1687	1505	2179	1933	1505	1252	1771	1460	1102
2	1702	1348	1216	1757	1569	1247	1042	1466	1211	930
3	1222	1023	939	1343	1215	998	841	1172	971	763
4	263	290	315	519	502	440	388	513	434	431
5	-654	-336	-218	-366	-259	-38	0	52	-27	76
6	-1625	-1003	-786	-1108	-899	-547	-413	-653	-517	-221
7	-2427	-1543	-1249	-1888	-1572	-960	-750	-1143	-918	-536
8	-3264	-2114	-1736	-2607	-2192	-1399	-1106	-1661	-1340	-825
9	-4038	-2642	-2187	-3176	-2684	-1802	-1434	-2137	-1728	-1091
10	-4626	-3116	-2592	-3773	-3200	-2164	-1729	-2565	-2078	-1330
11	-5265	-3473	-2898	-4322	-3674	-2497	-2000	-2958	-2399	-1550
12	209	222	194	228	201	181	150	185	151	162
13	388	454	428	435	427	410	361	412	368	368
14	727	744	699	782	752	684	593	718	623	579
15	1076	1013	937	1134	1060	923	788	997	847	750
16	1398	1240	1132	1451	1329	1119	946	1239	1039	882
17	1689	1424	1287	1728	1561	1278	1072	1445	1202	979
18	1955	1571	1409	1969	1761	1404	1173	1621	1341	1050
19	2314	1816	1813	2474	2239	1907	1629	2078	1710	1343
20	2380	1832	1806	2492	2282	1908	1644	2133	1775	1331
21	2321	1779	1676	2365	2161	1750	1498	2023	1689	1226
22	2274	1742	1614	2293	2089	1673	1391	1919	1600	1166
23	2005	1603	1411	1973	1757	1398	1157	1630	1345	1066

Table C.12 Quarter-point Restraints, Multiple Span, Exterior ¼ Span

	Purlin Designation									
Combination	**P1**	**P2**	**P3**	**P4**	**P5**	**P6**	**P7**	**P8**	**P9**	**P10**
1	1190	956	762	1216	957	719	531	826	614	532
2	933	787	626	1002	784	603	443	690	509	454
3	682	624	494	794	617	491	359	559	407	379
4	180	258	200	377	281	242	171	266	182	229
5	-300	-55	-53	-67	-77	27	9	14	-13	69
6	-806	-389	-321	-444	-380	-201	-163	-254	-219	-66
7	-1227	-662	-542	-839	-698	-388	-304	-474	-390	-208
8	-1664	-950	-773	-1204	-991	-585	-452	-705	-567	-339
9	-2067	-1216	-987	-1495	-1226	-767	-589	-918	-731	-460
10	-2378	-1455	-1180	-1799	-1470	-930	-712	-1109	-878	-569
11	-2712	-1638	-1327	-2079	-1694	-1081	-825	-1285	-1013	-669
12	187	225	191	223	187	176	136	173	133	156
13	444	420	344	479	387	322	243	343	257	261
14	594	556	449	641	509	418	312	447	332	335
15	724	666	537	777	617	500	373	539	401	396
16	848	760	612	903	716	571	426	625	465	445
17	969	839	674	1019	807	631	469	702	523	483
18	1083	903	723	1123	887	680	504	769	572	511
19	1574	1650	1364	1818	1484	1291	986	1322	994	1008
20	1466	1409	1161	1648	1339	1119	849	1191	889	825
21	1331	1134	935	1426	1161	920	695	1036	774	650
22	1273	1050	864	1338	1090	820	618	946	705	585
23	1015	858	694	1022	825	648	479	739	546	514

Table C.13 Quarter-point Restraint, Multiple Span, Interior ¼ Span

	Purlin Designation									
Combination	**P1**	**P2**	**P3**	**P4**	**P5**	**P6**	**P7**	**P8**	**P9**	**P10**
1	1032	836	642	1065	818	615	435	708	509	475
2	794	687	525	871	664	515	361	587	417	408
3	562	543	412	682	514	418	289	470	327	343
4	99	221	160	303	214	202	132	211	131	214
5	-371	-75	-65	-132	-121	15	-10	-28	-49	77
6	-828	-362	-290	-470	-388	-186	-150	-260	-224	-41
7	-1214	-600	-478	-820	-664	-345	-271	-453	-372	-165
8	-1607	-847	-676	-1143	-918	-516	-396	-652	-527	-278
9	-1971	-1080	-860	-1404	-1128	-673	-511	-840	-670	-383
10	-2256	-1291	-1025	-1672	-1345	-815	-614	-1010	-799	-477
11	-2558	-1453	-1152	-1920	-1543	-946	-709	-1165	-917	-564
12	146	204	167	187	150	151	110	141	103	148
13	372	375	296	422	330	283	204	295	211	244
14	488	489	383	555	430	363	260	381	272	308
15	599	583	456	673	522	433	310	461	331	361
16	714	665	519	786	610	493	352	536	386	403
17	827	733	570	889	689	543	387	603	434	434
18	933	791	611	983	758	584	414	660	475	458
19	1397	1575	1289	1667	1235	1235	934	1234	921	1030
20	1292	1312	1067	1504	1050	1050	783	1096	808	817
21	1171	1017	823	1285	832	832	612	934	682	612
22	1115	931	748	1194	724	724	527	836	608	537
23	850	736	571	863	541	541	380	616	439	450

Table C.14 Quarter-point Restraints, Multiple Span, ½ Span

	Purlin Designation									
Combination	**P1**	**P2**	**P3**	**P4**	**P5**	**P6**	**P7**	**P8**	**P9**	**P10**
1	2137	1719	1473	2176	1862	1466	1169	1690	1351	1113
2	1659	1409	1202	1778	1517	1225	977	1405	1120	951
3	1194	1114	941	1399	1180	991	791	1131	896	795
4	273	452	373	642	511	482	376	518	399	501
5	-622	-207	-146	-259	-210	60	29	19	-32	186
6	-1558	-842	-680	-972	-817	-457	-361	-572	-483	-135
7	-2336	-1361	-1117	-1719	-1453	-847	-672	-1031	-856	-434
8	-3144	-1906	-1576	-2409	-2040	-1258	-999	-1515	-1248	-708
9	-3890	-2411	-2001	-2957	-2507	-1637	-1301	-1960	-1608	-961
10	-4462	-2865	-2384	-3531	-2995	-1979	-1572	-2360	-1932	-1188
11	-5079	-3209	-2674	-4058	-3444	-2292	-1822	-2728	-2230	-1397
12	204	229	200	236	201	186	148	186	146	163
13	476	528	468	546	487	451	373	463	380	395
14	821	848	741	927	811	726	592	763	619	617
15	1136	1117	962	1266	1089	946	773	1013	827	787
16	1413	1329	1137	1552	1327	1122	914	1228	998	909
17	1680	1495	1278	1794	1536	1266	1023	1411	1138	997
18	1920	1619	1389	1996	1713	1379	1106	1564	1255	1066
19	2321	2030	2030	2613	2290	2055	1674	2130	1694	1668
20	2386	1955	1955	2625	2320	2022	1660	2174	1744	1562
21	2298	1711	1711	2432	2149	1782	1458	2017	1622	1324
22	2236	1619	1619	2330	2054	1632	1327	1883	1513	1216
23	1904	1356	1356	1916	1659	1341	1067	1543	1225	1058

Table C.15 Third-point plus Support Restraint, Single Span, Exterior

	Purlin Designation									
Combination	**P1**	**P2**	**P3**	**P4**	**P5**	**P6**	**P7**	**P8**	**P9**	**P10**
1	829	587	500	881	728	537	424	659	509	313
2	638	462	395	714	587	440	346	541	414	255
3	452	341	294	551	448	346	271	427	321	199
4	80	74	72	226	172	138	106	175	119	86
5	-276	-159	-123	-118	-119	-43	-39	-45	-58	-32
6	-648	-403	-326	-414	-370	-232	-190	-276	-243	-132
7	-961	-605	-496	-719	-628	-390	-316	-468	-398	-237
8	-1281	-817	-670	-1001	-867	-554	-447	-667	-558	-333
9	-1577	-1007	-831	-1230	-1061	-704	-567	-850	-705	-421
10	-1809	-1181	-976	-1464	-1259	-840	-674	-1015	-836	-500
11	-2053	-1316	-1089	-1679	-1441	-945	-773	-1166	-957	-573
12	23	17	15	23	20	17	14	20	18	14
13	155	149	131	187	156	139	109	143	108	96
14	254	245	215	309	258	226	178	239	181	151
15	369	336	292	439	367	308	243	338	258	200
16	491	417	360	566	471	381	301	432	331	241
17	611	485	416	682	566	443	350	517	398	272
18	724	542	463	787	652	495	391	593	457	296
19	1016	1063	919	1206	1016	908	723	935	729	671
20	946	936	815	1115	935	821	650	861	666	585
21	891	758	673	1009	852	709	565	787	609	467
22	867	687	613	960	814	636	508	736	571	398
23	728	427	384	716	616	443	355	574	449	255

Table C.16 Third-point plus Support Restraints, Single Span, Interior

	Purlin Designation									
Combination	**P1**	**P2**	**P3**	**P4**	**P5**	**P6**	**P7**	**P8**	**P9**	**P10**
1	1734	1592	1365	1853	1569	1295	1030	1409	1110	1003
2	1362	1287	1111	1514	1284	1079	861	1175	926	848
3	1000	994	866	1181	1006	871	698	949	748	699
4	278	334	315	518	450	404	331	442	349	401
5	-412	-229	-156	-195	-148	4	17	8	7	82
6	-1146	-829	-658	-793	-649	-422	-318	-454	-356	-184
7	-1750	-1317	-1067	-1423	-1177	-768	-590	-831	-653	-468
8	-2383	-1834	-1498	-2004	-1665	-1135	-878	-1229	-967	-727
9	-2968	-2309	-1897	-2462	-2050	-1473	-1144	-1596	-1256	-967
10	-3412	-2737	-2256	-2946	-2455	-1777	-1384	-1926	-1516	-1182
11	-3896	-3060	-2527	-3390	-2828	-2006	-1603	-2230	-1754	-1380
12	267	304	262	308	263	242	193	242	190	212
13	534	573	495	596	511	458	367	466	371	397
14	775	815	705	857	733	653	523	666	529	561
15	991	1025	886	1090	932	823	660	844	670	696
16	1189	1206	1042	1304	1113	972	778	1006	798	806
17	1378	1359	1172	1503	1280	1099	878	1155	914	891
18	1560	1487	1279	1686	1432	1206	962	1289	1018	955
19	1725	1592	1420	1894	1620	1372	1110	1453	1147	999
20	1773	1644	1459	1935	1660	1403	1137	1493	1184	1039
21	1768	1637	1434	1913	1640	1377	1111	1479	1173	1037
22	1756	1620	1412	1893	1621	1344	1080	1454	1152	1023
23	1665	1547	1320	1763	1497	1247	990	1356	1068	993

Table C.17 Third-point plus Support Restraints, Multiple Span, Exterior Support

	Purlin Designation									
Combination	**P1**	**P2**	**P3**	**P4**	**P5**	**P6**	**P7**	**P8**	**P9**	**P10**
1	791	605	508	855	709	537	419	637	495	338
2	605	481	405	690	570	441	343	521	402	281
3	423	361	305	530	434	348	269	410	311	225
4	59	97	86	209	162	144	107	165	112	114
5	-289	-133	-106	-129	-125	-34	-35	-50	-62	-2
6	-651	-374	-307	-419	-371	-221	-183	-274	-243	-102
7	-957	-575	-474	-719	-626	-376	-307	-462	-396	-206
8	-1269	-782	-647	-996	-860	-538	-435	-655	-552	-301
9	-1558	-974	-806	-1221	-1051	-686	-552	-833	-696	-389
10	-1784	-1145	-949	-1452	-1246	-819	-658	-993	-826	-468
11	-2022	-1280	-1061	-1663	-1425	-942	-755	-1144	-945	-540
12	24	17	16	23	20	17	14	20	18	14
13	154	164	140	187	156	143	111	142	108	112
14	248	262	225	304	255	230	180	234	179	172
15	355	354	303	427	359	312	245	330	255	223
16	469	434	371	548	461	384	302	421	327	265
17	582	503	427	661	554	446	350	503	391	297
18	690	559	472	763	637	496	389	574	447	321
19	927	1025	902	1109	952	889	720	892	708	730
20	871	923	810	1038	885	807	646	823	647	629
21	836	769	678	962	820	704	561	761	594	501
22	820	702	620	923	788	633	503	715	557	428
23	704	444	391	702	602	444	350	562	436	276

Table C.18 Third-point plus Support Restraints, Multiple Span, Interior Support

	Purlin Designation									
Combination	**P1**	**P2**	**P3**	**P4**	**P5**	**P6**	**P7**	**P8**	**P9**	**P10**
1	1274	894	682	1336	1051	757	548	925	680	492
2	944	718	539	1068	830	620	442	747	538	417
3	623	546	401	806	614	487	338	574	400	344
4	19	174	102	283	182	198	114	199	101	198
5	-634	-157	-166	-263	-266	-58	-85	-134	-165	45
6	-1265	-498	-440	-739	-659	-323	-290	-477	-438	-88
7	-1807	-790	-676	-1225	-1057	-549	-466	-770	-672	-225
8	-2351	-1085	-912	-1673	-1425	-778	-643	-1066	-907	-350
9	-2852	-1357	-1130	-2044	-1731	-989	-806	-1339	-1124	-407
10	-3254	-1602	-1327	-2416	-2036	-1179	-953	-1584	-1318	-572
11	-3667	-1800	-1486	-2758	-2315	-1353	-1087	-1809	-1496	-668
12	46	24	24	44	39	32	27	39	35	25
13	302	311	237	371	295	263	189	264	188	218
14	464	464	356	567	449	389	281	403	288	304
15	639	588	453	753	598	496	360	536	388	368
16	813	692	533	926	735	584	426	656	479	416
17	979	776	596	1081	857	656	478	761	558	450
18	1130	842	644	1216	960	712	517	849	624	474
19	1611	1834	1521	1947	1609	1495	1134	1469	1096	1304
20	1539	1612	1334	1831	1510	1362	1028	1382	1026	1124
21	1425	1241	1025	1614	1330	1116	837	1224	906	829
22	1366	1094	901	1507	1241	956	713	1107	818	672
23	1039	591	480	1004	824	584	428	769	563	375

Table C.19 Third-point plus Support Restraints, Multiple Span, Third-point

	Purlin Designation									
Combination	**P1**	**P2**	**P3**	**P4**	**P5**	**P6**	**P7**	**P8**	**P9**	**P10**
1	1709	1611	1362	1849	1552	1290	1010	1392	1086	1026
2	1342	1312	1114	1514	1271	1080	846	1162	906	876
3	985	1025	875	1186	997	876	688	941	731	730
4	271	413	337	535	451	420	332	446	341	457
5	-454	-176	-123	-170	-146	53	27	21	-23	172
6	-1170	-766	-614	-759	-629	-387	-297	-431	-363	-133
7	-1766	-1246	-1014	-1380	-1149	-726	-563	-801	-645	-411
8	-2383	-1753	-1435	-1954	-1628	-1086	-843	-1191	-948	-665
9	-2954	-2221	-1825	-2407	-2008	-1417	-1100	-1550	-1230	-900
10	-3392	-2643	-2177	-2884	-2406	-1715	-1333	-1874	-1485	-1111
11	-3864	-2961	-2442	-3322	-2773	-1988	-1546	-2171	-1719	-1305
12	270	317	272	319	270	252	198	249	191	223
13	541	584	504	604	517	465	373	472	376	408
14	776	828	715	862	738	661	530	671	534	581
15	986	1041	897	1095	934	832	664	849	672	720
16	1180	1225	1052	1308	1114	981	779	1010	797	829
17	1365	1379	1178	1506	1276	1105	874	1154	907	915
18	1541	1507	1282	1686	1423	1208	950	1281	1003	980
19	1713	1731	1519	1933	1648	1460	1167	1497	1174	1182
20	1756	1741	1523	1963	1677	1466	1173	1523	1198	1165
21	1749	1685	1459	1927	1643	1407	1120	1493	1173	1102
22	1735	1654	1425	1899	1617	1357	1075	1457	1142	1066
23	1629	1549	1306	1740	1466	1232	961	1332	1034	1007

APPENDIX D: REGRESSION ANALYSIS SAMPLE REPORTS

This appendix contains two sample regression reports, one for the constant panel stiffness regression and one for variable panel stiffness regression. The reports were generated by the computer software program *SigmaPlot 5.0* (1999). The following descriptions of each result in the regression reports are quoted from the *SigmaPlot 5.0* User's Manual (1999).

Equation Code

This is a printout of the code used to generate the regression results.

R and R^2

R, the multiple correlation coefficient, and R^2, the coefficient of determination, are both measures of how well the regression model describes the data. R values near 1 indicate that the equation is a good description of the relation between the independent and dependent variables.

R equals zero when the values of the independent variable does not allow any prediction of the dependent variables, and equals 1 when you can perfectly predict the dependent variables from the independent variables.

Adjusted R^2

The adjusted R^2, R^2_{adj}, is also a measure of how well the regression model describes the data, but takes into account the number of independent variables, which reflects the degrees of freedom. Larger R^2_{adj} values (nearer to 1) indicate that the equation is a good description of the relation between the independent and dependent variables.

Standard Error of the Estimate

The standard error of the estimate is a measure of the actual variability about the regression plane of the underlying population. The underlying population generally falls within about two standard errors of the observed sample.

Statistical Summary Table

The standard error, t and P values are approximations based on the final iteration of the regression.

Estimate *The value for the constant and coefficients of the independent variables for the regression model are listed.*

Standard Error *The standard errors are estimates of the uncertainties in the estimates of the regression coefficients (analogous to the standard error of the mean). The true regression coefficients of the underlying population generally fall within about two standard errors of the observed sample coefficients. Large standard errors may indicate multicollinearity.*

t statistic *The t statistic tests the null hypothesis that the coefficient of the independent variable is zero, that is, the independent variable does not contribute to predicting the dependent variable. t is the ratio of the regression coefficient to its standard error.*

You can conclude from "large" t values that the independent variable can be used to predict the dependent variable (i.e., that the coefficient is not zero).

P value *P is the P value calculated for t. The P value is the probability of being wrong in concluding that the coefficient is not zero (i.e., the probability of falsely rejecting the null hypothesis, or committing a Type I error, based on t). The smaller the P value, the greater the probability that the coefficient is not zero.*

Traditionally, you can conclude that the independent variable can be used to predict the dependent variable when $P < 0.05$.

Analysis of Variance (ANOVA) Table

The ANOVA (analysis of variance) table lists the ANOVA statistics for the regression and the corresponding F value for each step.

SS (Sum of Squares) *The sum of squares are measures of variability of the dependent variable.*

The sum of squares due to regression measures the difference of the regression plane from the mean of the dependent variable.

The residual sum of squares is a measure of the size of the residuals, which are the differences between the observed values of the dependent variable and the values predicted by regression model.

DF (Degrees of Freedom) *Degrees of freedom represent the number observations and variables in the regression equation.*

The regression degrees of freedom is a measure of the number of independent variables.

The residual degrees of freedom is a measure of the number of observations less the number of terms in the equation.

MS (Mean Square) *The mean square provides two estimates of the population variances. Comparing these variance estimates is the basis of analysis of variance.*

The mean square regression is a measure of the variation of the regression from the mean of the dependent variable.

The residual mean square is a measure of the variation of the residuals about the regression plane.

F statistic

The F test statistic gauges the contribution of the independent variables in predicting the dependent variable.

If F is a large number, you can conclude that the independent variables contribute to the prediction of the dependent variable (i.e., at least one of the coefficients is different from zero, and the "unexplained variability" is smaller than what is expected from random sampling variability of the dependent variable about its mean). If the F ratio is around 1, you can conclude that there is no association between the variables (i.e., the data is consistent with the null hypothesis that all the samples are just randomly distributed).

P value *The P value is the probability of being wrong in concluding that there is an association between the dependent and independent variables (i.e., the probability of falsely rejecting the null hypothesis, or committing a Type I error,*

based on F). The smaller the P value, the greater the probability that there is an association.

Traditionally, you can conclude that the independent variable can be used to predict the dependent variable when P < 0.05.

Regression Diagnostics

The regression diagnostic results display the values for the predicted values, residuals, and other diagnostic results. All results that qualify as outlying values are flagged with a < symbol.

Row *This is the row number of the observation.*

Predicted Values *This is the value for the dependent variable predicted by the regression model for each observation.*

Residuals *These are the unweighted raw residuals, the difference between the predicted and observed values for the dependent variables.*

Standardized Residuals *The standardized residual is the raw residual divided by the standard error of the estimate .*

If the residuals are normally distributed about the regression, about 66% of the standardized residuals have values between -1 and +1, and about 95% of the standardized residuals have values between -2 and +2. A larger standardized residual indicates that the point is far from the regression; the suggested value flagged as an outlier is 2.5.

Constant Panel Stiffness Regression: Support Restraints, Single Span

Nonlinear Regression

[Variables]
y = col(1)
n = col(2)
θ = col(3)
b = col(4)
d = col(5)
t = col(6)
L = col(7)
Ixy = col(8)
Ix = col(9)
w=1/abs(col(1))
[Parameters]
C1 = 0.5 '{{previous: 0.482717}}
C2 = 6.0 '{{previous: 5.82341}}
[Equation]
nmax=0.5+d/(2*C2*t)
P=((0.5*Ixy/Ix+0.3333*b/d)*cos(θ)-sin(θ))*100*L
f=if(n>nmax,P*C1*nmax*(1-C2*(t/d)*(nmax-1)),P*C1*n*(1-C2*(t/d)*(n-1)))
fit f to y with weight w
[Constraints]
[Options]
tolerance=0.000100
stepsize=100
iterations=100

R = 0.99889532 Rsqr = 0.99779186 Adj Rsqr = 0.99777780

Standard Error of Estimate = 1.6724

	Coefficient	**Std. Error**	**t**	**P**
C1	0.4827	0.0038	125.9753	<0.0001
C2	5.8234	0.0853	68.2860	<0.0001

Analysis of Variance:

	DF	**SS**	**MS**	**F**	**P**
Regression	1	198414.3094	198414.3094	70943.5869	<0.0001
Residual	157	439.0960	2.7968		
Total	158	198853.4054	1258.5659		

Regression Diagnostics:

Row	**Predicted**	**Wtd Resid**	**Wtd Std Resid**
1	786.2594	-1.8526	-1.1078
2	665.6563	-2.2112	-1.3222
3	544.9182	-2.2909	-1.3699
4	302.9242	-2.7969	-1.6724
5	-163.1989	-2.9821	-1.7832
6	-380.2566	-2.3988	-1.4344
7	-583.0401	-2.0239	-1.2102

8	-769.9923	-1.8477	-1.1049
9	-940.9248	-1.6216	-0.9697
10	-1096.4003	-1.4941	-0.8934
11	474.1318	0.5384	0.3219
12	630.4955	-0.6657	-0.3981
13	733.0577	-2.1945	-1.3122
14	781.8184	-2.8138	-1.6826
15	786.2594	-2.3526	-1.4068
16	786.2594	-2.0055	-1.1992
17	1314.4738	-1.2765	-0.7633
18	1089.7206	-1.2888	-0.7706
19	864.9749	-1.0726	-0.6414
20	415.2748	-3.0271	-1.8101
21	-448.1763	-1.7157	-1.0259
22	-849.0302	0.0698	0.0417
23	-1222.8048	0.0516	0.0309
24	-1566.7628	-0.0060	-0.0036
25	-1880.6892	0.0390	0.0233
26	-2165.7394	-0.0056	-0.0033
27	452.6558	0.7093	0.4241
28	647.9744	1.1155	0.6670
29	822.6201	0.8716	0.5211
30	976.5928	0.3629	0.2170
31	1109.8927	-0.2680	-0.1603
32	1222.5197	-0.8254	-0.4935
33	1643.0923	-1.1534	-0.6897
34	1362.1507	-0.6327	-0.3783
35	1081.2186	-0.4661	-0.2787
36	519.0935	-1.6423	-0.9820
37	-560.2204	0.4358	0.2606
38	-1061.2878	2.3646	1.4139
39	-1528.5059	2.1697	1.2974
40	-1958.4535	2.0928	1.2514
41	-2350.8615	2.1695	1.2973
42	-2707.1743	2.1619	1.2927
43	565.8198	1.3954	0.8344
44	809.9680	1.8711	1.1189
45	1028.2751	1.5739	0.9411
46	1220.7411	0.9113	0.5449
47	1387.3659	0.1242	0.0743
48	1528.1497	-0.6227	-0.3724
49	1022.2022	-0.8302	-0.4965
50	846.9375	-0.7991	-0.4778
51	671.6836	-0.5334	-0.3190
52	321.0273	-1.6987	-1.0157
53	-352.2019	-0.7725	-0.4619
54	-664.7228	-1.2226	-0.7311
55	-956.1180	0.7237	0.4328
56	-1224.2561	0.6128	0.3665
57	-1468.9718	0.7103	0.4247
58	-1691.1684	0.6413	0.3835
59	441.0891	1.0636	0.6360
60	615.2490	1.2099	0.7235

61	758.4858	0.4864	0.2908
62	870.7995	-0.4026	-0.2407
63	952.1902	-1.0278	-0.6146
64	1002.6577	-1.2451	-0.7445
65	1277.7527	-0.8995	-0.5379
66	1058.6719	-0.8934	-0.5342
67	839.6045	-0.6493	-0.3883
68	401.2841	-2.2317	-1.3344
69	-440.2524	-1.1927	-0.7132
70	-830.9035	0.7345	0.4392
71	-1195.1475	0.5290	0.3163
72	-1530.3201	0.3936	0.2354
73	-1836.2148	0.5689	0.3402
74	-2113.9606	0.4801	0.2871
75	551.3613	1.5509	0.9274
76	769.0612	1.6092	0.9622
77	948.1072	0.7664	0.4583
78	1088.4994	-0.2892	-0.1729
79	1190.2377	-1.0667	-0.6379
80	1253.3221	-1.3040	-0.7797
81	1827.9748	-0.6119	-0.3659
82	1490.9699	-0.7313	-0.4373
83	1154.2221	-0.5706	-0.3412
84	481.1309	-0.0516	-0.0309
85	-808.6283	-0.1883	-0.1126
86	-1406.2246	-0.6811	-0.4073
87	-1962.7629	-0.9654	-0.5772
88	-2474.2958	0.2680	0.1603
89	-2940.6294	0.0301	0.0180
90	-3363.5978	-0.2306	-0.1379
91	629.4864	0.9202	0.5502
92	901.1064	1.6179	0.9674
93	1143.9777	1.5043	0.8995
94	1358.1001	1.0408	0.6223
95	1543.4738	0.4184	0.2502
96	1700.0987	-0.1725	-0.1032
97	2132.6373	0.7808	0.4669
98	1739.4649	0.5842	0.3493
99	1346.5925	0.6324	0.3782
100	561.3194	0.8979	0.5369
101	-943.3997	-0.7272	-0.4348
102	-1640.5953	-1.7257	-1.0319
103	-2289.8901	-2.1078	-1.2604
104	-2886.6784	-1.0382	-0.6208
105	-3430.7343	-1.4380	-0.8598
106	-3924.1974	-1.7443	-1.0430
107	734.4008	1.3181	0.7882
108	1051.2909	2.1976	1.3141
109	1334.6406	2.2909	1.3699
110	1584.4502	1.9980	1.1947
111	1800.7195	1.5340	0.9172
112	1983.4485	1.0771	0.6440
113	1210.7847	-1.4911	-0.8916

114	986.3095	-1.4770	-0.8832
115	762.0172	-1.7197	-1.0283
116	-545.1230	-3.5298	-2.1106
117	-943.0105	-1.7714	-1.0592
118	-1313.5280	-1.8156	-1.0857
119	-1654.0538	-1.8964	-1.1340
120	-1964.4648	-1.8892	-1.1296
121	-2245.9876	-0.9818	-0.5871
122	603.0798	0.5604	0.3351
123	827.4341	0.1928	0.1153
124	1000.3314	-1.0719	-0.6409
125	1121.7715	-2.2149	-1.3244
126	1191.7546	-2.7037	-1.6167
127	1210.7847	-2.2188	-1.3268
128	1412.5822	-1.1504	-0.6879
129	1150.6945	-1.6831	-1.0064
130	889.0201	-2.1206	-1.2680
131	-635.9768	-6.2397	-3.7311
132	-1100.1789	-4.5552	-2.7238
133	-1532.4494	-4.4310	-2.6495
134	-1929.7294	-4.7095	-2.8161
135	-2291.8757	-4.6773	-2.7968
136	-2620.3189	-3.8691	-2.3135
137	703.5931	0.4266	0.2551
138	965.3398	0.0855	0.0511
139	1167.0532	-1.1023	-0.6591
140	1308.7334	-2.1861	-1.3072
141	1390.3804	-1.3207	-0.7897
142	1412.5822	-1.1504	-0.6879
143	2208.7573	-2.1945	-1.3122
144	1745.2570	0.1849	0.1106
145	1282.6349	-2.1771	-1.3018
146	359.4788	-2.2069	-1.3197
147	-542.4841	0.5863	0.3506
148	-1403.8521	-0.6128	-0.3664
149	-2218.3659	1.0166	0.6079
150	-2975.4414	0.5609	0.3354
151	-3669.9835	0.1485	0.0888
152	-4302.0011	1.4335	0.8572
153	-4874.2329	1.0569	0.6320
154	673.3536	-0.1683	-0.1006
155	979.7394	0.4208	0.2516
156	1265.9311	0.3932	0.2351
157	1531.9287	0.0018	0.0011
158	1777.7323	-0.6388	-0.3820
159	2003.3418	-1.4150	-0.8461

Variable Panel Stiffness Regression: Support Restraints, Single Span

Nonlinear Regression

[Variables]
y = col(1)
G = col(2)
n = col(3)
m = col(4)
P = col(5)
α = col(6)
w=1/abs(col(1))
[Parameters]
C3 = 0.5 '{{previous: 0.27669}}
[Equation]
C1=0.50
X=m*α+n*C3*log(G/2500)
f=if(X<n,P*C1*X,P*C1*n)
fit f to y with weight w
[Constraints]
[Options]
tolerance=0.000100
stepsize=100
iterations=100

R = 0.98584812 Rsqr = 0.97189651 Adj Rsqr = 0.97189651

Standard Error of Estimate = 2.4679

	Coefficient	**Std. Error**	**t**	**P**
C3	0.2767	0.0094	29.3891	<0.0001

Analysis of Variance:

	DF	**SS**	**MS**	**F**	**P**
Regression	0	12426.6169	12426.6169	2040.3834	(NAN)
Residual	59	359.3297	6.0903		
Total	59	12785.9466	216.7110		

Regression Diagnostics:

Row	**Predicted**	**Wtd Resid**	**Wtd Std Resid**
1	1707.0923	-3.6977	-1.4983
2	1392.5755	-0.1497	-0.0607
3	1103.7275	-0.5379	-0.2180
4	970.6502	-1.5684	-0.6355
5	806.1905	-2.6646	-1.0797
6	682.1957	-2.7948	-1.1325
7	1960.0000	-2.6293	-1.0654
8	1877.6809	-2.3884	-0.9678
9	1618.9322	-0.2476	-0.1003
10	1499.7222	-0.5650	-0.2290
11	1352.4000	-2.3412	-0.9487
12	1241.3261	-4.5835	-1.8573

13	2452.0000	-2.1041	-0.8526
14	2336.9263	-3.4276	-1.3889
15	2013.2133	-1.6854	-0.6829
16	1861.6434	-2.3983	-0.9718
17	1691.2901	-1.8729	-0.7589
18	1538.6052	-4.5552	-1.8458
19	1851.8366	-1.7753	-0.7194
20	1570.6689	2.0490	0.8303
21	1312.4483	2.2881	0.9272
22	1193.4816	0.9569	0.3877
23	1046.4600	-1.5989	-0.6479
24	935.6128	-3.8139	-1.5454
25	2300.5966	-2.0141	-0.8161
26	1950.4818	2.1117	0.8557
27	1627.8249	2.2225	0.9006
28	1476.7495	0.7792	0.3158
29	1306.9520	-1.7267	-0.6997
30	1154.7653	-4.1863	-1.6963
31	2728.0000	-2.7116	-1.0988
32	2563.9814	-1.7272	-0.6999
33	2202.3835	0.3104	0.1258
34	2085.3278	-0.0072	-0.0029
35	1882.3200	-1.9162	-0.7765
36	1674.4480	-5.3324	-2.1607
37	3180.0000	-2.4650	-0.9988
38	2930.2157	-0.5051	-0.2047
39	2510.4092	1.4089	0.5709
40	2374.2772	0.9496	0.3848
41	2194.2000	-0.5411	-0.2193
42	1895.8044	-4.9031	-1.9868
43	2304.0049	-1.6965	-0.6874
44	1918.8102	2.0122	0.8154
45	1559.3331	1.3118	0.5315
46	1442.9640	0.2371	0.0961
47	1241.1468	-2.0800	-0.8428
48	1034.4940	-4.0562	-1.6436
49	2633.1314	-2.3760	-0.9628
50	2180.3171	1.5727	0.6373
51	1762.6228	0.7174	0.2907
52	1627.1758	-0.4030	-0.1633
53	1448.0046	-2.1075	-0.8540
54	1151.1103	-4.1719	-1.6905
55	2872.0000	-2.9736	-1.2049
56	2872.0000	-4.2720	-1.7311
57	2554.8516	-1.3403	-0.5431
58	2431.9718	-0.7349	-0.2978
59	2280.3680	-0.6827	-0.2766
60	1999.8486	-2.8594	-1.1587

VITA

Michael Christopher Neubert was born on March 19, 1976 in Manchester, Connecticut. He attended RHAM High School in Hebron, Connecticut, and graduated in June 1994. Michael graduated Summa Cum Laude from the Virginia Polytechnic Institute and State University with a Bachelor of Science degree in civil engineering in May 1998. In August 1999, he received a Master of Science degree in Civil and Environmental Engineering, also from the Virginia Polytechnic Institute and State University. He has worked summers at the Rhode Island Department of Transportation in Providence, Rhode Island and at Pratt & Whitney in East Hartford, Connecticut. After graduation, Michael will work for Skidmore, Owings & Merrill in Chicago.

_____

Michael Neubert